JOINT CONFERENCES
ON ADVANCED MATERIALS AND TECHNOLOGIES

The 14th Conference
on Functional and Nanostructured Materials

FNMA'17

The 7th International Conference
on Physics of Disordered Systems

PDS'17

25–29 September 2017
Lviv & Yaremche, Ukraine

ABSTRACT BOOK

TITLE

Joint Conferences on Advanced Materials and Technologies:
The 14th Conference on Functional and Nanostructured Materials – FNMA'17
The 7th International Conference on Physics of Disordered Systems – PDS'17
25–29 September 2017, Lviv & Yaremche, Ukraine – Abstract Book

EDITORS

Ihor Shtablavyi and Jarosław Rybicki

TYPESETTING USING TEX

BOP, www.bop.com.pl

Printed from camera-ready copy by
the publishing house PAIS (Lviv, Ukraine)

The Abstract Book printing was funded by
the Ministry of Education and Science of Ukraine
(Agreement No MK/63 of June 12, 2017)

TASK PUBLISHING 2017
GDAŃSK

ISBN 978-83-947070-3-3

FNMA'17 PDS'17

Joint Conferences on Advanced Materials and Technologies

The 14th Conference on Functional and Nanostructured Materials

The 7th International Conference on Physics of Disordered Systems

Organizers

Ministry of Education and Science of Ukraine
Ivan Franko National University of Lviv, Ukraine
Vasyl Stefanyk Precarpathian National University, Ukraine
Department of Solid State Physics, Gdansk University of Technology, Poland
The Gdansk Branch of the Polish Physical Society
Institute of Physics, Faculty of Mechanical Engineering and Mechatronic, West Pomeranian University of Technology, Szczecin, Poland
Department of Solid State Physics, Faculty of Physics, University of Athens, Greece
Institute of Molecular Physics, Polish Academy of Sciences, Poznan, Poland
University of Zielona Gora, Poland
PWSZ im. Prezydenta St. Wojciechowskiego, Kalisz, Poland

In cooperation with:

TASK – Academic Computer Centre in Gdansk, Poland
Poznan Supercomputing and Networking Centre, Poland
Intel Corporation

Honorary Committee

V. Melnyk (Lviv, Ukraine) • B. Ostafiychuk (Ivano-Frankivsk, Ukraine)
G. J. Papadopoulos (Athens, Greece) • M. Strikha (Kyiv, Ukraine)

Scientific Committee

A. Alderson (Bristol, UK) • J. Bernholc (Raleigh, USA) • T. Bryk (Lviv, Ukraine)
A. Continenza (L'Aquila, Italy) • A. Di Cicco (Camerino, Italy) • X. M. Duan (Beijing, China) • J. Felba (Wroclaw, Poland) • I. Gasyuk (Ivano-Frankivsk, Ukraine)
V. Girzhon (Zaporizhzhya, Ukraine) • R. Gladyshevskii (Lviv, Ukraine) • J. Grima (Msida, Malta) • M. Grinberg (Gdansk, Poland) • B. Grzybowski (Evanston, USA)
I. Grygorchak (Lviv, Ukraine) • N. Gouskos (Szczecin, Poland) • W. G. Hoover (Ruby Valley, USA) • V. Kazimirov (Kyiv, Ukraine) • A. B. Kolomeisky (Houston, USA)
A. A. Kornyshev (London, UK) • A. Morawski (Szczecin, Poland) • S. Mudry (Lviv, Ukraine) • U. Narkiewicz (Szczecin, Poland) • V. Radmilovic (Berkeley, USA)
W. Sadowski (Gdansk, Poland) • F. Scarpa (Bristol, UK) • A. Sikorski (Warsaw, Poland) • I. Vakarchuk (Lviv, Ukraine) • A. Voloshinovskii (Lviv, Ukraine)
K. W. Wojciechowski (Poznan, Poland) • N. I. Zheludev (Southampton, UK)

Programme Committee

C. Aidinis (Athens, Greece) • I. Budzulyak (Ivano-Frankivsk, Ukraine)
M. Dudek (Zielona Gora, Poland) • V. Kotsyubynsky (Ivano-Frankivsk, Ukraine)
S. Mudry (Lviv, Ukraine) • B. Padlyak (Zielona Gora, Poland) • J. Rybicki (Gdansk, Poland) • I. Shcherba (Lviv, Ukraine) • P. Yakibchuk (Lviv, Ukraine)

Organizing Committee

P. Berczynski (Szczecin, Poland) • I. Budzulyak (Ivano-Frankivsk, Ukraine) • I. Gasyuk (Ivano-Frankivsk, Ukraine) • A. Koloryshyn (Lviv, Ukraine) • V. Kotsubinsky (Ivano-Frankivsk, Ukraine) • I. Lishchinsky (Ivano-Frankivsk, Ukraine) • S. Mudry (Lviv, Ukraine) • A. Rybicka (Gdansk, Poland) • J. Rybicki (Gdansk, Poland)
Yu. Plevachuk (Lviv, Ukraine) • I. Shtablavyi (Lviv, Ukraine) • V. Sklyarchuk (Lviv, Ukraine) • Sz. Winczewski (Gdansk, Poland) • I. Yaremiy (Ivano-Frankivsk, Ukraine)

CONTENTS

Can auxetic mechanisms be used to make domes?

D. Attard[1], D. Calleja[1], J. N. Grima[1,2]

[1] *Metamaterials Unit, Faculty of Science, University of Malta Msida MSD 2080, Malta*

[2] *Department of Chemistry, Faculty of Science, University of Malta Msida MSD 2080, Malta*

Over the years, a number of planar systems have been identified for their potential to exhibit in-plane auxetic behaviour. It has been shown that a number of these systems adopt a double curvature in response to bending. This work proposes a novel concept through which a doming effect can be obtained in auxetic systems. The concept is illustrated on a chiral honeycomb, one of the earliest systems identified to exhibit auxetic behaviour. It is shown that by introducing constraining elements to the system to suppress its in-plane expansion, the structure can be forced to deform out-of-plane, providing that the same mechanism that leads to auxeticity in-plane can be induced by means other than uniaxial loading. This doming effect is confirmed through 3D printed ABS prototypes. Simple mathematical models show that the extent of doming can be controlled by the parameters that define these system.

"Spin-Battery" – Effect on Dielectric Nanofibers in a System of Magnetic Nanoclusters

O. Balaban, I. Grygorchak, B. Lukiyanets

Department of Applied Physics and Nanomaterials Science
Lviv Polytechnic National University
Bandera 12, 79013 L'viv, Ukraine

Attempts have been made recently to actively introduce nanotechnology into the practical use. The objects of such research have been nanofibers, as a type of two-dimensional nanoscale materials. They have large specific surface due to small fiber diameters and high porosity. Continuous ultra-thin polymer sheets, from tens to hundreds of nanometers in diameter, may be obtained by a widely used method of electrospinning. They are interesting as materials for the manufacture of filters, tissue engineering, protective clothing, catalysis, ceramic fibers, drug delivery systems and many other applications. A set of unique properties of nanofibers opens up wide possibilities for their use in nanoelectronics and molecular power engineering.

In this paper, we synthesized a polymer-inorganic nanofiber (NF/γ-Fe_2O_3), based on polyvinyl-pyrrolidone, with magnetic γ-Fe_2O_3 nanoparticles, and modified by a polymer shell matrix compatible with the polyvinyl-pyrrolidone. Such technology allows achieving unique magnetosensor properties attractive for the practical use of the "spin-battery" effect, which is a basis of a fundamentally new kind of power generating devices – spin capacitors.

The impedance measurements were performed in the frequency range of 10^{-3}–10^{6} Hz in the measuring complex of "Autolab" firm "Eco chemie" (Netherlands), equipped with the FRA-2 and GPES computer programs. Cyclic voltammetry (CV)

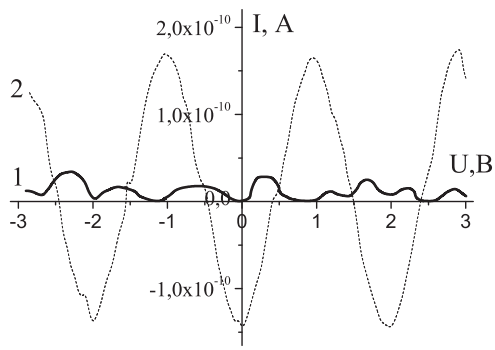

Figure 1: CV curves, measured along the NF/γ-Fe_2O_3 surface under normal conditions (1) and in magnetic field (2)

was recorded at a rate of the sweep voltage of 0.05 V/s. The magnetic field tension was 2.75 kOe.

A strong change of the polarization properties of NF/γ-Fe_2O_3 in the magnetic field can indicate the presence of a spin electromotive force. Indeed, as seen from the CV curves (Figure 1), the value of the "spin-battery" effect in the applied magnetic field reaches 410 mV, which is almost 23 times higher than found at the temperature of 3 K in a magnetic field of 10 kOe. The extraordinary behavior of the CV curves due to the appearance of spin EMF should be noted, namely the CV curves (Figure 1) show oscillation, both when measured in normal conditions and in a magnetic field. However, it still acquires a changeable character in a magnetic field (curve 2).

Such behavior of the CV curves may be related to the following. Based on the architecture of synthesized nanohybrids, it is most likely assumed that grafted magnetite nanoclusters are an ensemble of quantum dots, located on nanofibres. It means that the charge transfer will be determined by its tunneling and by its limitation by a localized charge, similar to the Coulomb blockade. Minority carriers will be localized in quantum wells creating an energy barrier for majority carriers. In these extraordinary cases, the behavior of the dynamic CV curves is peculiar.

Spin-1/2 XY Model of a Magnetoelectric on Zigzag Ladder: Exact Results

O. Baran[1], V. Ohanyan[2,3], T. Verkholyak[1]

[1] *Institute for Condensed Matter Physics, National Academy of Sciences of Ukraine Svientsitskii 1, 79011 L'viv, Ukraine*

[2] *Department of Theoretical Physics, Yerevan State University Alex Manoogian 1, 0025 Yerevan, Armenia*

[3] *Joint Laboratory of Theoretical Physics, ICTP Affiliated centre in Armenia Alikhanian Br. 2, 0036 Yerevan, Armenia*

We consider a spin-1/2 XY model of a magnetoelectric with the Katsura-Nagaosa-Balatsky mechanism (KNB) [1] on a chain with a zigzag structure of bonds between local magnetic moments. The Hamiltonian reads:

$$H = J\sum_{i=1}^{N}\left(S_i^x S_{i+1}^x + S_i^y S_{i+1}^y\right) - h\sum_{i=1}^{N} S_i^z - J\sum_{i=1}^{N}\mathbf{E}\cdot\mathbf{P}_{i,i+1}.$$

Here h is an external magnetic field, J is the nearest-neighbors exchange interaction, $\mathbf{E}$ is an external electric field normal to the z-axis (*i.e.*, the electric field is $(E_x, E_y, 0)$), and $\mathbf{P}_{i,i+1} \propto [\mathbf{l}_{i,i+1} \times [\mathbf{S}_i \times \mathbf{S}_{i+1}]]$ is the bond polarization, where $\mathbf{l}_{i,i+1}$ is the unit vector pointing from the ith site to the $(i+1)$th site. It should be noted that the x, y, and z axes coincide in the real space and in the spin space.

Using the Jordan-Wigner transformation, the Hamiltonian is reduced to a free-fermion form, and can be solved exactly. The ground-state phase diagrams are constructed and the magnetic and electric field dependence of magnetization and polarization at zero temperature and different values of angles θ and α (see Figure 1) is

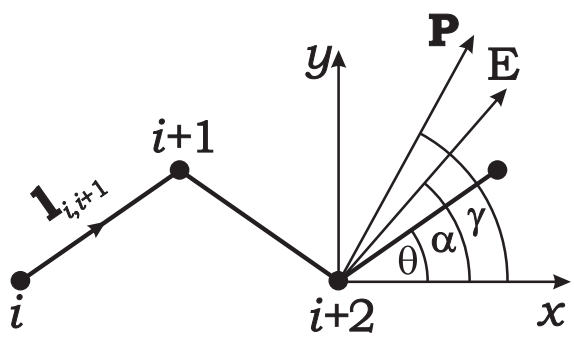

Figure 1: Zigzag ladder with indicated system axes, electric field vector $\mathbf{E}$, polarization $\mathbf{P}$, and unit vector pointing from ith site to $(i+1)$th site

calculated. It is shown that zigzag geometry leads to the appearance of additional quantum phase transitions in comparison with the case $\theta = 0$ [2]. It turns out that the polarization vector in the xy-plane is not collinear to the electric field. Thus, the zigzag geometry and the KNB mechanism lead to the anisotropy of the dielectric properties. Furthermore, it is established that it is only in the case $\alpha = \theta$ that the direction of polarization (*i.e.*, angle γ) does not depend on absolute values of magnetic and electric fields.

References

[1] Katsura H, Nagaosa N, Balatsky A V 2005 *Phys. Rev. Lett.* **95** 057205
[2] Menchyshyn O, Ohanyan V, Verkholyak T, Krokhmalskii T, Derzhko O 2015 *Phys. Rev.* **B 92** 184427

Mono- and Multi-Layer Film Structures Based on Au Nanostars

T. H. Beinyk, N. A. Matveevskaya

Institute for Single Crystals, National Academy of Sciences of Ukraine
Nauky 60, 61001 Kharkiv, Ukraine

The development of new materials based on noble metal nanoparticles (Au, Ag, Pt) has been of great interest recently due to their application in various fields of science and technology, including surface enhancement Raman spectroscopy. The use of materials based on branched gold nanoparticles enables achieving the greatest Raman signal enhancement due to the electric field concentration on the nanoparticle surface inhomogeneities.

In this connection, the development of new materials based on branched gold nanoparticles (nanostars, nanoflowers) with a precision controlled size and morphology is a current task.

The aim of the work was to produce mono- and multilayer film structures based on Au nanostars, to study their optical properties and establish a correlation between the morphology of Au nanoparticles and their properties. Monolayer film structures based on Au nanostars on glass substrates were obtained by template synthesis which allowed controlling the degree of filling the substrate with Au nanoparticles in the 30–80% region. Multilayer film structures based on alternating polycation/nanostar layers were produced by the layer-by-layer method using poli(diallildimethyl)ammonium bromide as the polycation, the number of adsorption cycles varied in the range of 1–5. The layer-by-layer method allows producing film structures with different thickness without nanoparticle aggregation on the substrate surface.

The film morphology and structure were investigated by transmission and scanning electron microscopy, the film composition was studied by X-ray photoelectron spectroscopy. The optical properties were investigated by Raman spectroscopy and optical spectrophotometry.

The study of the optical properties of the obtained film structures based on Au nanostars showed that two surface plasmon resonance (SPR) maxima in absorption spectra for monolayer films based on Au nanostars with (72±16) nm average nanoparticle size and the 30–80% filling degree of the substrate were observed: transverse SPR in the region of 620 nm and longitudinal SPR in the region of 950 nm. In the case of multilayer films based on nanostars with the (55±14) nm average nanoparticle size, one SPR maximum was observed in the region of 600 nm. With increasing the substrate surface filling degree in the case of monolayer structures and the number of adsorption cycles in the case of multilayer structures, the intensity of the lines in the absorption spectra increased. The obtained mono- and multi-layer film structures based on gold nanostars were studied as substrates for surface enhanced Raman spectroscopy. The Raman signal enhancement factor of the

test molecules of a rhodamine 6G dye using monolayer structures was at 10^4 times higher than that for multilayer structures and reached 10^6, the dye concentration was 10^{-5} M.

Ionic-Liquid Based Thermo-Electric Converters. Redox Reactions

M. Bobrowski[1,2], S. Freza[1], P. Skurski[1]

[1] *Department of Solid State Physics, Gdansk University of Technology Narutowicza 11/12, 80-233 Gdansk, Poland*

[2] *TASK Computer Center, Gdansk University of Technology Narutowicza 11/12, 80-233 Gdansk, Poland*

The acceleration of growth of the world's primary energy consumption in the past 30 years (reaching 13000 MToe (million tons of oil equivalent) in 2014) and the continued heavy reliance on fossil fuels over renewable energy sources (despite intergovernmental regulation policies such as the Electronic Vehicles Initiative, the Mandatory CO2 gas emission reduction targets, etc.) paint an alarming picture of today's energy situation. Meanwhile, much of the consumed energy is lost to waste heat through all levels of human activity. For example, the thermal loss consists of 20 to 50% of the total energy consumption across different industrial sectors [1] and as much as 60–70% in the current gasoline and/or diesel powered vehicles (see, for example, https://energy.gov/eere/vehicles/waste-heat-recovery). In such context, if even a small fraction of the waste-heat could be converted into more useful forms of energy (e.g., electrical, mechanical, etc.), it would result in tremendous savings to the global energy consumption.

It is known that heat recovery can be practically accomplished in the Peltier device, where the temperature gradient is utilized to achieve some amount of potential difference between the junctions, and in turn – the electrical current and the power. Two unique semiconductors, one n-type and one p-type, are used because they need to have different electron densities. The semiconductors are placed thermally in parallel to each other and electrically in series and then joined with a thermally conducting plate on each side. The Peltier systems are commonly utilized, for instance, in radioisotope thermoelectric generators (RTGs) in many satellites and space probes as a power source. One good example is Voyager 1 – a space probe launched by NASA on September 5, 1977 to study the outer Solar System. The Voyager 1 probe is still operating in space.

The problem with the traditionally used thermoelectric materials is their efficiency, typically measured by the Seebeck coefficient. The best semiconductor for those applications currently known on the market is bismuth telluride, for which the Seebeck coefficient is 287 μV/K at 54°C. This material is also toxic and expensive. Actually solid semiconductors achieved their upper limit in thermoelectric conversion several years ago. Fortunately there are other possibilities.

It has been demonstrated that ionic liquids – and an appropriate redox couple dissolved in them – can play a role similar to that played by a bismuth telluride

semiconductor in "traditional" thermoelectric devices. The ionic liquid is a salt in the liquid state and it is mostly made of ions and short-lived ion pairs. When dissolved in ionic liquids, redox couples were thought to play the same role as typical redox couples in typical solvents, *i.e.* being responsible for the current flow in liquids. Like the ions present in the system (ionic liquid + redox couple(s)) they take part in the reduction/oxidation processes occurring at electrodes in cells which leads to a potential difference between two electrodes. It was also assumed that the flow of ions was caused by the heat flow whereby it was possible to speak about the thermodiffusion of ions. In the current work we show the idea of a novel type of a thermo-electric device based on the ionic-liquid material, and the results of quantum calculations of the redox reactions which were theoretically developed according to the types of ions present in thermogalvanic cells. We utilized the so-called Born-Haber cycle to determine the redox potentials of all the assumed half-reaction reactions and thereby determined which ions were responsible for the involvement in the current flow in the cells. The tendency of any ion to lose or gain electrons can be determined by calculation of the redox potentials. Moreover, its value calculated for all selected reactions can be widely compared and can indicate the mechanism of electron conductivity present in ionic-liquid based thermogalvanic cells.

Acknowledgements
The investigations were supported by Grant No. 731976 from the European Union through the MAGENTA project granted within the Horizon 2020 Programme.

References

[1] U. S. Department of Energy 2008 *Waste Heat Recovery: Technology and Opportunities in U. S. Industry*

What Do We Know about the Structure and Dynamics of Liquid Metals at High Pressure?

T. Bryk[1,2]

[1] *Institute for Condensed Matter Physics, National Academy of Sciences Svientsitskii 1, 79011 L'viv, Ukraine*

[2] *Lviv Polytechnic National University Bandera 12, 79013 L'viv, Ukraine*

I will review the results of recent *ab initio* simulations of liquid Li, Na, Rb, Pb and Si metals in a wide pressure range. Special interest is given to pressure-induced new features in the structure of liquid metals and how these new features are reflected in their single-particle and collective dynamics.

References

[1] Bryk T, de Panfilis S, Gorelli F A, et al, 2013 *Phys. Rev. Lett.* **111** 077801
[2] Bryk T, Klevets I, Ruocco G, Scopigno T, Seitsonen A P, 2014 *Phys. Rev.* **B 90** 014202
[3] Bryk T, Ruocco G, Scopigno T, Seitsonen A P, 2015 *J. Chem. Phys.* **143** 110204
[4] Bryk T, Wax J-F, 2016 *J. Chem. Phys.* **144** 194501

Structure and Electrical Properties of $NiCr_xFe_{2-x}O_4$ Ferrites

V. S. Bushkova, B. K. Ostafiychuk, I. P. Yaremiy

Vasyl Stefanyk Pre-Carpathian National University
Shevchenko 57, 76025 Ivano-Frankivsk, Ukraine

Nano-sized spinel ferrites with the generic formula $MeFe_2O_4$ are very important materials because of their interesting structural, electrical and magnetic properties as well as their chemical and thermal stabilities. Spinel ferrites have exceptional potential applications in many fields, such as satellite communication, memory devices, filters, microwave absorbing materials, computer components, antenna rods, magnetic recording media, ferro-fluids, transformer cores, cancer treatment, and magnetic resonance imaging [1]. Inter alia, ferrite $NiFe_2O_4$ has been the subject of an extensive technical and fundamental study both in its pure form as well as its substituted form in which various isovalent and non-isovalent metals are made to replace the Fe^{3+} ions.

Synthesis of ferrite nanoparticles through the sol-gel auto-combustion (SGA) method is a unique combination of ignition and chemical gelation processes. This method has the advantages of simple preparation, cost-effectiveness and a gentle chemistry route resulting in ultra-fine and homogeneous powder. The ability to obtain a single-phase ferrite nano-sized magnetic nanostructure with a controllable particle size and size distribution will improve its adequacy in a wide range of potential and technological applications. This synthesis method can produce fine, high-purity, stoichiometric particles of single and multi-component metal oxides.

The aim of this work was to create and study nanoparticles of $NiCr_xFe_{2-x}O_4$ systems, using the SGA technology. After completing the auto-combustion process, the only phase which corresponds to the cubic structure of the spinel space group Fd3m was obtained. Distances between ions of the elementary lattice of the spinel structure were calculated. The average size of coherent scattering regions of powders was found to be in the range of 23 to 43 nm. It was found that the X-ray density d_x and anionic parameter u increased, however, the lattice parameter a decreased linearly with the increasing content of Cr^{3+} ions [2]. The specific surface area S_Σ of the investigated powders was in the range 7.2–17.1 m^2/g. In nickel-chromium ferrite powders micro- and mesopores are present. Mesopores with effective diameter of 3.9 nm are dominating.

The results of the study of the dielectric properties of nickel-chromium ferrites are shown in the temperature range 298–723 K in the frequency range of 10^{-2}–10^6 Hz. With increasing frequency the real ε' and imaginary ε'' components of the dielectric permeability decrease through the contribution to the polarization processes at grain boundaries. It is shown that the conductivity of $NiCr_xFe_{2-x}O_4$ ferrites also increases with the increasing temperature. It is found that the Vervey jump conductivity mech-

anism is dominated at low temperatures and the conductivity is described by the band model in the high temperature range.

References

[1] Koledintseva M, Drewniak J, Zhang Y, Lenn J, Thoms M 2009 *J. Magn. Magn. Mater.* **321** 730

[2] Bushkova V S, Yaremiy I P, Lisovskiy R P, Karpyk B V 2017 *J. Nano El. Phys.* **9** (2) 02011

Are Wine-Rack Systems Auxetic?

R. Caruana-Gauci[1], E. P. Degabriele[1], D. Attard[1], J. N. Grima[1,2]

[1] *Metamaterials Unit, Faculty of Science, University of Malta Msida MSD2080, Malta*

[2] *Department of Chemistry, Faculty of Science, University of Malta Msida MSD 2080, Malta*

"Wine-rack" systems are arguably the simplest mechanical systems which are known to potentially exhibit various anomalous mechanical properties such as negative linear compressibility, negative thermal expansion and a very high positive Poisson's ratio.

This paper asks a simple question: Can these systems be auxetic for particular loading conditions? This question is answered trough an analysis which involves analytical and molecular modelling where it is shown that even the simplest of wine-rack systems, that which have all sides equal in length, may exhibit auxetic behaviour when loaded in particular directions.

X-Ray Excited Luminescence of SrF_2 Nanoparticles at Low Temperatures

M. Chylii, V. Vistovskyy, T. Demkiv, A. Voloshinovskii

Ivan Franko National University of Lviv
Kyrylo i Mephodiy 8, 79005 L'viv, Ukraine

Recently, considerable attention of scientists has been aimed at studying the properties of nanosized materials. One of the aspects of such studies is clarification of the dependence of the luminescence intensity on the nanoparticle size. Such studies will allow us to determine the optimum size of nanoparticles with acceptable scintillation parameters.

At present, the dependence of the luminescence intensity on the nanoparticle sizes has been investigated for a number of compounds [1,2], including SrF_2 [3], however, such studies have been conducted at room temperature only. The literature data on how temperature affects the processes of relaxation of electronic excitations in nanoparticles is not available. Therefore, it is important to compare the dependence of the X-ray excited luminescence intensity of SrF_2 nanoparticles on their sizes at different temperatures.

In the work, SrF_2 nanoparticles were synthesized by chemical co-precipitation. As a result of such synthesis nanoparticles with sufficiently small sizes of ≈ 20 nm were obtained. In order to obtain SrF_2 nanoparticles of a different size, the nanoparticles were annealed at the temperatures of 200, 400, 600 and 800°C and their sizes were 30, 45, 65 and 85 nm, respectively.

The intensity of self-trapped exciton luminescence under X-ray excitation at the temperature of 77 K in SrF_2 nanoparticles reveals weaker dependence on the nanoparticle size than at room temperature. For nanoparticles with the smallest size (20 nm) at the temperature of liquid nitrogen the relative intensity of X-ray excited luminescence is 6 times higher than at room temperature. At the same time the intensity of luminescence almost does not change with decreasing temperature for a single crystal.

It is assumed that such difference in the dependence of the intensity of X-ray excited self-trapped exciton luminescence on the temperature in a single crystal and in nanoparticles is caused by the diffusion of self-trapped excitons, which leads to their non-radiative relaxation on the nanoparticle surface. As the temperature decreases, the average diffusion length of the self-trapped excitons decreases too, therefore, in the case of $T = 77$ K the relative intensity of the X-ray excited luminescence of small SrF_2 nanoparticles is higher than that at room temperature.

The study of the influence of nanoparticle sizes on the intensity of self-trapped exciton emission can be used to evaluate the mean diffusion length of nanoparticles.

References

[1] Vistovskyy V, Zhyshkovych A, Halyatkin O et al. 2014 *J. Appl. Phys.* **116** (5) 342

[2] Zhyshkovych A, Vistovskyy V, Mitina N et al. 2014 *Funct. Mater.* **21** 10
[3] Demkiv T, Chylii M, Vistovskyy V et al. 2017 *J. Lumin.* **190** 10

Structure and Dynamics of Molten Silicon at High Pressures: *Ab initio* Molecular Dynamics Study

T. Demchuk[1], T. Bryk[1,2], A. P. Seitsonen[3]

[1] *Institute for Condensed Matter Physics, National Academy of Sciences of Ukraine*
Svientsitskii 1, 79011 L'viv, Ukraine

[2] *Lviv Polytechnic National University*
Bandera 12, 79013 L'viv, Ukraine

[3] *Département de Chimie, École Normale Supérieure*
24 rue Lhomond, F-75005 Paris, France

We report changes in structural and dynamical properties of molten silicon by ab initio molecular dynamics simulations. Seven thermodynamic points in the pressure range from 10.2 to 27.5 GPa above the melting line were studied by means of simulations of 300 particles interacting via PAW potentials (VASP package). The exchange-correlation functional was taken in generalized gradient approximation in the form of PBE (Perdew-Burke-Ernzerhof). The studied pressure range is especially interesting because there are several different phases for the crystalline silicon and one of the issues to clarify by the simulations was a possible correlation in structural changes in the liquid and crystalline phases.

Pair distribution functions $g(r)$, angular three-particle distribution functions and the number of nearest neighbours were calculated for analysis of structural features in the liquid Si at high pressures. Diffusion coefficients, spectral representation of velocity autocorrelation functions, longitudinal and transverse dispersion curves are reported for the pressure dependence of dynamical properties of liquid Si.

Luminescence of Polystyrene Composites with YVO_4:Eu Nanoparticles under X-Ray Excitation

T. Demkiv[1], O. Halyatkin[2], M. Chylii[2], T. Malyi[2], A. Zhyshkovych[2], L. Demkiv[3], V. Vistovskyy[2], A. Voloshinovskii[2]

[1] *Department of General Physics, Ivan Franko National University of Lviv Kyrylo i Mephodiy 8a, 79005 L'viv, Ukraine*

[2] *Department of Experimental Physics, Ivan Franko National University of Lviv Kyrylo i Mephodiy 8a, 79005 L'viv, Ukraine*

[3] *Department of System Design, Ivan Franko National University of Lviv Kyrylo i Mephodiy 8a, 79005 L'viv, Ukraine*

Luminescent nanocomposite biomarkers based on fluorescein have been recently used for identification and separation of biological objects [2]. The main disadvantage of organic based biomarkers is their rapid photodegradation. Therefore, methods of controlled nucleation of luminescent inorganic salts, oxides and colloids of nanoparticles doped with lanthanide ions based on borates and vanadates (Y, La, Lu and Gd) compounds with luminescence that is effectively excited in the range of 340-390 nm are actively developed. In addition, these nanocomposites are promising materials for ionizing radiation sensors due to their high operation speed and low cost of manufacture.

YVO_4:Eu nanoparticles obtained by the precipitation method were about 10 nm in size. As-synthesized nanoparticles were annealed at the temperatures of 400, 600 and 800°C resulting in an increase in the nanoparticle size to 39, 40 and 45 nm, respectively. The composite was based on polystyrene containing luminescent impurity p-Terphenyl and the POPOP wavelength shifter. The method of chemical homogenization involving a solvent with subsequent evaporation was used for composite film preparation. Polystyrene film composites with YVO_4:Eu nanoparticles obtained in this way have good transparency and homogeneity.

The luminescence intensity of YVO_4 nanoparticles increases linearly with the increasing concentration of europium to 10% and decreases with the decreasing nanoparticle size due to the escape of photoelectrons from the nanoparticle volume. The luminescence spectra of polystyrene without inorganic nanoparticles contain a weak peak with a maximum at 420 nm, which is typical for the emission of the POPOP wavelength shifter. The emission band of p-Terphenyl at 380 nm is not observed, which indicates effective energy transfer from p-Terphenyl to POPOP.

The luminescence spectra of the polystyrene nanocomposite contain bands characteristic for luminescent impurities of p-Terphenyl (370 nm) and POPOP (420 nm) and for YVO_4:Eu nanoparticles (main band at 617 nm). It should be noted that an increase in the luminescence intensity of both polystyrene nanocomposites and YVO_4:Eu nanoparticles is observed in such system.

It should be noted that the luminescence intensity of YVO_4:Eu nanoparticles 20 nm in size is very weak, and the luminescence intensity of these particles embedded in a polystyrene matrix is significant. On the other hand, the energy of ionizing radiation absorbed by a polystyrene nanocomposite with embedded YVO_4:Eu nanoparticles results in the presence of luminescence of YVO_4:Eu nanoparticles and a polystyrene matrix. The intensity of the X-ray excited luminescence of the YVO_4:Eu nanoparticle is significant which indicates the possibility of energy transfer from the polystyrene matrix to the YVO_4:Eu nanoparticles.

References

[1] Wang F, Xue X, Liu X 2008 *Angew. Chem. Int. Ed.* **47** 906

Domain Evolution in the Magnetic Auxetic System Subjected to a Deformation

K. K. Dudek[1], W. Wolak[2], M. R. Dudek[2], R. Caruana-Gauci[1], R. Gatt[1], K. W. Wojciechowski[3], J. N. Grima[1,4]

[1] *Metamaterials Unit, Faculty of Science, University of Malta Msida MSD 2080, Malta*

[2] *Institute of Physics, University of Zielona Gora Szafrana 4a, 65-069 Zielona Gora, Poland*

[3] *Institute of Molecular Physics, Polish Academy of Sciences M. Smoluchowskiego 17, 60-179 Poznan, Poland*

[4] *Department of Chemistry, Faculty of Science, University of Malta Msida MSD 2080, Malta*

Over the years, the Ising model was used in order to investigate a wide range of physical processes. This model has proven to be of particular importance in the field of statistical physics as it allowed to gain a fundamental understanding of critical phenomena. In a vast majority of studies involving the use of the Ising model, it is assumed that distances between the Ising spins within the lattice defined by means of the Ising model are constant. In such cases it was shown in a number of papers that an average size of domains within the system increases accordingly to a particular power law. In this work, a different scenario was investigated with the Ising model being deformed as the magnetic domains were evolving [1,2]. In order to induce a deformation of the Ising model it was assumed that it represents a non-magnetic mechanical system with magnetic inclusions. A deformation process of such mechanical system corresponds to the rotation of respective rigid units constituting the system. Upon investigating this model, it was shown that the aforementioned power law associated with a growth of magnetic domains is not satisfied for the considered system. This result may prove to be of great significance as it indicates that one may expect a different domain evolution than is normally the case for examples known from the literature upon subjecting the system to some form of a deformation. Another interesting result reported in this work corresponds to the fact that the change in the rate of deformation of the system may affect the magnetic domain evolution. This in turn leads to the conclusion that it may be possible to fine-tune the magnetic domain evolution by a variation in the rate of deformation of the system.

References

[1] Cirillo E N M, Gonnella G, Saracco G P 2005 *Phys. Rev.* **E 72** 026139

[2] Dudek K K, Wolak W, Dudek M R, Caruana-Gauci R, Gatt R, Wojciechowski K W, Grima J N, 2017 *Phys. Status Solidi Rapid Res. Lett.* **11** 1700122

Synthesis and Physico-Chemical Properties of Polymer-Polymer Composites Based on Polyaniline and Polyvinyl Alcohol

V. Dutka, Ya. Kovalskyi, N. Oshchapovska, O. Aksimentyeva, H. Halechko

Department of Physical and Colloidal Chemistry, Faculty of Chemistry
Ivan Franko National University of Lviv
Kyrylo i Mephodiy 6, 79005 L'viv, Ukraine

Polymer-polymer composites based on polyaniline (PANi) and polyvinyl alcohol (PVA) have unique properties due to their flexibility, high conductivity and light density. In these composites a polyvinyl alcohol matrix provides film-forming properties. This allows obtaining conductive polymer films on different surfaces. In this paper we studied the kinetics of conductive polymer formation in a PVA matrix. The addition of aniline (AN) to polymerization mixtures changes the parameters of the viscosity, the optical absorption and the electrical conductivity of PVA solutions. Conductive PANi formed in a PVA matrix in the presence of an oxidant (ammonium peroxydisulfate). The resulting composite was precipitated, purified and dried, after oxidation of AN in the PVA matrix. We can regulate the amount of the conductive component in the composite changing the ratio between PVA and AN. The thermomechanical properties of PVA and the composites were investigated. It is shown that an increase in the conductive polymer content in the composite leads to an increase in the glass transition temperature of PVA. The electrical conductivity of the obtained composites increases with the increasing PANi content in the PVA matrix. The existence of intermolecular interaction between the macromolecules of PVA and PANi in the composite was confirmed by the IR spectroscopy method.

The conductive polymer network is formed in the PVA matrix when the percolation threshold ($> 2\%$) is achieved. High electrical conductivity is observed above this threshold and with high PANi content it is approaching the conductivity of the individual conductive polymer (PANi). In studying the morphology of PVA – PANi films a significant influence of the sample composition on their structure was observed. A conductive polymer is located in the dielectric polymeric PVA matrix in the form of globular aggregates which are not interconnected. This is observed at a low content of PANi (before reaching the percolation threshold). Linear chains of the conductive polymer are forming with an increase in the PANI content in the PVA matrix.

Threshold Switching and Hysteresis in Transport Characteristics of Mesoscopic Ag-LCMO Junctions

A. D'yachenko[1], V. Tarenkov[2], V. Krivoruchko[2], O. Boliasova[2], M. Belogolovskii[1,3]

[1] *Department of Superconducting Electronics*
G. V. Kurdyumov Institute for Metal Physics, the NAS of Ukraine
Ac. Vernadsky Av. 36, 03142 Kiev, Ukraine

[2] *Department of High Pressure Physics and Advanced Technologies*
A. A. Galkin Donetsk Institute for Physics and Engineering, the NAS of Ukraine
Nauki Av. 46, 03680, Kyiv, Ukraine

[3] *Faculty of Physics and Technology, Vasyl' Stus Donetsk National University*
600-letiya 21, 21021, Vinnytsia, Ukraine

Introduction

Applications of manganites in nanoelectronic devices with extremely short working times need more knowledge about their non-equilibrium and near-equilibrium properties. Particular interest is given to such processes in contacts of manganites with metals which can be used in memory devices [1,2]. In manganites, oxygen ions are weakly bound to the lattice and easily go out of the crystal bulk [3]. This feature is of decisive importance for the formation of near-surface layers, as well as for the structure of an interface formed between the manganite and a normal metal. Due to the presence of oxygen vacancies on the manganite surface, the concentration of holes in the near-surface layers decreases and, in the limiting case, the surface can transform into a dielectric phase with magnetic ordering at low temperatures [1,4,5]. As a result, a high-resistive several atomic-layer region appears at the manganite surface.

In this report, we present our experimental results concerning the threshold switching effects and hysteretic behavior in the current-voltage characteristics of mesoscopic manganite-normal metal heterostructures.

Experimental results and discussion

The studied samples $La_{0.6}Ca_{0.3}MnO_3$ (LCMO) were prepared by the solid-phase synthesis method from oxides La_2O_3 and carbonate $CaCO_3$. $0.1 \times 1 \times 10$ mm plates were prepared using ceramics fabricated by high uniaxial pressures $P = 6$ GPa, and annealed at $T = 1050°C$ for six hours.

The plates were pressed again and re-annealed at $T = 1100°C$ to get a well-developed texture. As a result, the samples consisting of oriented 10–15 μm sized microcrystals were fabricated. The current and potential contacts for measurements of transport characteristics were obtained by burning colloidal silver into the surface of the plates. The contact resistance of the contacts was less than 10^{-8} Ohm·cm^2. Ag-LCMO contacts for tunneling experiments were prepared by rubbing colloidal silver into the plate surface. The resistance of the tunnel junctions was $50 - 200$ Ohm.

Current-voltage recording was performed by both an automated measuring system and with an ordinary two coordinate recorder to exclude instrument errors. The results of the two measuring techniques coincided completely. In Figure 1, a typical current-voltage characteristic (CVC) of an Ag-LCMO contact is shown as well as the temperature effect on it. Anomalous sharp vertical growth of the tunnel current was observed at voltages $\sim \pm 1$ V. For decreasing voltage, the current decreased smoothly and the contact resistance followed the initial, equilibrium way. The CVCs studied did not exhibit a jump-like transition from the high-resistive to the low-resistive state. There was no memory effect, usually observed in metal-manganite contacts, the contact resistance (at $V \approx 0$) does not change for a long time after switching to a new state. The absence of significant hysteresis and memory effects are apparently due to the fact that the mechanism causing the observed specific CVC features is realized only in a narrow region of the 2D tunneling barrier.

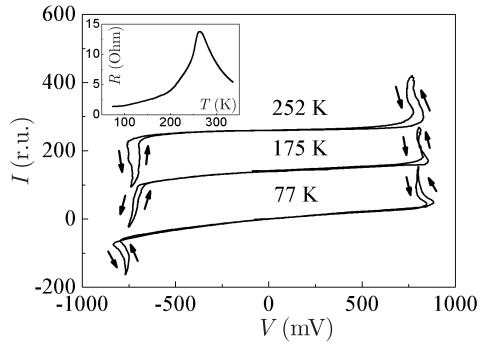

Figure 1: Temperature effect on current-voltage characteristics of Ag-LCMO contact; the inset demonstrates the resistance-vs-temperature dependence of a manganite plate

Some of the measurements were carried out in the pulsed mode to avoid effects caused by possible sample heating during the recording procedure. The experiment showed that in the pulsed regime, the current also increased at the same voltage values ~ 1 V as during the continuous recording mode. In addition, the current increase in the CVC occurred at the same voltage applied to the contact. Thus, the thermal effects did not determine the shape of the CVC.

Since the injector in the Ag-LCMO contact is a noble metal, it is reasonable to assume that the tunnel barrier is due to the oxygen deficiency at the manganite surface. The escape of oxygen ions from the barrier and near-barrier regions generates a system of localized levels capable to trap tunneling electrons. Such behavior is typical for barriers based on perovskites [5] where the tunneling electrons with the energy of junction bias eV can be captured by excited states (the so-called F-centers). The relaxation of the excited state is similar to the usual process of an electron-hole pair recombination that is trapped into the defect.

Typically, the excess energy of the F-center $E = eV$ is partly transferred to the vibrational degrees of freedom of the center and is scattered as a result of the emission of phonons. However, there is another possibility, when the entire vibrational energy E is localized on one of the oxygen ions surrounding the vacancy. Then, when the

condition $eV = E_a$ is satisfied (here E_a is the activation energy of the oxygen ion), the ion can jump to another vacancy. Thus, due to the capture of high-energy electrons by the excited localized state of the vacancy, it is possible for the oxygen vacancy to jump over.

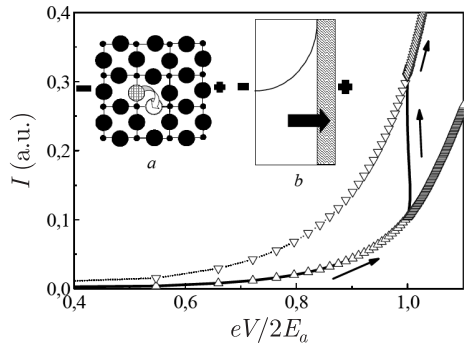

Figure 2: Expected current-voltage characteristic of tunnel junction as a result of transition (at $V = V_c$) of barrier surface layer into metallic-like phase; triangles correspond to the "equilibrium" characteristics; the insets show schematically an oxygen ion jumping to a vacancy (a) and a partial metallization of the tunnel barrier due to di usion of oxygen ions

As is known, the preferred direction of the jump of the activated ion is given by both the direction of the electric field and the electron flow. In our case, the direction of the tunneling electron flow plays a significant role. For a practically fixed voltage $V = V_c \sim 1$ V, the current increases above the intensity of the oxygen ion hopping processes which enhances the inhomogeneous metallization process (see the inset (a) in Figure 2) and accordingly the ohmic resistance $R = V/I$ of the contact decreases. When the voltage decreases the hopping processes in the direction of the electron flow are slowed down, but the activation of the oxygen ions is maintained. As a result, the direction of the jumps becomes more and more random, and the distribution of the oxygen vacancies along the barrier cross section gradually returns to the initial state. As a result of directed activated diffusion of vacancies, a non-equilibrium state with a more metallic nature of conductivity is formed in the region adjacent to the interface, with the effective number of carriers in this region growing monotonically with the increasing transport current. It leads to the appearance of a vertical current section in the $I(V)$ dependence (see Figure 2).

According to [1], the activation energy of oxygen ions is 450–500 meV, it agrees with the observed value of $eV_c \approx 2E_a \approx 1$ eV.

Conclusions

In summary, the current-voltage characteristics of Ag-LCMO contacts with tunneling conductivity exhibit anomalously nonlinear effects, in the absence of "remembering" of the reconstructed state. It is shown that these nonlinearities cannot be explained by thermal effects and are, in all probability, related to the motion of oxygen ions in the region of the tunnel barrier which are stimulated by the tunnel current and the electric field applied to the contact.

Acknowledgements
Financial support from the State Fund for Fundamental Research (Grant/Project No. F76/65-2017) is kindly acknowledged.

References
[1] Nian Y B, Strozier J, Wu N J, Chen X, Ignatiev A 2007 *Phys. Rev. Lett.* **98** 146403
[2] Waser, Aono M, 2007 *Nature materials* **6** 833
[3] Yunoki S, Dagotto E, Costamagna S, Riera J A 2008 *Phys. Rev.* **B 78** 024405
[4] Mazur A S, Krivoruchko V N, Danilenko I A 2007 *Low Temp. Phys.* **33** 931
[5] Tarenkov V Yu, D'yachenko A I, Krivoruchko V N 2001 *JETP* **93** (1) 180

Minimal-parameter Implicit Solvent Model for Large-scale DFT Calculations

J. Dziedzic[1,2], J. C. Womack[1], C.-K. Skylaris[1]

[1] *School of Chemistry, University of Southampton Highfield, Southampton, UK*

[2] *Faculty of Applied Physics and Mathematics, Gdansk University of Technology Narutowicza 11/12, 80-233 Gdansk, Poland*

Accurate studies of crucial biochemical processes, such as protein folding or protein-ligand binding, require the inclusion of their solvent environment [1]. Explicit inclusion of the solvent with full atomic detail is usually computationally infeasible, not only because it substantially increases the number of atoms in the system, but also because it necessitates extensive averaging over the solvent degrees of freedom. The implicit solvent (IS) approach introduces an unstructured dielectric continuum to represent the solvent, which seeks to address this difficulty. This averaging property makes IS the prime candidate for use within density functional theory (DFT) calculations on biological systems. Owing to the low directionality and low specificity of most of the solvent's effects, this simplified description is often sufficient for capturing the relevant phenomena, yielding solvation energies in good agreement with experiment.

A multitude of IS models of differing sophistication have been proposed to date (see [2] for a review). One approach for determining the electrostatic component of solvation involves solving the nonhomogeneous Poisson equation (NPE), or, in saline solutions, the Poisson-Boltzmann equation (PBE), for a system where the solute is placed within a suitably defined cavity, with the dielectric kept outside of the cavity. The exact shape of the cavity usually depends on a number of parameters. The elegant, iso-density formulation originally proposed by Fattebert and Gygi (FG) [3] instead chooses to define the cavity naturally in terms of the electronic density, which eliminates the need to carefully tune the many parameters related to the shape of the cavity that are present in most other models.

In this work [4–7] we present an implementation of NPE-based solvation models in the ONETEP [7] linear-scaling density functional theory (DFT) program and in the CASTEP [8] density functional theory code. ONETEP achieves CPU and memory requirements that increase linearly with the number of atoms by employing a density matrix formulation of DFT using strictly localized basis functions (Non-orthogonal Generalized Wannier Functions or NGWFs) [9–10], and CASTEP is a well-established plane-wave DFT code. We start from the FG formulation and extend it by a consistent application of open boundary conditions, approximately including dispersion-repulsion interactions and reducing the computational overhead. In so doing, we obtain a fully self-consistent approach, where the electronic density is optimized in the presence of implicit solvent. Solutions to the NPE (or PBE) are obtained using a high-order defect-corrected multigrid method, [11] which we demonstrate is efficient and

accurate. We show how the proposed approach consistently gives predictions in excellent agreement with experiment on a test set of 100+ molecules and demonstrate how it can be used to obtain binding energies in solvent for entire proteins with thousands of atoms, while maintaining good parallel scalability.

Acknowledgements
J. D. acknowledges the support of the Engineering and Physical Sciences Research Council (EPSRC grant No. EP/J015059/1), of the Ministry of Science and Higher Education (grant IP2012 043972) C.-K. S. would like to thank the Royal Society for a University Research Fellowship. We would like to thank the University of Southampton for access to the Iridis4 HPC facilities that were used in this work and to the TASK Academic Computer Centre for access to the tryton supercomputing facility.

References

[1] Baker N A, 2005 *Current Opinion in Structural Biology* **15** 137
[2] Tomasi J, Mennucci B, Cammi R 2005 *Chem. Rev.* **105** 2999
[3] Fattebert J-L, Gygi F 2003 *Int. J. Quantum Chem.* **93** 139
[4] Dziedzic J, Helal H, Skylaris C-K, Mostofi A A, Payne M C 2011 *Europhys. Lett.* **95** 43001
[5] Dziedzic J, Fox S J, Fox T, Tauterman C S, Skylaris C-K 2013 *Int. J.Quantum Chem.* **113** 771
[6] Fox S J, Dziedzic J, Fox T, Tautermann C S, Skylaris C-K 2014 *PROTEINS* **82** 3335
[7] Howard J, Womack J, Dziedzic J, Skylaris C-K, Pritchard B, Crawford T D, 2017 *JCTC*, submitted
[8] Clark S J, Segall M D, Pickard C J, Hasnip P J, Probert M J, Refson K, Payne M C 2005 *Zeitschrift fuer Kristallographie* **220** (5–6) 567
[9] Skylaris C-K, Haynes P D, Mostofi A A, Payne M C 2005 *J. Chem. Phys.* **122** 084119
[10] Skylaris C-K, Mostofi A A, Haynes P D, Dieguez O, Payne M 2002 *Phys. Rev.* **B 66** 035119
[11] Anton L, Dziedzic J, Skylaris C-K, Probert M 2013 *dCSE project report:* www.hector.ac.uk/cse/distributedcse/reports/onetep/onetep

Synthesis, Structure and Magnetic Properties of Yttrium-Iron Garnet Prepared by Sol-Gel Method

V. D. Fedoriv[1], I. P. Yaremiy[1], N. V. Stashko[2], P. I. Kolkovsky[1]

[1] *Vasyl Stefanyk PreCarpathian National University*
Shevchenko 57, 76018 Ivano-Frankivsk, Ukraine

[2] *Ivano-Frankivsk National Medical University*
Halytska 2, 76018 Ivano-Frankivsk, Ukraine

Yttrium Iron Garnet (YIG – $Y_3Fe_5O_{12}$) is the most representative and well-known compound among the rare-earth garnets. $Y_3Fe_5O_{12}$ is a material used widely in electronic devices for the microwave region as well as in magnetic bubble domain-type digital memories. Recently, polycrystalline YIG has also found application in magneto-optical recording media devices. In recent years, the interest of scientists has been focused on the research of the properties of garnet structures depending on the size of particles. Some magnetic properties, such as saturation magnetization, remanence and coercitivity, depend critically on the structure and microstructure of the materials. Therefore, it is important to develop techniques to produce garnets with strict control of the composition, homogeneity, size and particle shape [1]. In this regard, alternative methods of synthesis of garnet structures that ensure weak-agglomerated nanoparticles that are homogeneous in size, have actively started to be developed and implemented.

The studied material was synthesized by the sol-gel method of auto-combustion. This method provides the chemical homogeneity and activity of the obtained powders, which enables obtaining a finely dispersed polycrystalline porous material with particles of a homogeneous size. The sol-gel technique appears to be the favorable technique as it provides a 40 and 50% reduction of the sintering temperature and the sintering time. The developed surface of an initial oxide system obtained from the solution of $pH = 1$ allowed obtaining a high dispersed yttrium iron garnet at the temperature of subsequent isothermal annealing of 700°C under static air. The XRD pattern of the sample with $pH = 1$ indicates that the powder is a single-phase YIG. The direct formation of a crystalline YIG during combustion and heat treating at 700°C is surely due the a higher degree of compositional homogeneity and greater heat generated from the exothermic reaction of nitrates metals and citric acid.

It has been found that a mesoporous structure is formed at isothermal annealing in the temperature range 700÷1100°C, the pores with dimensions of 5 and 30 nm make the main contribution to the porous volume of which, with the gradual disappearance of smaller pores with the increasing annealing temperature. The sizes of blocks of coherent scattering of annealed samples vary in the range of 40÷80 nm. At the synthesis temperature of 700°C each particle is a single block of coherent scattering, while at the 1100°C synthesis the particles contain several regions of coherent scattering. The increase in the temperature of isothermal annealing leads to

a decrease in the lattice constant of the garnet. Structural changes caused by increasing the temperature of isothermal annealing of the garnet forming systems lead to corresponding changes of the magnetic microstructure and the resulting changes of the magnetic macroparameters of $Y_3Fe_5O_{12}$. The calcined $Y_3Fe_5O_{12}$ nanopowder samples are ferromagnetic. Specific saturation magnetization (M_s) values of 18.3, 19 and 20.6 emu/g were observed for the $Y_3Fe_5O_{12}$ samples calcined at 900, 1000 and 1100°C, respectively. Saturation magnetization of the samples increases with the increasing annealing temperature due to the increasing size of the particles and the repair of the surface defective layer.

References

[1] Sanchez R D, Rivas J, Vaqueiro P, Lopez-Quintela M A, Caeiro D 2002 *J. Magnetism Magnetic Materials* **247** 92

Nano- and Micro-Sized Silver Particles for Electronic Packaging

J. Felba[1], K. Stojek[1], T. Falat[1], A. Moscicki[2]

[1] *Faculty of Microsystem Electronics and Photonics*
Wroclaw University of Science and Technology
ul. Janiszewskiego 11/17, 50-372 Wroclaw, Poland

[2] *Amepox Microelectronics Ltd.*
Łódź, Poland

Production of modern microelectronic devices needs advanced materials and packaging technologies oriented onto miniaturization and high reliability of the systems. Micro- and nano-sized silver can be treated as such advanced material and it is used in advanced packaging technologies, especially for high-density packaging electronics as well as for flexible electronics. At the FNMA'14 conference information on the practical use of silver with particle sizes ranging from 4 nm to several dozen of nm in electronic packaging technologies was presented – mostly for ink-jet printing electrically conductive structures, especially on temperature sensitive flexible substrates.

In this paper, another aspect of the use of nano- and micro-sized silver is presented, namely, the efficient transport of heat. The miniaturization trends with combining faster operation of electronic devices cause a larger amount of the heat generation issue. Highly conductive materials become essential for heat dissipation systems, especially in the 1st level of packaging. Thermal, as well as mechanical, joints can be created in the silver particle sintering process. The impact of both the materials and the process parameters was analyzed. The research area was focused on obtaining mechanically acceptable joints between non-metalized silicon chips and the substrate.

Acknowledgements
All the presented achievements are a result of the work carried out in the Laboratory of Interconnecting and Packaging Electronics Circuits at the Wroclaw University of Science and Technology.

Influence of Different Thermal Treatment Regimes on the Microstructure of *n*-Si Single Crystals

G. Gaidar[1], P. Baranskii[2]

[1] *Institute for Nuclear Research, National Academy of Sciences of Ukraine*
Prospect Nauky 47, 03680 Kyiv, Ukraine

[2] *Lashkaryov Institute of Semiconductor Physics*
National Academy of Sciences of Ukraine
Prospect Nauky 45, 03028 Kyiv, Ukraine

The modern scientific and technological progress is largely determined by the level of development of physics and technology of semiconductor devices [1,2]. Silicon is the base material of solid state electronics. The production of semiconductor devices is associated with the need to use different regimes of thermal treatment of plates on the basis of which these devices are created [3]. At the development and substantiation of a sequence of necessary thermal annealings, most of the focus is usually on the selection of the temperatures of annealing under which they are carried out, at the same time, an unjustifiably small amount of attention is paid to the choice of optimal cooling conditions, despite the fact that the cooling conditions have a significant influence both on the structure of the semiconductor material and on the characteristics of the devices created on its basis.

The aim of this work was to reveal the features of the microstructure change in *n*-Si single crystals depending on the conditions of thermal treatments widely used in research work with semiconductors and in the development of devices based on them.

A study of dislocation-free *n*-Si crystals with a phosphorus impurity ($\rho_{77\mathrm{K}} \approx 5.84$ Ohm·cm), grown by the floating-zone method was carried out. The crystals were subjected to high-temperature annealing at 1200°C for 2 and 72 h with the subsequent rapid (1000°C/min) or slow (1°C/min)cooling from the annealing temperature to room temperature. The microstructure of silicon crystals was investigated after different thermal treatment regimes by studying X-ray topograms taken using the Lang method [4], and also by analysis of surface micrographs after selective etching of samples. For this, the samples were cut parallel to the (111) plane from the same ingot. The mechanical and chemical treatment of all samples was carried out under the same conditions.

In the initial sample of silicon the structural defects were not detected either by the X-ray method or by the selective etching method (Figure 1*a*).

In the *n*-Si samples annealed at 1200°C for 2 h (irrespective of the rate of their subsequent cooling), the large etching pits belonging to the outlets of dislocation loops on the surface of the crystal with a relatively uniform density $\sim 10^6$ cm^{-2} were detected by the selective etching method. Small very heterogeneously distributed hillocks, apparently belonging to the impurity precipitates, are also revealed (Figure 1*b*). And in these cases X-ray topography clearly did not detect any of the structural defects.

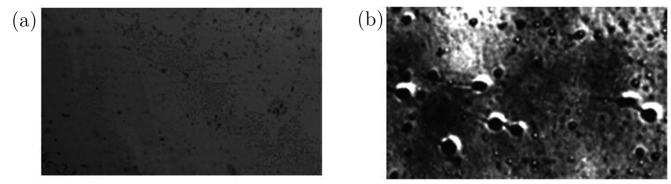

Figure 1: Micrographs of the surface (×200) after selective chemical etching of n-Si samples: a – initial, b – thermal treated (1200°C; 2 h) and cooled with rates $v_{cl} = 1$ and 1000°C/min

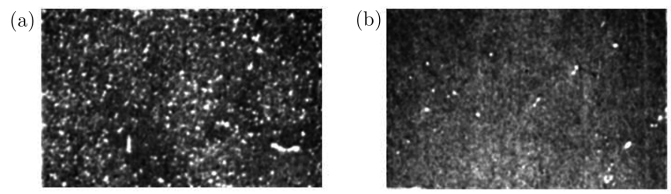

Figure 2: X-ray topograms (×5) of thermal treated (1200°C, 72 h) samples of n-Si with consequent slow (1°C/min) (a) or fast (1000°C/min) (b) cooling

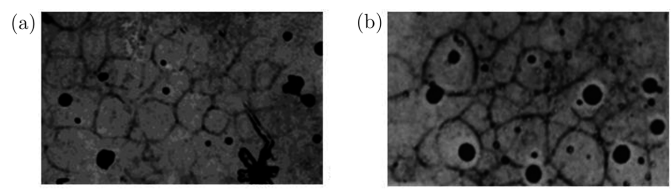

Figure 3: X-ray topograms (×5) of thermal treated (1200°C, 72 h) samples of n-Si with consequent slow (1°C/min) (a) or fast (1000°C/min) (b) cooling

It is established that annealing (1200°C, 72 h) depending on the cooling conditions, affects the release of impurities in the volume of crystals in different ways. Structural defects in the rapidly cooled samples on topograms were detected in small amounts in the form of separate points (Figure 2b), meanwhile the selective etching revealed both dislocation loops (of the same density $\sim 10^6$ cm^{-2}) and impurity precipitates, evenly distributed throughout the volume, with a density of $\sim 5 \cdot 10^9$ cm^{-2} (Figure 3b).

It is shown that after such annealing in the rapidly cooled samples, the size of etch pits, due to the dislocation loops, is 1.5–1.7 times larger than in the case of annealing (1200°C, 2 h), which is associated with the different density of halos of impurities around the dislocations. In slowly cooled samples analogous etch pits associated with the dislocation loops were not only of large dimensions, but also of a more complex structure, as can be seen from the comparison in Figure 3a and b. Meanwhile the structural defects were well detected both by the X-ray method (Figure 2a) and by the selective etching method (Figure 3a). However, it was only the pits of dislocation loops with the same density $\sim 10^6$ cm^{-2} that were found on the surface of the samples after selective etching, and traces of impurity precipitates were almost absent (Figure 3a).

As a result of the performed experiments, it has been established that the degree of the defectiveness of annealed crystals, controlled by selective chemical etching and

X-ray topography, depends not only on the time of high-temperature annealing, but also on the cooling rate of samples from the annealing temperature to room temperature.

References

[1] Belous A I, Solodukha V A, Shvedov S V 2015 *Space Electronics*, Tekhnosfera, 696 (in Russian)
[2] Green M A, Zhao J, Wang A, Wenham S R 1999 *IEEE Transactions on Electron Devices* **46** (10) 1940
[3] Baranskii P I, Belyaev O Ye, Gaidar G P, Kladko V P, Kuchuk A V 2014 *Problems of Real Semiconductor Crystals Diagnostics*, Naukova Dumka, 462 (in Ukrainian)
[4] Murin L I, Lindstrom J L, Davies G, Markevich V P 2006 *Nucl. Instrum. Meth. Phys. Res.* **B253** (1–2) 210

Features of Formation of Microdefect n-Si Structure under the Influence of Irradiation by High-Energy Ions with Different Masses

G. Gaidar, M. Starchyk, L. Marchenko, G. Shmatko, M. Pinkovska, V. Varnina

Institute for Nuclear Research, National Academy of Sciences of Ukraine
Prospect Nauky 47, 03680 Kyiv, Ukraine

At the present stage, the urgency of the study of the influence of irradiation by ions of light nuclei on semiconductors is brought about by the extensive application of ion-beam modification methods of materials in micro- and nanoelectronics [1,2]. Such methods are used to create thin layers in the matrix volume with preassigned characteristics which are necessary for the operation of semiconductor devices [3].

The aim of this work was to establish the features of the formation of a microdefect silicon structure under the influence of high-energy particles (protons, deuterons, α-particles) irradiation.

Single crystals of n-Si grown by the Czochralski and floating-zone methods, dislocation-free and with a dislocation density of $\sim 10^3$ cm^{-2} ($\rho = 3$ up to 4 kOhm·cm) were investigated. Silicon crystals were irradiated by protons (hydrogen ions) with an energy of 6.8 MeV, by 13.6 MeV deuterons (deuterium ions) and 27.2 MeV α-particles (helium ions) with fluences $\Phi \geq 10^{16}$ to 10^{17} cm^{-2} at cyclotrons U-120 and U-240 of the Institute for Nuclear Research of the NAS of Ukraine. The dislocation-free crystals were irradiated by protons and α-particles, and crystals containing dislocations were irradiated by deuterons. During the irradiation, the samples were cooled by running water. In this case the temperature of samples did not exceed 100°C.

To study the topographic image of the defective silicon microstructure, the sample was cut into plates along the direction of irradiation, the mechanical (grinding) and chemical (polishing) surface treatments were carried out. The structural properties of the irradiated samples were studied using a complex of techniques: X-ray topography, selective etching, metallography, scanning electron microscopy, multiangular monochromatic ellipsometry, microprofileometry, atomic-force microscopy.

The silicon microstructure was compared under a variation of the ion beam current magnitude and under irradiation with ions of different energies and masses (protons, deuterons, and α-particles) in the regions of their path, braking and beyond the ion path region (Figure 1). A series of the features of the behavior of radiation defects in the conditions of their high concentration and inhomogeneous distribution was revealed. The projection path length of the protons and α-particles of the used energies in the silicon crystal was approximately the same, about 360 μm, and it was 780 μm in case of the deuterons.

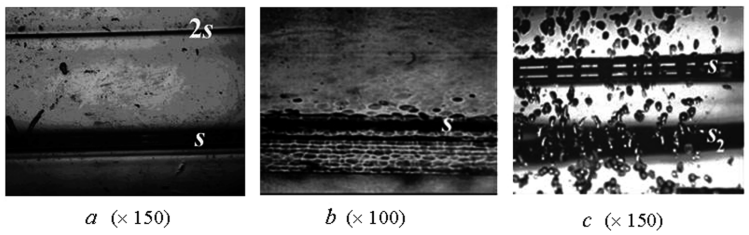

Figure 1: Micrographs of selective etching after irradiation of n-Si: dislocation-free – by 6.8 MeV protons (a) and 27.2 MeV α-particles (b); with dislocations – by 13.6 MeV deuterons (c); the fluence of irradiation is $\Phi = 10^{17}$ cm^{-2}; the arrow indicates the direction of irradiation; s is the braking band of ions; $2s$ is the defect band beyond the proton path in the sample at the double proton path distance (~ 720 μm)

The dependence of the degree of damage of the silicon defective structure on the mass of the irradiating particles was established: the structure of the path region after irradiation with protons did not change significantly (Figure 1a), in contrast to the strongly damaged structure (probably, polycrystalline) after irradiation with α-particles (Figure 1b).

According to the data of X-ray topography and selective etching it was found that the highest damage of the structure (disordering) was observed for all types of irradiation in the braking region of ions, where concentration of defects was the highest (band s in Figures 1 and 2). The width of the etched braking line was varied for light ions of different masses in the direction from the edge to the center of irradiation as follows: 30 to 80 μm (H^+), 30 to 130 μm (D^+, Figure 2 a–f), 140 to 200 μm (He^{2+}). The minimal value of this magnitude for all types of irradiation was obtained at the edge of the irradiation region, where the sample temperature was lower due to cooling.

When the silicon was irradiated with high-energy protons and α-particles, the propagation of the periodic defect structure, located perpendicular to the ion flux, was found into the part of samples beyond the ion path (long-range effect), which is not provided for by the existing ion implantation theory (Figure 1a). In addition, it has been established that when irradiated with α-particles, under conditions of high fluences, the formation of defects in the range of the path (Figure 1b) passes through the stage of ordering (layered structures in the form of "walls" of defects) as a result of their self-organization (large dose effect).

When the dislocation silicon was exposed to deuterons, the long-range effect was not observed, but the deuteron braking region in silicon was not only wider than when irradiated with protons, but also had a more complex structure (band s, Figure 1c). In addition, another line of stresses, ~ 100 μm in width, was etched near the irradiated surface at a distance of approximately 130 μm from the first disturbed region (band s_2, Figure 1c). In the case of proton irradiation, the braking region was a rather narrow band, under α-irradiation it consisted of pores, whereas in the case of deuteron irradiation, the braking region consisted of a broad band of damages located parallel to the plane of braking, and "bridges" from defects, probably, dislocations, which at right angles crossed the damaged region (band s, Figure 2e, f).

The complex studies of the influence of high-energy light ion irradiation on sil-

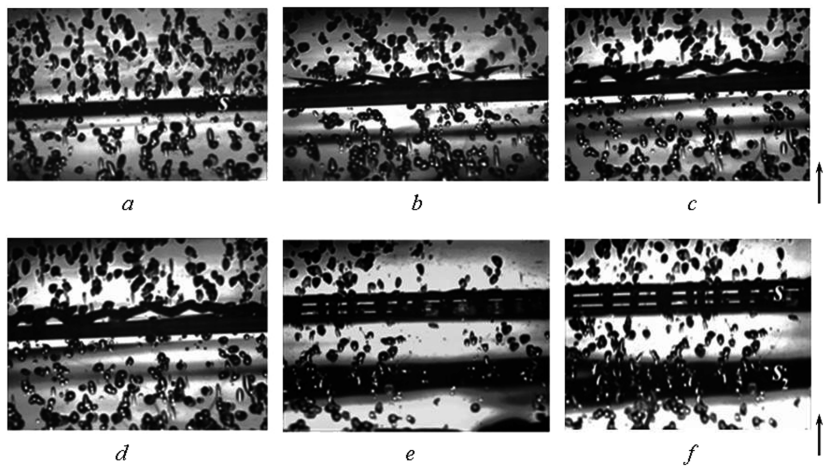

Figure 2: Micrographs (×150) of modification of braking line (s) of 13.6 MeV deuterons in silicon from edge to center (a–f) of irradiation region after selective etching; the fluence of irradiation is $\Phi = 10^{17}$ cm^{-2}; the arrows indicate the direction of irradiation

icon single crystals have shown that, with a large-energy release in a thin crystal layer, under irradiation, favorable conditions can be created for the appearance of effects of large doses and long-range action. The detected effects can be applied in the development of a modern theory of interaction of radiation with matter.

References

[1] Vavilov V S, Chelyadinskiy A R 1995 *Uspekhi Fizicheskikh Nauk* **165** (3) 347 (in Russian)
[2] Komarov F F, Pogrebnyak A D 2005 *Ion-Beam and Ion-Plasma Modification of Materials*, Moscow State University, 639 (in Russian)
[3] Brodie I, Muray J J 1982 *The Physics of Microfabrication*, Springer, 504

Optical Properties of Polytetrafluorethylene-Carbon Nanotube Composite in Light Spectrum Range 320–3000 nm

I. Ye. Galstyan[1], M. M. Nishenko[1], M. M. Yakimchuk[1], L. I. Herunenko[2], G. P. Prikhodko[3]

[1] *G. V. Kurdyumov Institute for Metal Physics of the N.A.S. of Ukraine Ac. Vernadsky Av. 36, 03142 Kiev, Ukraine*

[2] *Institute of Physics of NAS of Ukraine Nauki Av. 46, 03680 Kiev, Ukraine*

[3] *Chuiko Institute of Surface Chemistry of the N.A.S. of Ukraine General Naumov 17, 03164 Kiev, Ukraine*

The influence of carbon nanotube (CNT) concentration (in wt.%) on the optical properties of polytetrafluorethylene (PTFE) was investigated by the spectrophotometric analysis. The effect of increasing transparency at 4–25 times was detected in the spectrum range $\lambda = 320$–3000 nm during the addition of a CNT to PTFE. It was

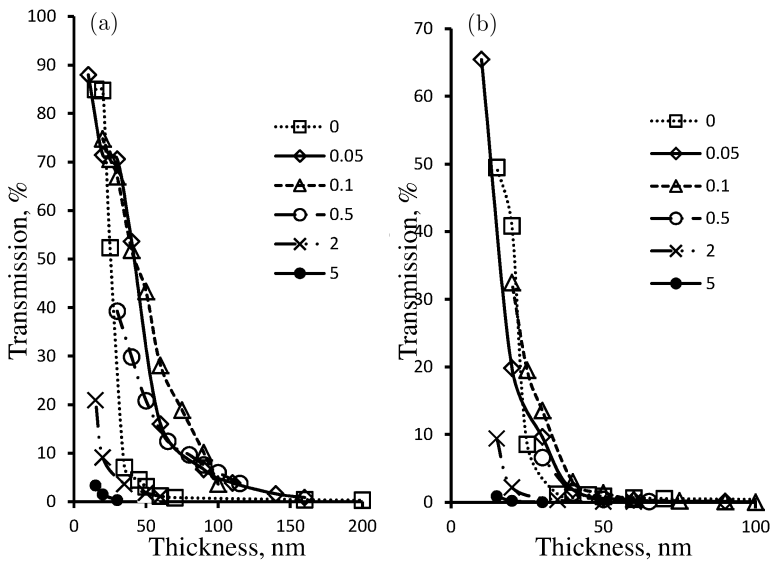

Figure 1: Dependences of monochromatic light transmission on thickness of CNT-PTFE composite with different CNT concentration: 0.05 wt.% (a) and 5.0 wt.% (b)

shown that increasing the CNT concentration and thickness of the sample led to decreasing the transparency of the composite in the ultraviolet (UV) band, and also to increasing the transparency in the infrared (IR) band.

The dependences of the monochromatic light transmission factor ($K_{\text{tr.}}$) for PTFE films in the spectrum range 320–3000 nm with the thickness in the wide range from 25 to 500 μm are shown in Figure 1. Most light transmission (80%) at $\lambda = 3000$ nm is observed for the thinnest (15 and 20 μm) samples. It was shown that the light transmission factor monotonically decreased to 38–45% with reducing the wavelength down to $\lambda = 320$ nm. For the samples with the maximum thickness (500 μm) the light transmission factor decreased to 1–2%. It should be noted that the $K_{\text{tr.}} = f(\lambda)$ curves are convex for the minimal thickness (< 25 μm), however, on the contrary, the curves have a concave form for larger thicknesses (> 35 μm). The thickness of the sample at which the inversion occurs is approximately 30 μm. Thus, at low concentrations of the CNT in PTFE the light transmission increases in the IR band for a wide range of thicknesses, contrary to the Beer–Lambert–Bouguer law. In the UV band the effect was observed for very small thickness (30–60 μm).

Investigation of Li^+-ion Mechanism of Conductivity of Li_2O-Fe_2O_3-Al_2O_3 Ceramics

I. M. Gasyuk[1], V. M. Vakalyuk[2], B. Y. Deputat[2], V. V. Uhorchuk[1], A. V. Vakalyuk[1]

[1] *Vasyl Stefanyk Precarpathian National University Shevchenko 57, Ivano-Frankivsk, Ukraine*

[2] *Ivano-Frankivsk National Technical University of Oil and Gas Karpatska 15, Ivano-Frankivsk, Ukraine*

At present intensive investigations of the conductivity of complex spinel ceramics are being carried out because they contain movable Li^+ – ions and in this way can be used as the material for manufacturing cathodes of portable lithium power sources.

A series of samples with the expected composition $(1-y)LiFe_5O_8 + (y)LiAl_5O_8$ were obtained by a ceramic method at the synthesis temperature of 1273 K that corresponds to the lithium-aluminum-iron spinel formula [1]. The high-dispersion powders of the OCh mark served as the original material. The thermal processing at the final stage of synthesis was carried out at an average cooling rate of $v = 0.03$ K/s.

The conductive and dielectric properties of the synthesized compounds were calculated on the basis of the experimental impedance spectra obtained with an Autolab PGSTAT 12/FRA-2 spectrometer in the frequency range of 0.01–100 kHz and the temperature range of 293–773 K. The temperature was recorded isothermally at every 25 K.

The temperature conductivity dependences show that electron conductivity in the synthesized ceramics dominates in the temperature range of 295–475 K [2]. It can be obtained due to the two mechanisms: the hopping conduction mechanism and the activation mechanism of conductivity. The hopping conduction mechanism in these ceramics is obtained mainly by means of electron hopping between ions of the same element (these are Fe^{2+} and Fe^{3+} ions in this case) that can stay in more than one valence state, randomly distributed in crystallographically equivalent lattice positions. The hopping conduction mechanism dominates in the temperature range of 295–350 K. The value of its activation energy is within the range of 0.1–0.14 eV. The activation mechanism of conductivity dominates in the temperature range of 295–350 K. The value of its activation energy is about 0.35 eV.

Ion conductivity becomes the predominant mechanism in synthesized Li_2O-Fe_2O_3-Al_2O_3 ceramics at temperatures higher than 475 K. The activation energies of conductive ions were determined by slopes of linier sections of the dependences $\sigma_{0*}T(1/T)$. Their values depending on the aluminum content are within the range of 0.9–1.4 eV. A jump in the activation energy was revealed in the temperature range of 520–540 K for samples corresponding to $y = 0.8$ and $y = 1.0$. It may be evidence of the two-type transition and formation of domains.

Considering the prevailing contribution of the ionic Li^+ component in the resulting charge transfer, the frequency dispersion of lithium-aluminum-iron spinel conductivity was calculated within the phenomenological model of the dynamic super ionic conductivity [3]. This model considers the resonance growth of the kinetic energy of ions in the charge-mass transfer process along with energy dissipation in a periodic lattice field.

The values of concentration of carriers, their macroscopic μ_1 and microscopic (transitional) μ_2 mobility for a wide range of concentration of Al^{3+} ions and the temperature range of 400–700 K were obtained by approximation of the experimental dependencies with the theoretical equation:

$$\sigma = \frac{ne^2}{m} \times \frac{\gamma(1 - i\omega\tau)}{\gamma\tau(\omega_0^2 - \omega^2) - i\gamma\omega(1 + \gamma\tau) + \gamma^2 - \omega_0^2}$$

where γ is the frequency of ions scattering on lattice defects; ω_0 is the frequency of natural oscillations of ions relatively to the equilibrium positions; τ is the characteristic time of ion localization.

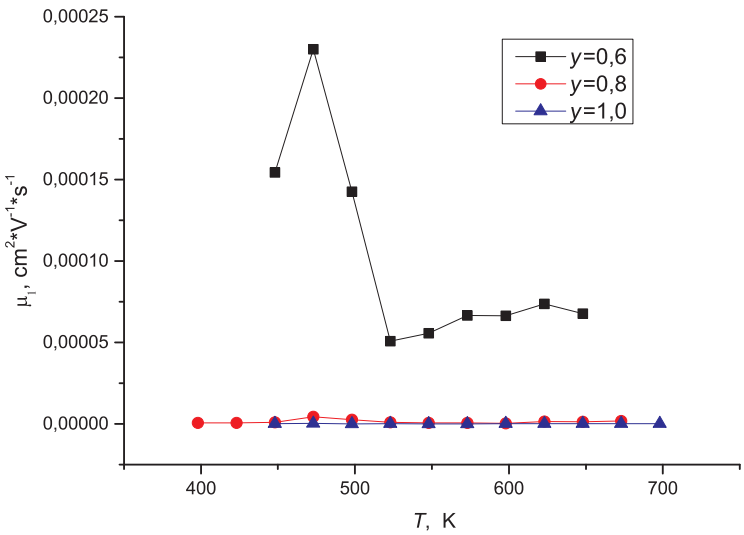

Figure 1: Dependences of macroscopic mobility μ_1 on temperature for different values of aluminum content in synthesized samples

It has been determined that the macroscopic Li^+ ion mobility μ_1 in the samples decreases with the increasing aluminum amount and the curves μ_1(T) have distinct maxima at the temperatures of 470 K (Figure 1). At the same time, the transitional mobility μ_2 increases from 400 K up to 475 K, and then decreases sharply even assuming negative values which can be evidence of the earlier observed manifestations of ferroelectric properties of samples and the existence of a temperature transition to a ferroelectric state (Figure 2).

References

[1] Ostafiychuk B K, Gasyuk I M, Deputat B Y, Yaremiy I P, Kaykan L S, Grabko T V 2008 *J. Physics and Chemistry of Solid State* **9** (1) 24

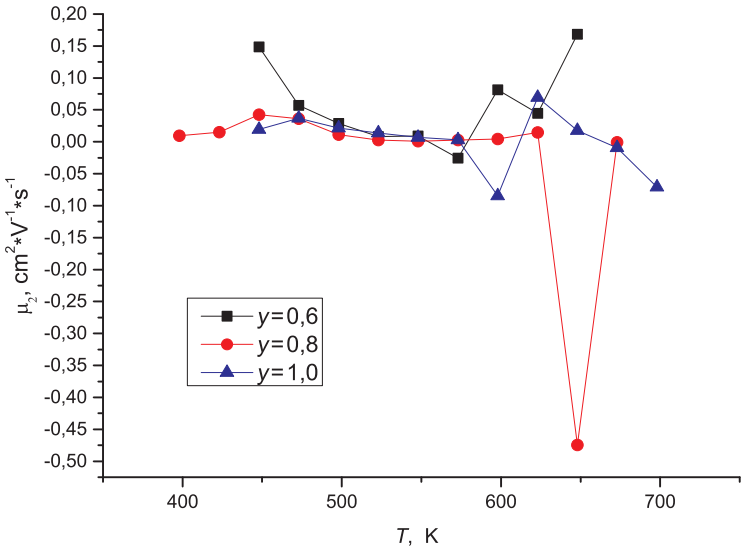

Figure 2: Dependences of microscopic (transitional) mobility μ_2 on temperature for different values of aluminum content in synthesized samples

[2] Deputat B Y 2014 *J. Physics and Chemistry of Solid State* **14** (1) 186
[3] Volkov A A, Kozlov G V, Lebedyev S P, Rakitin A S 1990 *J. Solid State Physics* **32** (2) 329

Simulation of Two-Dimensional Quasi-Periodic Lattices

V. V. Girzhon, O. V. Smolyakov

Zaporizhzhya National University
Zhukovsky 66, 69063 Zaporizhzhia, Ukraine

It has been experimentally established that as for now there are quasicrystals (QC) having the axis of symmetry of the fifth, eighth, tenth and twelfth orders. The last three types of QCs are quasiperiodic in only two dimensions, and they are periodic along the third dimension. Despite a large number of research studies on QC, problems relating to the correct description of their structure remain unresolved in their entirety. This is mainly due to the impossibility of selecting an elementary cell.

The interpretation of the patterns of electron diffraction and X-ray rays from QC is also incomplete, which is due to the ambiguity in the indexation of diffraction reflexes. This uncertainty is a consequence of the inflation-deflation symmetry inherent in QC, resulting in a correlation between the absolute values of the inverse lattice vectors expressed through the so-called scale factor. In electron studies of QC, the vectors, which are closest to the trace of the primary reflexes beam, and which, as a rule, are of a very low intensity, are often placed in correspondence with the base vectors. As a result, the minimum (basic) vectors of the inverse lattice determined in the diffraction experiment are dependent on the experimental conditions.

In this paper we propose a method of two-dimensional QC structure modeling that consists of recurring multiplication of groups of nodes which have the required symmetry. Formally, the simulation algorithm is written identically for octagonal, decagonal and dodecagonal quasicrystals, and can be represented in the form of recurrent relations:

$$D_n = D_{n-1} + \left\{k^{n-2}\mathbf{q}_i\right\} D_{n-1}$$

This record means adding to the group of nodes, labeled as D_{n-1}, the same groups, shifted from the start of coordinates (center of symmetry) to vectors $\pm k^{n-2}\mathbf{q}_i$, where $\pm\mathbf{q}_i$ – are the base vectors, which specify the vertices of the output correct polygon. For octagonal QCs, vertices of the correct octagon are selected as the output group of nodes, and the parameter $k = 1+\sqrt{2}$ is a number known as the silver section. In the case of decagonal QC, the output group of nodes is the vertex of the right decagonal, and $k = (1+\sqrt{5})/2$ – is the golden section. For a dodecagonal lattice, the output group of nodes are the vertices of a correct dodecahedron and $k = 1+\sqrt{3}$.

An analysis of two-dimensional model lattices has shown that they are in good agreement with the corresponding electronograms of quasicrystals and enable the correct indexing of diffraction reflexes, since they show reflexes that correspond to the base vectors $\pm\mathbf{q}_i$. On the basis of a comparison of the model with the traditional method of projection of multidimensional periodic lattices [1], it is possible to index

the diffraction reflexes from the above mentioned types of QC using three integer indexes (N, M, L). This indexation is similar to the index proposed by Kan, in the form of two indices [2] for icosahedral QC.

The obtained results have shown that the proposed modeling method can be used to analyze the atomic structure of QC with axes of symmetry of the 8th, 10th and 12th orders. The possibility of variation by numerical parameters in the simulation algorithms (equation above) opens the possibility for a certain description of varieties of quasicrystalline structures.

References

[1] Steurer W, Deloudi S 2009 *Crystallography of Quasicrystals: Concepts, Methods, and Structures* Springer-Verlag, Berlin, 384

[2] Cahn J W, Shechtman D, Gratias D 1986 *J. Mater. Res.* **1** 30

Laser Fusion of Zr-Nb-Alloys in Different Gas Environments

V. V. Girzhon, O. V. Smolyakov, T. Dmytrenko

Zaporizhzhia National University
Zhukovsky 66, 69063 Zaporizhzhia, Ukraine

The interest in Zr-Nb-alloys is, first of all, due to their widespread use in reactor construction. At the same time, alloys of the Zr-Nb system are an interesting object for fundamental research, since they are characterized by a number of features in equilibrium transformations: congruent melting, polymorphic transformation, monotectoid decomposition, concentration layering. The evolution of the structure of these alloys with different types of thermal action on them may have different effects on the service characteristics of products. Therefore, the purpose of this work is to study the structural changes in the surface layers of the Zr-Nb alloy in highly equilibrium conditions, which are achieved by pulsed laser melting in different gas environments.

Samples of zirconium alloy E125 containing 2.5 wt.% of niobium, 10×10 mm in size, cut from a sheet 3 mm in thickness, were selected for the object of investigations.

Laser melting (LM) was carried out in argon, nitrogen and air atmospheres using a pulsed YAG laser ($\lambda = 1.06$ nm) with 30% overlapping of laser spots. The laser melting zone (LMZ) depth was about 200 microns. The sample surface layer phase composition after the LM was controlled by X-ray diffraction. The microhardness was measured with a PMT-3 device.

According to the results of the X-ray phase analysis, the samples studied in the initial state were single-phase. Due to the insignificant content of niobium in the original eutectic, reflections from the lattice of niobium were not detected.

The X-ray studies of the samples processed in the atmosphere of argon showed that there was only one α-phase in the alloy, the lattice parameters of which were slightly lower compared to its parameters in the initial state. At the same time, the LMZ structure was no longer a mixture of Zr + eutectic Zr-Nb. High (~ 104 K/s) melt cooling rates resulted in the formation of a supersaturated solid solution of niobium in zirconium. And since the atomic radius of niobium is smaller than the atomic radius of zirconium, the lattice parameters of the α-solid solution (α-phase) decreased.

After laser surface treatment in the air atmosphere, four phases were observed in the structure of the surface layers of the alloy: α-solid solution, ZrN nitride and two ZrO_2-type oxides with different types of lattice-high-temperature cubic and low-temperature monoclinic, which is associated with different concentration-time conditions of structure formation at various points of the LMZ. Due to the formation of a complex solid solution, the lattice parameters of the α-phase were slightly higher than in the initial state.

Laser treatment in the nitrogen atmosphere allowed finding the reflections from the α-phase lattice and ZrN cubic nitride. In this case, the parameters of the α-phase

lattice turned out to be higher than after the LM in the air atmosphere, which may be due to larger sizes of nitrogen atoms introduced in the face-centered close-packed-lattice, in comparison with the size of the oxygen atoms.

The absence of the β-phase after LM in different atmospheres may be due to several reasons. First, the cooling rates of the melt in the LM were insufficient to fix the β-phase at room temperature and could contribute to the martensitic nature of the $\beta \rightarrow \alpha$ transformation. Secondly, although the niobium contained in the alloy refers to β-stabilizers, its insignificant content in the α-solid solution has no significant effect on the transition temperature. On the other hand, the introduction of nitrogen (oxygen) atoms in the α-solid solution could increase the temperature of the polymorphic $\beta \rightarrow \alpha$ transformation, *i.e.*, the introduced nitrogen and oxygen atoms could act as stabilizers of the α-phase.

Measurement of the microhardness of the surface of the samples after the LM showed that the maximum microhardness (4.7 GPa) was achieved after the LM in the atmosphere of nitrogen. The microhardness of the surfaces, both after treatment in the argon atmosphere and after treatment in the air atmosphere, was low, and amounted to 3.6 GPa and 3.7 GPa, respectively. The initial microhardness of the alloy did not exceed 2.4 GPa.

Features of Structural State of Magnetron Coating of High-Entropy FeCoNiCrMn Alloy

V. F. Gorban[1], M. V. Karpets[1], O. V. Kantsyr[2], T. V. Homko[1]

[1] *Frantsevich Institute for Problems of Materials Science of NASU*
Kryzhanovsky 3, 03680 Kyiv, Ukraine

[2] *National Technical University of Ukraine "Igor Sikorsky Kyiv Politechnic Institute"*
Kyiv, Ukraine

A target (rectangular form, 20×60 mm) was made from the ingot of the equiatomic FeCoNiCrMn alloy smelted with argon-arc melt in an atmosphere of high purity argon in order to obtain magnetron coatings by mechanical means. After that the ingot was sprayed, then it was cut into three equal parts 20 mm in length, in order to determine the phase composition and mechanical characteristics in each of these particles. The crystal coating characteristics were studied by full-profile analysis of the diffraction patterns (DRON-UM1, monochromatic Cu-K_α radiation) with use of the complex PowderCell 2.4 program.

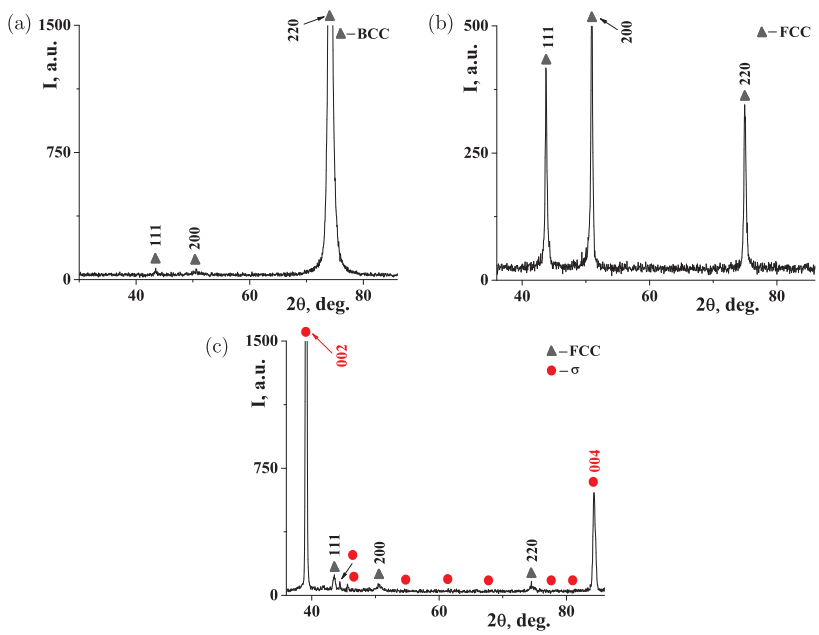

Figure 1: FeCoNiCrMn HEA coatings on steel X18N9T from different parts of the sample: (a) beam center, (b) beam middle, (c) beam edge

The initial phase composition of the target structure is a solid solution on the basis of a phase with an FCC lattice with the lattice period $a = 0.3617$ nm. The spraying of this alloy in vacuum resulted in a decrease in the period of the FCC lattice in the coating compared with the cast state. The phase with the FCC lattice is characteristic for the first part of the coating (beam center), the lattice period $a = 0.3618$ nm has a clearly expressed texture along the direction [220], the texture coefficient $\tau = 0.12$ (Figure 1a), the 2$^{\text{nd}}$ part of the coating (beam middle) also has a phase with the FCC lattice with the lattice period $a = 0.3577$ nm, it has a slight structure along the direction [200], the texture coefficient $\tau = 0.79$ (Figure 1b), the third part of the coating (beam edge) has a basic phase σ with the lattice periods $a = 0.88777$ nm, $c = 0.4584$ nm, textured along the direction [002], the texture coefficient $\tau = 0.17$, and the phase traces from the FCC lattice, the lattice period $a = 0.3594$ nm (Figure 1c). The decrease in the lattice periods was reflected in the characteristics of the modulus of elasticity and hardness, in the casting state with $E_r = 115$ GPa, $H_{IT} = 2.7$ GPa to $E_r = 194$ GPa, $H_{IT} = 11$ GPa (beam center), $E_r = 169$ GPa, $H_{IT} = 5.5$ GPa (mid-beam) in vacuum. For the 3$^{\text{rd}}$ part of the coating (beam edge), the mechanical characteristics were not taken into account, since the hardness was too low compared with other parts of the coating, which is characteristic of the intermetallic σ-phase.

It was established that the periods of the lattice decreased during the spraying of this alloy which manifested itself in increasing the alloy hardness. This is due to the cluster structure, the alloy nanostructure and the lattice distortion.

Recent developments in Auxetics and Related Systems

J. N. Grima[1,2], K. K. Dudek[1], R. Caruana-Gauci[1], M. C. Grech[1], E. P. Degabriele[1], J. N. Grima-Cornish[2], D. Calleja[1], S. De Vrieze[1], Ch. Mellos[1], P. S. Farrugia[3], R. Gatt[1], D. Attard[1]

[1] *Metamaterials Unit, Faculty of Science, University of Malta Msida MSD 2080, Malta*

[2] *Department of Chemistry, Faculty of Science, University of Malta Msida MSD 2080, Malta*

[3] *Department of Geosciences, Faculty of Science, University of Malta Msida MSD 2080, Malta*

Negative thermomechanical properties such as negative compressibility, negative thermal expansion and auxeticity (*i.e.* negative Poisson's ratio) are properties that can be exhibited at various scales of structure and may arise due to specific features within the system (geometry) deforming via some particular deformation mechanism/s. This work looks at some of the more recent advances made by the authors in these fields.

On Truss-Like Hexagonal Nanonetworks

J. N. Grima-Cornish[1,2], J. N. Grima[1,3], K. E. Evans[2]

[1] *Department of Chemistry, Faculty of Science, University of Malta*
Msida MSD 2080, Malta

[2] *College of Engineering Mathematics and Physical Science, Harrison Building*
University of Exeter
Exeter EX4 4QF, UK

[3] *Metamaterials Unit, Faculty of Science, University of Malta*
Msida MSD 2080, Malta

This paper presents some novel truss-like hexagonal hierarchical nanonetworks made from penta and tetra substituted polyphenlyacetylenes (see Figure 1) which are are modelled using force-field based simulations. These networks are shown to exhibit some interesting properties, including out-of-plane auxetic behaviour at high strains.

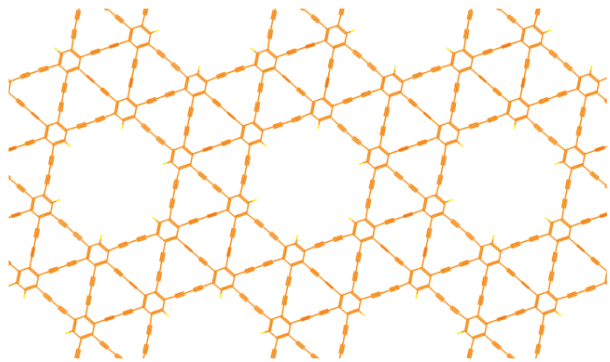

Figure 1: An example of the novel truss-like hexagonal hierarchical nanonetworks being studied

Chaotic Dynamics of the Metabolic Process in a Cell

V. I. Grytsay

Bogolyubov Institute for Theoretical Physics
Metrolohichna 14b, Kyiv 03680, Ukraine

We studied a model of self-oscillatory dynamics of the metabolic process in a cell. The full phase-parametric characteristics of variations of the form of attractors depending on the dissipation of a kinetic membrane potential were calculated. The bifurcations and the scenarios of "order-chaos", "chaos-order" and "order-order" transitions were found. We made projections of multidimensional phase portraits of attractors, Poincaré sections, and Poincaré maps. The process of self-organization of regular attractors was investigated through the torus formation. The total spectra of Lyapunov exponents and the divergences characterizing the structural stability of the determined attractors were calculated.

The obtained results demonstrate the possibility of application of classical tools of nonlinear dynamics to the study of self-organization and appearance of a chaos in the metabolic process in a cell.

Modeling Studies of Grid Connected p-Si Photovoltaic System in Polish Climate Conditions

S. Gulkowski[1], P. Dragan[2]

[1] *Institute of Renewable Energy Engineering, Faculty of Environmental Engineering*
Lublin University of Technology
Nadbystrzycka 38, 20-618 Lublin, Poland

[2] *PhD Studies, Faculty of Environmental Engineering*
Lublin University of Technology
Nadbystrzycka 38, 20-618 Lublin, Poland

The estimation of the power production of a photovoltaic system in dynamically changing environmental conditions is of great importance from the economic perspective in terms of the PV system energy generation. The commercial software available on the market is a perfect tool for designing and forecasting the energy yield of the installations. However, a more detailed analysis of the behavior of PV systems demands combined experimental and simulation studies with the use of more powerful engineering applications such as Matlab. Computational simulations and data analysis carried out using the Matlab software allow investigating the influence of various parameters such as solar radiation or cell temperature on the power generation and thus the energy output of the system.

In this paper a simulation study of a polycrystalline silicon grid connected PV system was shown in terms of the power output estimation for different environmental conditions. The temperature of the modules as well as the solar radiation intensity on the PV module plane were measured with the use of a sensor box commercial. These daily profiles of irradiance and temperature with the sampling period equal to 5 min were introduced into a one-diode model that allows obtaining the I-V electrical characteristics of p-Si modules with a high accuracy in variable conditions. Characteristic parameters of the modules used in the model were taken from the manufacturer's datasheet. As a result of the simulations, daily profiles of the power output for various irradiance and temperature were obtained. The modeling results were validated experimentally by comparison to the output power measurements of a PV commercial system of 17 kWp placed in the same location as the monitoring system. Relative errors were calculated to show the modeling approach effectiveness of predicting the output power generation for a photovoltaic system.

Art, Nature and Information

A. (Andreas) Guskos

Visual Arts Department, Academy of Art in Szczecin
Pl. Orła Białego 2, 70-562 Szczecin, Poland

In my presentation I will showcase art and design in which the artist/designer is not in total control of the process of creation, based on some of my projects and other examples. The approach to the creation process will be in general collecting and/or processing existing objects found in the environment or initiating processes that are producing information and collecting results by some assumed criteria. In the context of these examples I will refer to the notions of *casualty randomness* and it disorder and if/how they can be perceived by the spectator.

The presentation will include my projects: *Some components of nature* (video art), *3D structures in the space of information* (3D art), *Aheilos Region 9* (virtual world art), *You will not enter twice into the same river – today, yesterday, tomorrow. Impression on the variability of form in time* (spatial video installation), *Stones from Greek shores* (found objects), *Iconophagos|Stones* (algorithmic process/computer application).

EPR Study of N-TiO_2 Nanocomposites Subjected to Different Annealing and Rinsing Processes

A. (Aleksander) Guskos[1], N. Guskos[1], G. Zolnierkiewicz[1], J. Typek[1], D. Dolat[2], E. Kusiak-Nejman[2], A. W. Morawski[2]

[1] *Institute of Physics, West Pomeranian University of Technology Al. Piastow 48, 70-311 Szczecin, Poland*

[2] *Institute of Inorganic Chemical Technology and Environmental Engineering West Pomeranian University of Technology Pułaskiego 10, 70-322 Szczecin, Poland*

Nanocrystalline samples of N-TiO_2 annealed at 600°C and 650°C with and without water rinsing were successfully prepared. Electron paramagnetic resonance (EPR) spectra of the obtained samples registered at different temperatures in 4–300 K range were investigated. The recorded EPR spectra of the samples, rinsed and non-rinsed

Table 1: Physicochemical properties of investigated nanocomposites

Sample designation	**Phase composition [%]**		**Average crystallite size [nm]**		**S_{BET} [m^2/g]**
	Anatase (A)	Rutile (R)	Anatase (A)	Rutile (R)	
Amorphous TiO_2	84.7	15.3	9	23	265
TiO_2-600	94.0	6.0	46	98	42
TiO_2-600-R	94.2	5.8	47	86	51
TiO_2-650	94.0	6.0	39	77	62
TiO_2-650-R	93.7	6.3	39	102	55
TiO_2-350[1]	90.0	10.0	10	18	137
TiO_2-350-R[1]	92.0	8.0	8	17	146
TiO_2-400[1]	93.0	7.0	7	23	99
TiO_2-400-R[1]	94.0	6.0	6	25	102
TiO_2-450[1]	94.0	6.0	6	26	79
TiO_2-450-R[1]	93.0	7.0	7	27	82
TiO_2-500[1]	95.0	5.0	5	31	65
TiO_2-500-R[1]	95.0	5.0	5	32	61
TiO_2-300[2]	87.0	13.0	12		201
TiO_2-300-R[2]	88.0	12.0	12		235
TiO_2-350[2]	93.0	7.0	18		137
TiO_2-350-R[2]	93.0	7.0	17		146
TiO_2-100[3]	87.6	12.4	14		306
TiO_2-100-R[3]	87.7	12.3	13		318
TiO_2-200[3]	87.6	12.4	11		256
TiO_2-200-R[3]	89.4	10.6	12		284

with water, showed signals attributed to free radicals, centered between $g_{eff} = 2.0027$ and $g_{eff} = 2.0032$ with linewidths $\Delta H_{pp} = 5$ G and $\Delta H_{pp} = 8$ G at high temperatures. Additionally, resonance lines centered at $g_{eff} = 1.988$ with linewidth $\Delta H_{pp} = 17$ G and $g_{eff} = 1.956$ with linewidth $\Delta H_{pp} = 37$ G were detected in the samples annealed at 600°C but not in the samples annealed at 650°C.Those additional lines could arise from complexes of trivalent titanium ions. The intensities of the EPR lines strongly depended on thermal annealing and water rinsing processes. The concentration of the localized magnetic moments has strong influence on the physical properties of these nanocomposites. Parameters characterizing investigated nanocomposites are listed in Table 1. The sizes of nanocrystallites may have an impact on the type of magnetic defects. The EPR spectrum of the nanocomposites containing small sized nanoparticles is dominated by free radicals and may contain also magnetic agglomerates [1–3]. Nanocomposites containing nanoparticles with specific sizes display in their EPR spectrum complexes with trivalent ions of titanium located on nanoparticles surfaces.

Acknowledgements
This work was supported by the National Science Centre under Project No. DEC-2012/06/A/ST5/00226.

References

[1] Guskos N, Guskos A, Zolnierkiewicz G, Typek J, Berczynski P, Dolat D, Grzmil B, Ohtani B, Morawski A W 2012 *Materials Chemistry and Physics* **136** 889
[2] Guskos N, Typek J, Guskos A, Berczynski P, Dolat D, Grzmil B, Morawski A W 2013 *Central Eur. J Chem.* **11** 1994
[3] Guskos N, Guskos A, Typek J, Berczynski P, Dolat D, Grzmil B, Morawski A W 2012 *Materials Science and Engineering B* **177** 223

Dynamic and Static Magnetic Properties of Four Compounds from $FeVO_4$-$Co_3V_2O_8$ System

N. Guskos[1], G. Zolnierkiewicz[1], M. Pilarska[1], J. Typek[1], P. Berczynski[1], A. Blonska-Tabero[2], C. Aidinis[3]

[1] *Department of Physics, Faculty of Mechanical Engineering and Mechatronics*
West Pomeranian University of Technology
Al. Piastow 48, 70-311 Szczecin, Poland

[2] *Department of Inorganic and Analytical Chemistry*
Faculty of Technology and Chemical Engineering
West Pomeranian University of Technology
Al. Piastow 42, 70-065 Szczecin, Poland

[3] *Department of Electrical Engineering, Ajman University of Science and Technology*
PO Box 346, Ajman UAE

The dynamic and magnetic properties of four $n\mathrm{FeVO_4}/(1-n)\mathrm{Co_3V_2O_8}$ compounds obtained in reactions between $n\mathrm{FeVO_4}$ and $(1-n)\mathrm{Co_3V_2O_8}$ ($n = 0.82$, 0.80, 0.78 and 0.76) were investigated by dc magnetization in ZF and ZFC modes and electron paramagnetic resonance (EPR) spectroscopy. The XRD measurements revealed in all samples a mixture of the howardevansite-type structure (H-type phase) and the lyonsite-type structure (L-type phase). The magnetic susceptibility study showed the Curie-Weiss type behavior (with effective antiferromagnetic interaction) in all compounds in the high-temperature range. At low temperatures a phase transition to the antiferromagnetic state was registered, coexisting with the ferromagnetic behavior evidenced by the hysteresis loop, indicating a highly nonhomogeneous magnetic state of the studied materials. The coercive field and the remanent magnetization increased in composites with higher concentration of the starting $FeVO_4$. The paramagnetic component of the $n\mathrm{FeVO_4}/(1-n)\mathrm{Co_3V_2O_8}$ composites consisted of high-spin iron ions and magnetic agglomerates from coupled magnetic ions. Iron and cobalt ions had the largest contribution to the static magnetization of the investigated samples. The EPR measurements showed mainly asymmetric spectra (decomposed on two components) originating from iron ions and magnetic agglomerates, the former being the dominating one.

EPR Investigation of TiO_2-GO and TiO_2-rGO Nanocomposite Hybrids

N. Guskos[1], G. Zolnierkiewicz[1], J. Typek[1], A. (Aleksander) Guskos[1], E. Kusiak-Nejman[2], A. Wanag[2], J. Kapica-Kozar[2], Ł. Kowalczyk[2], A. W. Morawski[2]

[1] *Institute of Physics, West Pomeranian University of Technology Al. Piastow 48, 70-311 Szczecin, Poland*

[2] *Institute of Inorganic Chemistry and Environment Engineering West Pomeranian University of Technology Pułaskiego 10, 70-322 Szczecin, Poland*

A combination of graphene and semiconductors, especially the titanium dioxide has been intensively studied recently as a promising route to obtain new graphene–TiO_2 nanocomposites with an enhanced charge separation in the electron–transfer. Incorporation of the graphene or graphene oxide into TiO_2 provides a large specific surface area and high charge carrier mobility due to the moving of TiO_2 generated electrons across the graphene 2D–sheets, which minimizes the electron-hole recombination and enhances the oxidative reactivity [1,2].

The purpose of this study is to discuss the magnetic properties of hybrid nanocomposites obtained by the hydrothermal method using different types of graphene related materials (GO or rGO).

Figure 1 presents the electron paramagnetic resonance spectra (EPR) of the TiO_2-H_2O-rGO(5 wt.%)-A hybrid at liquid helium temperature. Hybrids for the EPR anal-

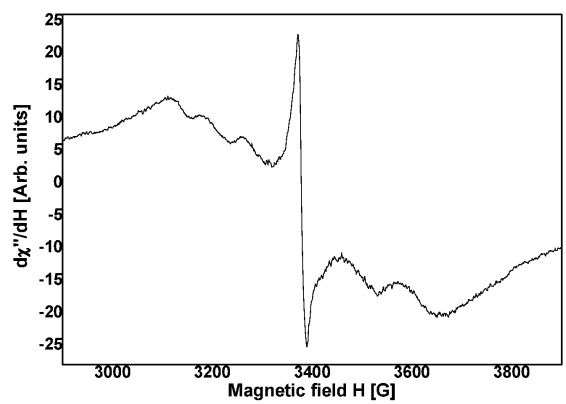

Figure 1: Magnetic resonance spectra of prepared hybrids at 4 K for TiO_2-H_2O-rGO(5 wt.%)-A

ysis were selected on the basis of the most noticeable structural and morphological changes. At low temperature it was possible to observe complicated EPR spectra originating from different magnetic centers. Table 1 shows the effective g-factors of EPR lines which could be due to the Ti^{3+} complexes and other paramagnetic centers [3].

Table 1: g_{eff} parameters for modified hybrid nanocomposites registered at 4 K

Sample code	g_1	g_2	g_3	g_4	g_5	g_6	g_7
TiO_2-ButOH-A	2.144	2.096	1.983	1.973	1.960	1.928	1.874
TiO_2-rGO(5 wt.%)-A	2.147	2.096	–	1.978	–	–	1.871
TiO_2-H_2O-rGO(5 wt.%)-A	2.144	2.096	–	–	–	1.926	1.874
TiO_2-ButOH-rGO(5 wt.%)-A	2.144	2.096	–	1.979	–	1.926	1.874
TiO_2-GO(5 wt.%)-A	2.144	2.096	–	–	–	1.927	1.873
TiO_2-H_2O-GO(5 wt.%)-A	2.144	2.096	–	–	–	1.930	1.871
TiO_2-ButOH-GO(5 wt.%)-A	2.144	2.096	–	–	–	1.926	1.872

The most significant changes after modification can be observed in the intensity of the resonance lines centered at g_{eff} between 2.0034 and 2.0039 [4]. The linewidth ΔH_{pp} varies in the 15 G–17 G range. Ratios of the integrated intensities are as follows: $I_1{:}I_5{:}I_7{:}I_9 = 1.0 : 0.3 : 1.0 : 0.9$ for the rGO-modified samples and $I_1{:}I_{13}{:}I_{15}{:}I_{17} = 1 : 2.0 : 60.0 : 115.0$ for GO-loaded composites. The most intensive increase is observed for the nanocomposite designated as TiO_2-ButOH-GO(5 wt.%)-A, whereas the smallest – for the TiO_2-rGO(5 wt.%)-A hybrid. In this region the GO gives a very narrow resonance line and it is overlapped by more intense resonance spectra [5].

Acknowledgements
This work was supported under the project Maestro 3 No. DEC-2012/06/A/ST5/ 00226 of the National Science Centre (Poland).

References

[1] Lightcap I V, Kosel T H, Kamat P V 2010 *Nano Lett.* **10** 577
[2] Huang Q, Tian S, Zeng D, Wang X, Song W, Li Y et al. 2013 *ACS Catal.* **3** 1477
[3] Guskos N, Glenis S, Zolnierkiewicz G, Guskos A, Typek J, Berczynski P et al. 2014 *J. Alloy Compd.* **606** 32
[4] Tryba B, Tygielska M, Colbeau-Justin C, Kusiak-Nejman E, Kapica-Kozar J, Wróbel R et al. 2016 *Mater. Res. Bull.* **84** 152
[5] Diamantopoulou A, Glenis S, Zolnierkiewicz G, Guskos N, Likodimos V 2017 *J. Appl. Phys.* **121** 34906

Influence of Calcination Temperature on Magnetic Properties of Benzene Modified TiO_2 Nanoparticles

N. Guskos[1], G. Zolnierkiewicz[1], J. Typek[1], E. Pilawska[1], A. (Aleksander) Guskos[1], E. Kusiak-Nejman[2], A. Wanag[2], J. Kapica-Kozar[2], A. W. Morawski[2]

[1] *Institute of Physics, West Pomeranian University of Technology Al. Piastow 48, 70-311 Szczecin, Poland*

[2] *Institute of Inorganic Chemistry and Environment Engineering West Pomeranian University of Technology Pułaskiego 10, 70-322 Szczecin, Poland*

Four TiO_2 samples subjected to modification with benzene vapors at various calcination temperatures (300°C to 450°C, in steps $\Delta T = 50$°C) were investigated [1]. Electron paramagnetic resonance (EPR) measurements as a function temperature were carried out in the 4–290 K range [1]. A strong temperature variation of the EPR integrated intensity was observed for different samples and the maximal value was found for the nanocomposite calcined at 400°C. Additionally, measurements of dc magnetic susceptibility χ as a function of temperature were performed. The complex nature of magnetic interactions in the studied samples was reflected in $\chi(T)$ curves. Both the used magnetic characterization methods showed the occurrence of antiferromagnetic and ferromagnetic interactions, nevertheless dominating in different temperature ranges.

Acknowledgements
This work was supported under the project Maestro 3 No. DEC-2012/06/A/ST5/ 00226 of the National Science Centre (Poland).

References

[1] Guskos N, Zolnierkiewicz G, Typek J, Pilawska E, Guskos S A, Kusiak-Nejman E, Wanag A, Kapica-Kozar J, Morawski A W 2016 *Joint Conferences On Advanced Materials And Technologies, The 13th Workshopon Functional and Nanostructured Materials FNMA'16, and The 7th Workshope on Nanotechnology – PoWieFoNa'16, 26–30 September 2016, Swornegacie, Poland, Abstract book* (p. 77) ISBN 978-83-937979-7-4

Magnetic Properties of nCoO/$(1-n)$ZnO Nanocomposites

N. Guskos[1], G. Zolnierkiewicz[1], J. Typek[1], D. Sibera[2], U. Narkiewicz[2]

[1] *Institute of Physics, Faculty of Mechanical Engineering and Mechatronics*
West Pomeranian University of Technology
Al. Piastow 48, 70-311 Szczecin, Poland

[2] *Institute of Chemical and Environment Engineering, Faculty of Chemical Engineering*
West Pomeranian University of Technology
Pulaskiego 10, 70-322 Szczecin, Poland

nCoO/$(1-n)$ZnO ($n = 0.40$, 0.50, 0.60 and 0.70) nanocomposites were synthesized using a traditional wet chemistry method followed by calcination, a different method than used in [1]. At first, a mixture of cobalt and zinc hydroxides was obtained by addition of a 2M solution of KOH to the 20% solution of a proper amount of $Zn(NO_3)\cdot 6H_2O$ and $Co(NO_3)\cdot 6H_2O$ in water. The obtained hydroxides were filtered, dried and calcined at 600°C for 1 h. The synthesized product was filtered and dried. The morphology of the samples was investigated using a scanning electron microscope (SEM, Hitachi). The phase composition of the samples was determined by X-ray diffraction. The specific surface area of the obtained nanopowders was determined using the Brunauer-Emmett-Teller (BET) method with a Micromeritics Gemini 2360 analyzer. A Micromeritics AccuPyc 1330 helium pycnometer was used to determine the density of powders. The results of the helium density and specific surface area measurements of our samples showed essential differences in comparison to nanocomposites prepared by another method. The XRD spectra revealed the presence of ZnO and $ZnCo_2O_4$ phases. The spinel phase $ZnCo_2O_4$ content increased with increasing the CoO content, while the ZnO content decreased simultaneously.

The magnetic properties of nCoO/$(1-n)$ZnO ($n = 0.4$, 0.5, 0,6 and 0.7) nanocomposites were investigated using dc magnetometry. Table 1 displays the hysteresis loop parameters of these nanocomposites and the data obtained in [1] are shown

Table 1: Hysteresis loop parameters for analyzed samples; the values measured in [1] are in parentheses

Nanocomposite	H_c [Oe]	M_n [emu/gr]	M_s [emu/gr]	$\Delta(1/\chi)/\Delta T$ [Oe gr/emu K]
40%CoO/60%ZnO	10 (30)	0.001 (0.022)	2.98 (13.38)	2088 (327)
50%CoO/50%ZnO	9 (30)	0.004 (0.047)	2.90 (22.05)	1977 (191)
60%CoO/40%ZnO	(80)	0.004 (0.100)	(27.84)	
70%CoO/30%ZnO	7 (100)	(0.120)	9.67 (29.05)	(42)

in parentheses. All the magnetic parameters of the analyzed samples have significantly lower values in comparison to that in [1]. At room temperature the following values are obtained: $\Delta M/\Delta H = 14.2 \times 10^{-5}$ emu/gr Oe (5.7×10^{-5} emu/gr Oe) for $n = 0.40$, $\Delta M/\Delta H = 10 \times 10^{-5}$ emu/gr Oe (107×10^{-5} emu/gr Oe) for $n = 0.5$, $\Delta M/\Delta H = -17 \times 10^{-5}$ emu/gr Oe for $n = 0.6$ and $\Delta M/\Delta H = -16.8 \times 10^{-5}$ emu/gr Oe (120×10^{-5} emu/gr Oe) for $n = 0.7$. Such strong differences of these parameters describing the magnetic properties might result from different sizes of the nanoparticles obtained by different methods and stronger antiferromagnetic interaction in hydrothermal samples.

References

[1] Guskos N, Zolnierkiewicz G, Typek J, Sibera D, Narkiewicz U 2017 *to appear in Rev. Ad. Mat. Sci.*

Investigation of Equilibrium State of Water and Two-Component Gas Mixture of Dry Air and Water Vapor at Phase Separation Surface in Phase Transition Conditions

T. V. Holubets

Department of Physical-Mechanical Fields
Pidstryhach Institute for Applied Problems of Mechanics and Mathematics NAS Ukraine
Naukova 3b, 79060 L'viv, Ukraine

Scientific research of the phase transition properties (evaporation or condensation) between liquid (water) and gas (steam-air mixture) phases is considered in many fundamental works [1,2,3]. A characteristic feature of such dynamic physical processes is the formation of a near-surface layer [4] (boundaries of phase separation) whose properties are rarely investigated by experimental methods [5] and not sufficiently substantiated [6] in terms of the theoretical (mathematical) description of the phenomena under consideration.

The present paper discusses the phenomenological approach for describing the equilibrium state between water and a two-component gas mixture under phase transitions based on the assumption that, over time, under the influence of an external homogeneous stationary temperature field, which is supported by the constant temperature of the thermostat, an open thermodynamic system (water and a two-component or binary gas mixture of dry air and water vapor) comes to a state of thermodynamic steady (stationary) equilibrium. Then, from the point of view of the macroscopic description of evaporation or condensation processes, there is no mechanical displacement (Figure 1) of the phase separation surface (kinetic effect), while according to the microscopic (molecular) description, there is a distortion of the division surface meniscus (capillarity effect), which is associated with the change of the state (molar fraction of water vapor) of the two-component steam-air mixture at the phase separation surface.

A quasi-classical approximation (the equality of chemical potentials in the liquid and gas phases at the phase separation surface) in the approximation of the mixture components (described by the normalized molar masses specified by the author) were used in the macroscopic equation of the state of the fluid interacting through the evaporation (condensation) of the binary steam-air mixture. The equation of the state of a non-ideal (interacting) two-component mixture is obtained in the following differential form

$$\left\{1+\frac{1-\bar{\kappa}}{1+\bar{\kappa}}\frac{\tilde{\delta}_x}{2}\right\}\frac{dP_G}{P_G}=\frac{2\langle\bar{M}\rangle}{RT}\left\{\langle r\rangle+\frac{RT}{\bar{M}_{eff}}\right\}\frac{dT}{T}+d\left[\frac{\langle\bar{M}\rangle}{\bar{M}^*_{eff}}\right]$$

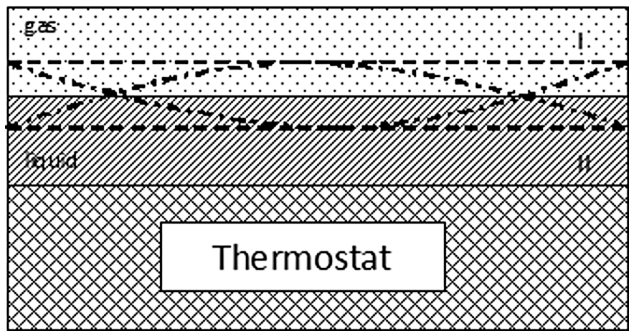

Figure 1: Schematic representation of equilibrium between liquid (I) and gas phases (II) during evaporation and condensation, respectively. Interphase surface movement – dashed lines, meniscus surface distortion – dashed dotted lines

where P_G is the current pressure in the steam-air mixture, T is the thermodynamic temperature, $\tilde{\delta}_x \in \{-2,2\}$ is the deviation of the molar fraction of the component ($x^*_\nu = 1/2(1+\tilde{\delta}_x/2)$ – water vapor and $x^*_a = 1/2(1-\tilde{\delta}_x/2)$ – dry air) from the equilibrium $x^*_\nu = x^*_a = 1/2$ ($\tilde{\delta}_x = 0$) value, $\bar{M}_{eff}$, $\bar{M}^*_{eff}$ and $\langle \bar{M} \rangle$ are the normalized effective, generalized and averaged molar masses of the mixture, respectively, $\bar{\kappa} = \bar{M}_\nu / \bar{M}_a$ is the ratio of normalized molar masses of water vapor $\bar{M}_\nu$ and dry air components $\bar{M}_a$ in the gas phase ($\bar{M}_\nu < \bar{M}_a$) at a mixed state, $\langle r \rangle$ is the latent heat of evaporation, R is the universal gas constant.

The principle of equivalence of mechanical and energy (macroscopic) characteristics of thermodynamic equilibrium on the surface of the phase separation between the liquid and gas phases is formulated. The conditions of the phase equilibrium in the near-surface layer under evaporation and condensation are determined, according to which an equilibrium curve Γ_{eqv} is obtained in the space of intensive (temperature T) and extensive (deviation of the molar fraction of components $\tilde{\delta}_x$ from the equilibrium value) of thermodynamic variables. The relative changes (displacement or fluctuations) of thermodynamic quantities (the increase in the pressure of the gas mixture or the ratio of the molar volumes) in the aforementioned space of thermodynamic variables in a sufficiently wide range of temperature T changes (between a fixed temperature of crystallization T_{Cr1} and boiling T_{Cr2} water) and a typical interval of change x^*_ν and x^*_a in the molar fraction of components relatively to the equilibrium ($\tilde{\delta}_x = 0$) value are shown by the graphical methods.

In the approach $P_G = p_\nu / x^*_\nu$, where $x^*_\nu = (1/2)\left(1+\tilde{\delta}_x/2\right)$, $\tilde{\delta}_x \in (-2,2)$ is the molar fraction of water vapor (neglecting the expansion factor [7]), p_ν is the partial pressure of the water vapor (here $\varphi = p_\nu / p_{\nu s}(T)$ is the relative humidity of air), and $p_{\nu s}(T)$ is the pressure of the saturated water vapor, as the known function [8] of the thermodynamic temperature T, obtained the dependence of the average curvature r the meniscus surface of the phase separation in the studied intervals of temperature variations $T \in (T_{Cr1}, T_{Cr2})$ and linear deviations $\tilde{\delta}_x \in \{-2,2\}$ of the molar particle components relative to the equilibrium value. The change of the maximum (at $T = T_{Cr1}$, when $\tilde{\delta}_x -> 2$ and $T = T_{Cr2}$ when $\tilde{\delta}_x -> -2$) weights of the effects of evaporation and con-

densation according to the ratio of amplitudes or modules of the relative increase in pressure on the surface of the phase separation at various fixed (equilibrium) values of surface temperature T_S under conditions of phase transition is considered.

References

[1] Kandlikar S G 1999 *Handbook of phase change: Boiling and Condensation*, Taylor & Francis, Philadelphia-London, 737
[2] Braut R 1967 *Fazovye perehody*, Mir, Moskva, 288
[3] Patashinskij A Z, Pokrovskij V L 1982 *Fluktuacionnaja teorija fazovyh perehodov*, Nauka, Moskva, 382
[4] Shtrauf E F 1949 *Molekuljarnaja fizika*, Leningrad-Moskva, Gos. izd. tehn.-teor. lit., 576
[5] Ahsan A 2011 *Evaporation, Condensation and Heat Transfer*, Rijeka, InTech, 582 (http://www.intechopen.com)
[6] Morrow N R 1970 *Industrial and Engineering Chemistry* **62** (6) 32-56
[7] http://www.mrc-eng.com/ 2007 *Thermodynamical Properties of Humid Air (Models and Background)*, M. Conde Engineering, Zurich, 22
[8] https://www.ashrae.org/ HandBook 2017, HandBook-Fundamentals

Reference System for Lennard-Jones Fluid

V. Hordiichuk[1], A. Trokhymchuk[1], J. Skvara[2], I. Nezbeda[2]

[1] *Institute for Condensed Matter Physics, National Academy of Sciences of Ukraine*
Svientsitskii 1, 79011 L'viv, Ukraine

[2] *Faculty of Science, J. E. Purkinje University*
400 96 Ústí nad Labem, Czech Republic

Recently it has been shown that thermodynamics as well as vapour-liquid equilibrium in the Lennard-Jones-like hard-core attractive Yukawa fluid can be rather accurately described within the augmented van der Waals theory. Within this theory the original pair interaction is represented as a sum of the short-ranged and long-ranged contributions where the former consists of both the hard-core repulsive and short-range attractive interactions and can be identified as the interaction energy of a target molecule with its nearest neighbour counterpart. The nearest neighbour molecules and the corresponding interaction energy are identified by means of the range (distance) criterion. According to this criterion the short-range interaction energy includes the full repulsion energy and the short-range part only of the full attraction energy, namely, the part that is responsible for the interaction of the target molecule with its nearest neighbour molecule. The long-range interaction energy corresponds to the interaction energy of the target molecule with any other molecule but from outside the first coordination shell. Then, the properties of the system as whole are the sum of two terms: (i) the corresponding properties of the system with short-ranged interaction, that is well suited to be evaluated from computer simulations, and (ii) the van der Waals correction term that can be evaluated analytically. In the present study this idea is discussed with respect to the Lennard-Jones interaction model that is most popular to describe real systems.

Photooxidation Effect on β-FeOOH Electrode in Aqueous KOH Electrolyte

A. Hrubiak[1], V. Kotsyubynsky[2], V. Moklyak[1], L. Mokhnatska[2], P. I. Kolkovsky[2], S. Fedorchenko[2]

[1] *1Institute of Metal Physics, National Academy of Science Ac. Vernadsky Av. 36, 03142 Kiev, Ukraine*

[2] *Vasyl Stefanyk Precarpathian National University Ivano-Frankivsk, Ukraine*

The problem of photooxidation of water and air pollutants has been the focus of intensive study in the last years. Iron hydroxides have excellent photocatalytic properties with their chemical stability, non-toxicity and a band structure depending on the morphology. Akaganeite (β-FeOOH) with a channel structure parallel to the c-axis, interesting sorption and ion exchange properties is a promising photo-Fenton catalyst in a heterogeneous system. The obtaining of nanostructured β-FeOOH allows combining a rapid charge transfer for carrier collection and a large surface area for increasing the number of reaction sites and enhancement of the photocatalytic performance.

Ultrafine β-FeOOH were synthesized by the sol-gel route combined with hydrothermal treatment. The iron citrate sol was obtained by slowly mixing $Fe(NO_3)_3{\cdot}9H_2O$ and $C_6H_8O_7{\cdot}H_2O$ aqueous solutions (0.4 M molarity) and processed under hydrothermal conditions at 120°C for 20 hours. The obtained materials were amorphous (XRD data). Mössbauer spectroscopy was used for the phase composition determination and magnetic microstructure control. The Mössbauer spectra of the samples consisted of a paramagnetic doublet component corresponding to the resonance absorption by the nucleus of tetrahedral coordinated Fe^{3+} ions in the high-spin state. The paramagnetic part of each spectra consisted of two doublet components with close values of the isomeric shift (about 0.34 mm/s) and different values of the quadrupole splitting (1.05 and 0.71 mm/s), which were close to the β-FeOOH characteristic parameters. The frequency dependences of the complex conductivity had peculiarities typical for disordered semiconductors – weak changes of the conductivity at low frequencies and an increase with the growing frequency. The DC component of conductivity was about $2{\cdot}10^{-8}$ $Om^{-1}{\cdot}m^{-1}$. The direct optical band gap for all materials was close to 2.9 eV and was comparatively higher to the bulk akaganeite ($E_g = 2.1$ eV) as a result of the quantum confinement effect.

The reversible charge accumulation on the surface of the ultrafine β-FeOOH electrode in a 1M KOH aqueous solution was studied. A three-electrode cell included an AgCl-electrode as a reference and a Pt anode. Cyclic voltammograms were measured in dark and under visible light (1000 W/m^2) irradiation (Figure 1). CVs in the dark are characterized by the presence of capacitive peaks associated with the charge accumulation at the electrode/electrolyte interface. The capacitive current

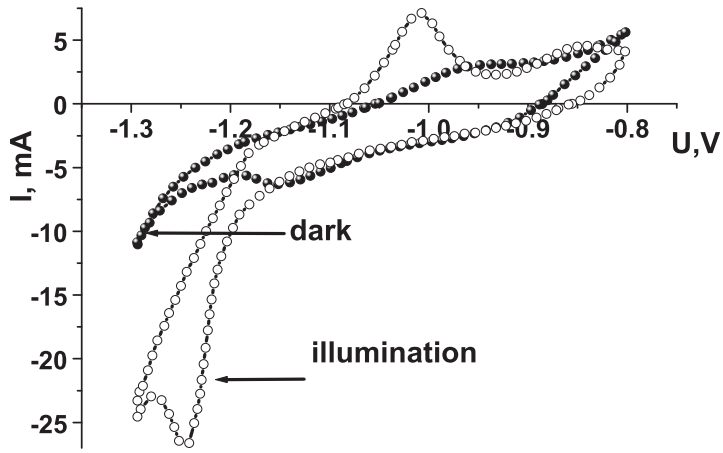

Figure 1: CVA curves for β-FeOOH electrode (scan rate 1 mV/s)

peaks at negative potentials on the anode and cathode branches were attributed to the conduction band filling and/or the exponential distribution of the surface states. The illumination caused a shift of capacitive peaks toward the negative potentials as a result of the space charge layer build-up on the surface of particle agglomerates. Light-induced electrochemical doping causes enlarging of the intrinsic material capacitance as a result of a depletion layer formation at the surface of particles. The presence of a depletion layer would enhance the efficiency of photogenerated electrons and holes separation which is important in photocatalytic applications.

Combined Effect of Thermal Annealing and Laser Irradiation on the Structure and Electrochemical Characteristics of Nano-dispersed TiO_2

R. V. Ilnitskiy, B. K. Ostafiychuk, I. I. Budzulyak, I. M. Lishchynskyy, M. I. Gasyuk

Vasyl Stefanyk Precarpathian National University
Shevchenko 57, Ivano-Frankivsk, Ukraine

A relative high electrical potential of titanium dioxide compared to metallic lithium, as well as the presence of corresponding "guest" positions, low cost and environmental friendliness makes it a perspective cathode material of lithium power sources (LPS). A high specific surface and the resulting large number of "guest" positions are inherent for nano-dispersed TiO_2. Thus, improving TiO_2 as a cathode material requires first of all determining the conditions of modification for which the intercalation lithium ions is most effective in terms of LPS functioning.

We investigated the combined influence of thermal annealing and laser irradiation of the rutile and anatase forms of a nano-dispersed TiO_2 compound in the ratio of 73:27 on the properties of an electrochemical system, formed on their basis [1,2]. Pyrogenic titanium dioxide with the average particle size of 10–60 nm was used for the purposes of the experiment. Titanium dioxide was thermally annealed at the temperatures of 573 K, 773 K, 973 K and 1173 K to improve the precursor material. The powder material annealing duration was set to 1 hour. After thermal annealing the samples were radiated with a laser operating in the modulated quality factor mode (impulse duration $\tau = 15$ ns, impulse energy $E = 0.02$ J, impulse frequency $f = 56$ Hz, duration of sample series irradiation $t = 3.5$ and 7 minutes.)

A set of complementary methods: X-Ray analysis, transmission electron microscopy, porometric analysis, thermal analysis, impedance spectroscopy and a "TIONiT P2.00-xx" device with the "Multicycle 2.0" software were used for testing the lithium power sources for the researched series of samples.

The average sizes of the coherent scattering anatase and rutile zones discovered by the Sherrer method coincided with the average particle sizes of the nanoparticles of related samples which were determined by their TEM images. The TEM also showed that most of the nanoparticles(around 70%) had the average size of 50 nm, while the sizes of the rest of the nanoparticles were roughly 25 nm. After annealing of TiO_2 at the temperatures of 773 K and 1173 K the sizes of nanoparticles increased relatively to 100–120 nm and 140–200 nm.

The X-ray diffractometry of laser irradiated materials showed an increase in the elementary lattice parameters in comparison with the thermally annealed materials and also a phase composition of the material was discovered.

In fact, the increase in the anatase nanoparticle size in the temperature range up to 773 K was not accompanied by a significant change in the structural parameters of the cell. A decrease in the elementary lattice parameters appeared, compared to the samples annealed at 573, 973 and 1173 K after laser irradiation of the series of samples thermally annealed at 773 K for three durations of irradiation.

Sintering of particles was observed depending on the laser irradiation duration, and there was a decrease in the intercalant degree for $t > 5$ min. The possible ways to increase the extent to which the lithium ions entered the cathode material structure were established experimentally using laser irradiation. In this experiment, an increase in the degree of "guest" loading of thermally annealed TiO_2 samples (at 773 K) accompanied the increase of discharge voltage on the surface. Laser irradiation of the material annealed at 973 K and 1173 K resulted in higher discharge pressure of LDS 20%, and reduced the amount of embedded lithium.

References

[1] Myronyuk I F, Ostafiychuk B K, Ilnitskiy R V et al. 2007 *Nanosystems, Nanomaterials, Nanotechnologies* **5** (1/2) 579

[2] Ostafiychuk B K, Ilnitskiy R V, Sehin M I et al. 2009 *Physics and Chemistry of Solid State* **10** (1/4) 773

Carbon Nanostructures and Metal Nanoparticles in Ion-Implanted Polymeric Materials: Possibilities of Positron Annihilation Spectroscopy Studies

T. S. Kavetskyy[1,2], O. Sausa[3], A. L. Stepanov[4,5]

[1] *Drohobych Ivan Franko State Pedagogical University*
I. Franko 24, 82100 Drohobych, Ukraine

[2] *The John Paul II Catholic University of Lublin*
Al. Raclawickie 14, 20-950 Lublin, Poland

[3] *Institute of Physics, Slovak Academy of Sciences*
Dubravska cesta 9, 845 11 Bratislava, Slovak Republic

[4] *Kazan Physical-Technical Institute, Russian Academy of Sciences*
Sibirskiy trakt 10/7, 420029 Kazan, Russian Federation

[5] *Kazan Federal University*
Kremlevskaya 18, 420008 Kazan, Russian Federation

Recent results of positron annihilation spectroscopy studies of carbon nanostructures and metal nanoparticles in ion-implanted polymeric materials exemplified by polymethylmethacrylate (PMMA) nanocomposites formed by boron and silver ion implantation are reviewed. Slow positron beam spectroscopy techniques, such as Doppler broadening of positron annihilation gamma rays as a function of incident positron energy, using a variable-energy slow positron beam, and positron annihilation lifetime at constant positron energy, using a pulsed slow positron beam, were applied to examine the carbonization and metal nanoparticles formation processes in the investigated ion-implanted PMMA nanocomposites. In addition, some important information on the ion-implanted polymeric materials and positronium formation probability in polymers was obtained with a conventional approach by means of low-temperature positron annihilation lifetime spectroscopy.

Efficient Second Harmonic Generation Signal from Chiral Organic Thin Films of 3D Octupolar Bipyrimidine Liquid Crystals

P. Kędziora[1], F. Camerel[2], S. Van Cleuvenbergen[3]

[1] *Institute of Molecular Physics, Polish Academy of Sciences Smoluchowskiego 17, 60-179, Poznań, Poland*

[2] *Institute des Sciences Chimiques de Rennes Université de Rennes 1, 35042 Rennes, France*

[3] *Department of Chemistry, University of Leuven Celestijnenlaan 200D, 3001 Leuven, Belgium*

The design of efficient noncentrosymmetric materials remains the ultimate goal in the field of organic second-order nonlinear optics. Unlike inorganic crystals currently used in second-order nonlinear optical applications, organic materials are an attractive alternative owing to their fast electrooptical response and processability, but their alignment into noncentrosymmetric film remains challenging. Here, symmetry breaking by judicious functionalization of 3D organic octupoles allows the emergence of multifunctional liquid crystalline chromophores which can easily be processed into large, flexible, thin, and self-oriented films with second harmonic generation responses competitive to the rototypical inorganic KH_2PO_4 crystals. The liquid-crystalline nature of these chiral organic films also permits the modulation of the nonlinear optical properties owing to the sensitivity of the supramolecular organization to temperature, leading to the development of tunable macroscopic materials.

Nanoparticles of Noble Metals as Efficient Peroxidase-Like Artificial Enzymes (Nanozymes) for Amperometric Biosensor on Primary Alcohols

H. Klepach[1,2], N. Stasyuk[2], G. Gayda[2], R. Serkiz[2,3], M. Gonchar[2]

[1] *Drohobych Ivan Franko State Pedagogical University*
Shevchenko 23, 82100 Drohobych, L'viv region, Ukraine

[2] *Institute of Cell Biology, National Academy of Sciences of Ukraine*
Drahomanov 14/16, 79005 L'viv, Ukraine

[3] *Ivan Franko National University of Lviv, Department of Solid State Physic*
Drahomanov 50, 79005 L'viv, Ukraine

Recent advances in nanotechnology have enabled the exploration of metallic nanocomposites for diverse applications, especially, for the development of amperometric biosensors. Some nanoparticles (NPs) of noble metals have been shown to be effective chemo-sensing catalysts on hydrogen peroxide, a final product of enzymatic oxidation of different substrates by correspondent oxidases. Such metallic NPs, as artificial peroxidase-like enzymes (nanozymes), may be promising platforms for fabrication of oxidase-based amperometric biosensors.

The aim of the current research is to construct an effective and cheap mono-enzyme biosensor on primary alcohols using yeast alcohol oxidase (AO) and selected, most effective nanozymes.

A number of metallic NPs were synthesized on the surface of a carbon electrode by electrochemical polymerization and characterized. The most electro-active bi-metallic chemo-sensor on H_2O_2 was chosen to be coupled with AO for analysis of primary alcohols. The developed biosensor exhibits a high sensitivity (357 ± 35 $A^{-1} \cdot M^{-1} \cdot m^{-2}$), a broad linear range (from 10 μM to 250 μM), a good selectivity toward ethanol and methanol, as well as a satisfactory storage stability.

The constructed biosensor was used for an ethanol assay in samples of wines and yoghurts. A high correlation of the obtained results and the values, declared by manufacturer, was demonstrated.

Acknowledgements
This work was financially supported by NAS of Ukraine ("Sensors for Medical, Environmental, Industrial, and Technological Needs" Program, Project 5/3–2017), by the Ministry of Education and Science of Ukraine (Project #0116U004737), and by the Fellowship of the President of Ukraine for Young Scientists in 2016–2017 (N. Stasyuk).

Interfacial Interaction in Elastically-Plastically Deformed Single Crystals of Semiconductors

B. P. Koman

Ivan Franko National University of Lviv, Faculty of Electronics and Computer Technologies
Dragomanova 50, Lviv, 79005, Ukraine

Modern investigations of plasticity carried out on the example of Si, Ge NaCl crystals have shown that deformation of crystals is accompanied by intensive dissipation of energy on all structural levels with the forming of local deformation-fragmented structures. They are divided by dislocation boundaries and have substantially different physico-mechanical properties [1,2]. However, their contribution to the deformation process has been not established until now. In addition, the conducted studies have not provided sufficient information about the peculiarities of the behavior of surface layers at different scale levels of deformation, what is an especially topical issue for structures of micro-and nanoelectronics. The aim of this paper is to establish to role of interfacial interactions with the participation of deformation fragments in the formation of an elastic-plastic state in semiconductor crystals at different structural levels of their deformation as well as in the transformation of the defect-impurity structure of the surface layers. The objects for the research were intrinsically defective crystals CdTe, HgTe and their solid solutions $Cd_xHg_{1-x}Te$ of the semiconductor composition ($x = 0,16$–$0,22$) grown by the Bridgman method and solid state recrystallization as well as Si, Ge, NaCl crystals grown by the Czochralski and Stockbarger methods. Deformation measurements were carried on a Regel-Dubov relaxometer with registration of "stress – strain" loading curves (σ – ε). The deformation of the samples ($2 \times 2 \times 6$ mm^3) was performed along the longer edge at a constant rate.

Analysis of the plastic deformation of crystals on the basis of a representation of dissipative structures allows us to understand some features of the macrofluidity of solids that do not find justification in the mechanics of deformed solids and exclusively in the deformation dislocation concept. The role of the near-surface layer of uniaxially deformed crystals during their deformation is studied. Forming of a "debris" – layer which serves as a barrier to dislocations generated by "bulk" sources under subsequent loading of the crystal at the pseudoelastic stage of deformation of CdHgTe crystals is revealed. It is found out that the deformation of CdHgTe crystals, along with the translational dislocation slipping, is accompanied by the rotational component of the lattice strain and the emergence of new structural elements of the strain which independently take part in the deformation process. New types of dissipative structures which ensure the most efficient dissipation of elastic energy at this stage of deformation of the crystal are revealed. The role of interfacial interactions in the formation of the elastic-plastic state of single crystals of semiconductors is clarified. The phenomenon of deformation-induced interfacial interaction which is realized in

the crystals uniaxially deformed at a constant speed is revealed: (1) at the pseudoelastic stage of the loading diagram as a result of the interfacial interaction between the "debris" –layer and the crystal volume; (2) at the stage of strain hardening – between deformation fragments with different moduli (E_1 ... E_N) which arise in the deformed crystal. The loading process of a crystal at the stage (L_2) of strain hardening in the diagram $\sigma(\varepsilon)$ is accompanied by the dislocation structure transformation in the fragmented form and by the internal interfacial interaction that quantitatively describes the energy parameters: $\sigma_h(\mathrm{CdHgTe}) = 0{,}493$ N/m, $\gamma_h(\mathrm{CdHgTe}) = 0.493$ J/m^2. A correlation of the "coefficient of strain hardening – interfacial tension" between the deformation fragments in the crystal volume is found.

References

[1] Alekhin V P 1983 *Physics of strength and plasticity of surface layer materials*, Moscow, Nauka

[2] Panin V E, Grinyaev Yu, Danilov V I 1990 *Structural levels of plasticity deformation and fracture*, Novosibirsk, Nauka (in Russian)

Generalized Diffusion Equation with Fractional Derivatives within Renyi Statistics

P. Kostrobij[1], B. Markovych[1], O. Viznovych[1], M. Tokarchuk[1,2]

[1] *Lviv Polytechnic National University*
Bandera 12, 79013 L'viv, Ukraine

[2] *Institute for Condensed Matter Physics, National Academy of Sciences of Ukraine*
Svientsitskii 1, 79011 L'viv, Ukraine

In the present work, we consider a way of obtaining a generalized (non-Markovian) diffusion equation with fractional derivatives by using the Zubarev nonequilibrium statistical operator method [1] and the maximum entropy principle for the Renyi entropy. The use of the Liouville equation with fractional derivatives proposed by Tarasov in [2] is an important and fundamental step for obtaining this equation. By using the Zubarev nonequilibrium statistical operator method and the maximum entropy principle for the Renyi entropy, we found a solution of the Liouville equation with fractional derivatives at a selected set of observed variables. We chose nonequilibrium average values of particle density as a parameter of reduced description, and then we received a generalized (non-Markovian) diffusion equation with fractional derivatives [3].

References

[1] Markiv B B, Tokarchuk R M, Kostrobij P P, Tokarchuk M V 2011 *Physica A: Statistical Mechanics and its Applications* **390** (5) 785
[2] Tarasov V E 2004 *Chaos* **14** (1) 123
[3] Kostrobij P, Markovych B, Viznovych O, Tokarchuk M 2016 *J Math. Phys.* **57** (9) 093301

Effect of Coulomb Interaction on Chemical Potential of Metal Film

P. Kostrobij, B. Markovych

Department of Applied Mathematics
Institute of Applied Mathematics and Fundamental Sciences
Lviv Polytechnic National University
Bandera 12, 79013 L'viv, Ukraine

The rapid development of nanotechnology involving processes of metal deposition on various substrates requires a theoretical analysis and understanding of electronic effects in nanoclusters and nanofilms. If the size of the nanostructure is comparable with the corresponding Fermi wavelength of electrons in the nanostructure, various physical properties may strongly depend on the size of this nanostructure. This phenomenon is called the quantum size effect [1] and is typical for many physical quantities of metal nanofilms, such as thermodynamic stability, electrical resistivity, work function, surface energy, etc. [2]. Due to possible differences in the properties of metal nanostructures from the properties of the bulk metal,the research of such properties is of considerable theoretical and experimental interest.

The first theoretical calculations of the chemical potential of the metal film within the jellium model without taking into account the Coulomb interaction between electrons are presented in [3,4,5]. However, as it is shown in [6,7], these calculations do not take into account the condition of electroneutrality and therefore the calculated values of the chemical potential are not correct.

In the present work, the metal film within the jellium model taking into account the Coulomb interactions between electrons is studied. The surface potential is modeled by the infinite rectangular potential well. In the limit of low temperatures, calculations of the chemical potential and the distance between the side of the film and the potential wall of an infinite height are performed for different values of the Wigner-Seitz radius. The chemical potential is found as a solution of the nonlinear equation which is obtained in [8] by using the functional integration method. The dependences of the calculated quantities on the film thickness are studied. It is shown that taking into account the Coulomb interaction between electrons leads to a significant decrease in the chemical potential and an increase in the distance between a side of the film and the infinite potential wall, and to an increase in the amplitudes of its oscillations, *i.e.* to an enhancement of the quantum size effect. It is shown that if the film thickness increases, the chemical potential of the film tends to the bulk chemical potential, *i.e.* to the chemical potential of the unbounded metal within the jellium model, and the distance tends to magnitude, which is obtained in [8] for the semi-infinite jellium.

References

[1] Cohen M L, Knight W D 1990 *Phys. Today* **43** 42

[2] Han Y, Liu D J 2009 *Phys. Rev.* **B 80** 155404
[3] Thompson C, Blatt J 1963 *Phys. Lett.* **5** 6
[4] Smith B 1965 *Phys. Lett.* **18** 210
[5] Paskin A, Singh A D 1965 *Phys. Rev.* **140** A1965
[6] Stratton R 1965 *Phys. Lett.* **19** 556
[7] Schulte F K 1977 *Physica Status Solidi (b)* **79** 149
[8] Kostrobij P P, Markovych B M 2015 *Phys. Rev.* **B 92** 075441

Carbon Monoxide Oxidation on Catalyst Surface: Modeling and Stability

P. Kostrobij, I. Ryzha

Department of Applied Mathematics
Institute of Applied Mathematics and Fundamental Sciences
Lviv Polytechnic National University
Bandera 12, 79013 L'viv, Ukraine

A two-dimensional mathematical model of carbon monoxide (CO) oxidation is investigated for the Langmuir-Hinshelwood mechanism [1] on the surface of a Platinum (Pt) catalyst. The adsorbate-driven $(1 \times 2) - (1 \times 1)$ structural phase transition of Pt(110) [2,3] is taken into account. The stability analysis of model solutions is carried out. It is shown that the spatio-temporal periodic chemical oscillations of the CO and the oxygen (O) surface coverage and a fraction of the surface in the non-reconstructed (1×1)-state occur in a narrow region of the phase diagram between two homogeneous steady states of high and low catalytic activity.

References

[1] Baxter R J, Hu P 2002 *J. Chem. Phys.* **116** (11) 4379
[2] Kellogg G L 1985 *Phys. Rev. Lett.* **55** (20) 2168
[3] Gritsch T, Coulman D, Behm R J, Ertl G 1989 *Phys. Rev. Lett.* **63** (10) 1086

Spectroscopic and Ellipsometric Studies of Photo- and Thermal Changes in Chalcogenide Glasses and Their Thin Films

M. Kozak[1], V. Zhickarev[1], V. Loya[2]

[1] *Department of Physics, Uzhgorod National University*
Voloshyna 54, 88000 Uzhgorod, Ukraine

[2] *Institute of Electron Physics, National Academy of Science of Ukraine*
Universitetska 21, 88000 Uzhgorod, Ukraine

The investigations of the optical properties of chalcogenide glasses and thin films based on them have their own peculiarities. For example, in the group of classical semiconductors they are distinguished by high thermal- and photosensitivity. On the one hand, photosensitivity makes them a material for optical recording of information. On the other hand, they change their optical characteristics in the process when investigated by the method of transmission spectroscopy. It turns out that the system behaves nonlinearly, which poses fundamentally new problems in optics. Unfortunately, there is no application for chalcogenide glasses regarding the high temperature sensitivity. On the contrary, they have a disadvantage as an irreplaceable material for IR optics in this respect.

This fact also stimulates research that is of a technological and materials science nature. Such studies should result in the production of a material with specified optical parameters and at a given temperature. It follows that the study of the optical properties of chalcogenide glasses at the photo-and thermal impact is significant [1,2].

We investigate chalcogenide glasses of various types and compositions, for example, As(Ge)-S(Se)-I(X) systems, which were prepared in our laboratory, as well as industrial high-purity glasses of IKS-# brands.

The material is illustrated by a variety of graphical representations. Some of them are given in this abstract. 1. Ellipsometry (Figures 1 and 2), 2. Transmission spectroscopy (Figure 3).

Moreover, the reflectance spectroscopy results will be presented. The latter area of investigations has been chosen recently. Here new theoretical results are obtained. They concern the processing of reflection spectra based on the Kramers-Kronig relationships. The Robinson-Yahoda equation is solved using a developed computer program. The investigations made it possible to obtain the optical characteristics of many glasses for which the reflection spectra were known. Numerous graphic illustrations on this item will be presented in the report.

References

[1] Kozak M, Zhickarev V, Studenyak I, Sejkovskij I 2006 *Opt. and Spectr.* **101** 604
[2] Kozak M, Loya V, Holub N, Onysko M 2009 *Theor. Exper. Chem.* **45** 59

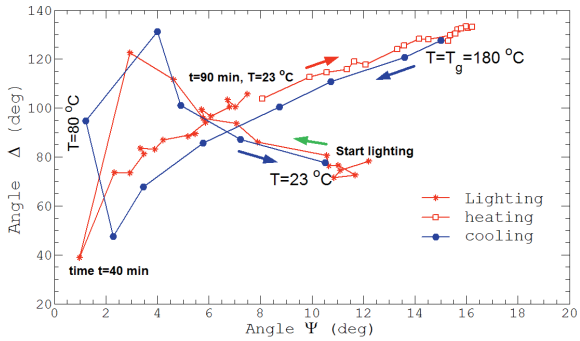

Figure 1: Evolution of ellipsometric parameters under photo- and thermal-transitions in As_2S_3 thin film with a thickness $d = 2$ μm

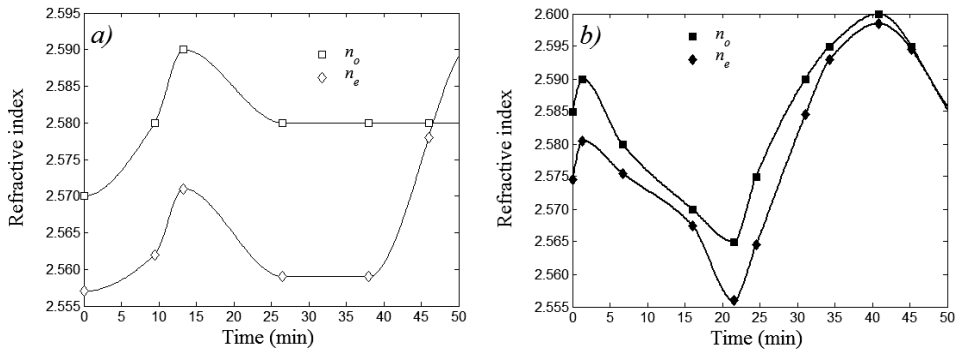

Figure 2: Kinetics of photodarkening and photobleaching under the influence of laser radiation (wavelenght about 465 nm) of the same thin film on a silicon substrate from ellipsometric measuements and calculation in an anisotropic film model: (a) fresh film; (b) thermally annealed film

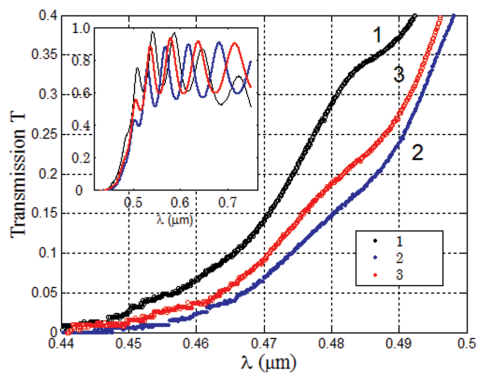

Figure 3: The transmission spectra of As_2S_3 film 2.15 μm-thick on fused quartz substrate: 1 – the fresh film, 2 – film after exposure, 3 – lighted film after heating to 170°C and cooling in air

Temperature Dependence of Short Range Order and Kinetics of Nanocrystalization in $Al_{86}Ni_{8-x}Co_xGd_6$ ($x = 0$; 2 at.%) Amorphous Alloys

Yu. Kulyk, S. Mudry

Physics of Metals Department, Ivan Franko National University of Lviv
Kyrylo i Mephodiy 8, 79005 L'viv, Ukraine

Nanocomposite materials attract the attention of researchers due to the unique properties which allow their wide application in various areas of engineering and technology. Al-based alloys occupy a central position among the family of such alloys owing to the low density, high electrical conductivity, good corrosive resistance and other properties. During the last decade growing interest in Al-Ni-REM alloys (REM-rare earth element) has been observed. Alloys with Y, La, Dy and Gd, containing 80–90 at.% Al, 5–10 Ni, 5–10 REM have been most promising for application. Fist of all it is due to the good mechanical properties of these alloys, it is particularly their yield strength which reaches 1.0-1.6 GPa that allows using them in the industry.

We investigated the short range order structure and nanocrystalization kinetics of an $Al_{86}Ni_{8-x}Co_xGd_6$ ($x = 0$; 2 at.%) amorphous alloy within a wide temperature range by means of the high temperature X-ray diffraction method. The main parameters of the short range order were estimated from the diffraction data and the variation of these parameters with heating was analyzed.

It was shown that the main feature of the structure was the formation of the medium range order due to the proffered interaction of Al and Gd atoms. Nonmonotonic behavior of the temperature dependence of relative integral intensity of the pre-peak in the intensity curves was observed which evidenced structure relaxation occurring within the temperature range of 135–1500°C. It was also pointed out that in both alloys the formation of the nanocomposite structure of Al nanocrystals, embedded in a residual amorphous matrix took place at the initial crystallization.

Partial substitution of Ni-atoms by Co-ones leads to an increase in the initial temperature of transformation by $\Delta T = 200$°C. The mean size of Al nanocrystals changes within the range of 5–20 nm over the entire temperature interval of the initial crystallization. The analysis of temperature changes of the size of nanocrystals, their volume fraction and density allowed us to reveal significant retardation of nucleation and growth processes at the finishing stage of transformation that was the evidence of transition from nucleation and the growth process to a diffusive-controlled one for Al nanocrystals. The variation of the phase content on the Co-atoms concentration was revealed by means of X-ray diffraction investigation of completely crystallized alloys.

Density Determination of Liquid Niobium by Means of Ohmic Pulse-Heating for Critical Point Estimation

M. Leitner, G. Pottlacher

Institute of Experimental Physics, Graz University of Technology
Petersgasse 16, 8010 Graz, Austria

Experimental determination of critical point data like critical temperature, critical pressure, critical volume and critical compressibility of high-melting metals such as niobium is very rare due to the outstanding experimental difficulties in reaching the necessary extreme temperature and pressure regimes.

The experimental techniques to achieve such extreme conditions could be diamond anvil devices, two stage gas guns or metal samples hit by explosively accelerated flyers. Electrical pulse-heating under increased pressures would be another choice. This technique heats thin wire samples, 0.5 mm in diameter and 40 mm in length from room temperature to melting and then further to the end of the stable phase, the spinodal line, within several microseconds. When crossing the spinodal line, the sample explodes and reaches the gaseous phase. In our laboratory, pulse-heating experiments can be performed under variation of the ambient pressure from 1 to 5000 bar and allow direct determination of critical point data for low-melting, but not for high-melting metals.

However, the critical point also can be estimated by extrapolating the liquid phase density according to theoretical models [1]. A reasonable prerequisite for the extrapolation is the existence of data that cover as much as possible of the liquid phase and at the same time exhibit small uncertainties. Ohmic pulse-heating was therefore applied to determine the thermal volume expansion, and from that the density of niobium over the entire liquid phase. As a first step, experiments under ambient pressure were performed. The second step will be to perform experiments under high pressure conditions.

During the heating process, shadow images of the expanding sample wire were captured at a frame rate of $4 \cdot 10^5$ fps to monitor the radial expansion as a function of time. Simultaneously, the sample radiance was measured with a pyrometer operating at a mean effective wavelength of 652 nm. To increase the temperature deduction accuracy, spectral emittance in the liquid phase is also taken into account. Due to the high heating rates of about $2 \cdot 10^8$ K/s, longitudinal expansion of the wire is inhibited which implies an increased radial expansion. As a consequence, measuring the temperature dependent radial expansion is sufficient to deduce density as a function of temperature. This is accomplished by evaluating the full widths at half maximum of the cup-shaped intensity profiles that are calculated from each shadow image of the expanding wire. Relating these diameters to the diameter obtained before the pulse-heating start, the temperature dependent volume expansion is calculated. With the help of the known room-temperature density, volume expansion is then converted

into density data. The so-obtained liquid density behavior is compared to existing literature data and provides another independent source of experimental data.

In this work, the newly determined off-critical liquid phase density was in the second step utilized as input data for the niobium critical point estimation. The approach used, heuristically takes into account the crossover from the mean field to the Ising behavior, as well as the non-linearity of the phase diagram diameter.

References

[1] Schröer W, Pottlacher G 2013 *High Temperatures-High Pressures* **43** 201

Phase-Separation in $(GeS_2)_{100-x}Ag_x$, $(Ge_{42}S_{58})_{100-x}Ag_x$ and $(GeS_3)_{100-x}Ag_x$ Glasses

I. M. Lishchynskyy[1], O. M. Voznyak[1], T. Wagner[2], I. G. Kaban[3]

[1] *Faculty of Phycics and Technology, Vasyl Stefanyk Precarpathian National University Shevchenko 57, 76000 Ivano-Frankivsk, Ukraine*

[2] *Department of General and Inorganic Chemistry, Faculty of Chemical Technology University of Pardubice Cs. legii. 565 square, 53210 Pardubice, Czech Republic*

[3] *Leibniz Institute for Solid State and Materials Research Dresden – IFW Dresden, Institute for Complex Materials PO Box 270116, D-01171 Dresden, Germany*

Due to the continuously increasing amounts of digital information with which people are dealing, the demand for memory devices capable of storing, communicating and computing this information is also growing. Currently, flash memories based on a charge storage are widely used and continuously replace hard disc drives. However, flash memories are challenged by a down-scaling problem because of the charge leakage from the storage layer. In this view, alternative memory technologies such as, for example, phase-change memories (PCM), redox conductive-bridge memories (RCBM) and conductive-bridge memories (CBM) have been suggested [1].

The chalcogenide glasses (*e.g.* Ge-S-Ag used for conductive-bridge memories) which are basically semiconductors become superionic conductors upon doping with metal species. Ge-S-Ag glasses are very attractive first of all due to a significantly higher glass transition temperature and consequently better thermal stability compared to the Ge-Se based glasses [2].

Also, Ge-S-Ag glasses are free of toxic elements.

We present the results of investigations of rapidly quenched $(GeS_2)_{100-x}Ag_x$ alloys ($x = 0$, 5, 10, 15, and 20 at.%), $(Ge_{42}S_{58})_{100-x}Ag_x$ and $(GeS_3)_{100-x}Ag_x$ alloys ($x = 0$, 5, 10, 15, 20, and 25 at.%) carried out at the Institute for Complex Materials, IFW Dresden and the Vasyl Stefanyk Precarpathian National University.

The microstructure of the Ge-S-Ag glasses, and particularly phase separation, was studied using a ZEISS (SEM) DSM 982 Gemini Digital Scanning Electron Microscope equipped with a Bruker energy dispersive X-ray spectrometer. The SEM micrographs of the binary GeS_3 and ternary $(GeS_3)_{75}Ag_{25}$ glasses revealed homogenous microstructures, whereas the samples with $x = 5$, 10, 15, 20 at.% were found to be phase separated. The SEM images and the EDX analysis of the $(Ge_{42}S_{58})_{100-x}Ag_x$ samples showed that they were constituted of an amorphous single phase up to $x = 20$ at.%. Ge crystals were detected in the glassy matrix at $x = 25$ at.%. A homogenous single phase glassy state was observed for the binary GeS_2 and ternary $(GeS_2)_{95}Ag_5$ and

$(GeS_2)_{80}Ag_{20}$ quenched alloys. On the other hand, the glasses with 10 and 15 at.% Ag were phase separated.

References

[1] Meena J S, Sze S M, Chand U, Tseng T Y 2014 *Nanoscale Research Letters* **9** 526
[2] Latif M R, Mitkova M, Thompa G, Coleman E 2013 *IEEE Workshop on Microelectronics and Electron Devices*, 12

Electron Tunneling in Intercalated Layered Crystal in External Magnetic Field

B. Lukiyanets, D. Matulka, I. Grygorchak

Department of Applied Physics and Nanomaterials Science
Lviv Polytechnic National University
Bandera 12, 79013 L'viv, Ukraine

It is known that layered crystals are a set of layers with covalent or ionic-covalent interactions within them and a weak, van der Waals, interaction between them.

Such specific interaction, under certain conditions, allows the insertion into the van der Waals gap (intercalation) or the withdrawal from it (deintercalation) of foreign atoms (molecules). The van der Waals gap may be considered as a nanoobject with a high specific surface, suitable for the high-capacity energy storage. Intercalation can significantly change the physical characteristics of layered crystals, and therefore their research is relevant.

We consider an ideal layered crystal with a potential along the normal to its layers (Figure 1). Here an electron behaves like a plane wave with some effective mass. Figure 1b shows the section of a layered crystal with intercalated atoms (black circles) in its van der Waals gap.

A penetrating atom (or molecule) in the van der Waals gap of the layered crystal causes local distortion of its potential, namely both growth and fall. Figure 1c shows local growth of the potential caused by an intercalated atom with some averaged potential outside the intercalated region.

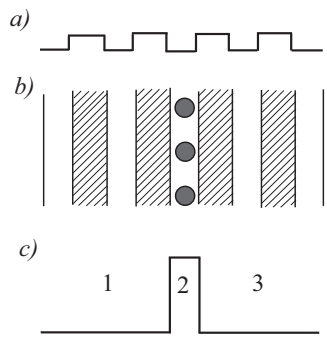

Figure 1: Schematic potential of layered crystals along C-axis – normal to the layers (a) and its section with intercalated atoms (black circles) in van der Waals gap (b); potential with an energy barrier formed by intercalated atoms with some averaged potential outside the intercalated region (c)

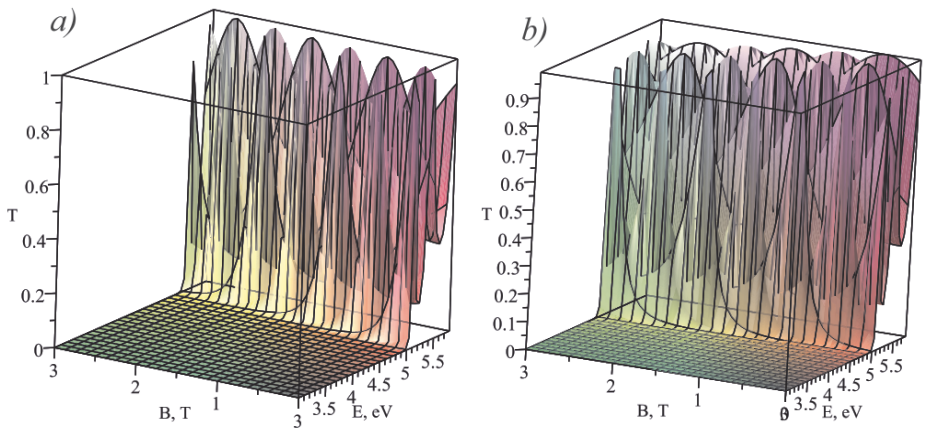

Figure 2: Tunneling probability T of an electron without (a) and with spin rotation (b)

We consider a system with a potential barrier in the constant magnetic field B. Two cases of electron tunneling through the barrier are analyzed: without and with spin rotation (The latter case is possible at antiferromagnetic spin-orbital interaction).

The obtained results of tunneling probability $T(E, B)$ without spin rotation (a) and with spin rotation (b) as function of the magnetic field B and energy of electron are shown in Figure 2. A nonmonotonic character is seen at both fixed magnetic field B and fixed energy.

The results indicate that magnetic field B is an effective means of control of the tunneling probability. In particular, in the case of fixed energy of an electron the tunneling can be controlled by a magnetic field in both cases – with and without electron spin rotation – in passing through the barrier. Moreover, if we consider a sub-barrier electron, its tunneling is practically absent. However, the magnetic field can transfer it into an over-barrier state, where tunneling probability is 1.

Structure and Conductivity Mechanisms of GaSb-GeTe Amorphous Films

N. Yu. Lutsyk, O. G. Mykolaychuk

Physics of Metals Department, Ivan Franko National University of Lviv
Kyrylo i Mephodiy 8, 79005 L'viv, Ukraine

Films of a GaSb-GeTe system with the thickness near 50 nm were prepared using the flash vacuum evaporation method. Ceramic, glass and spalling NaCl monocrystals were served as substrates. The structure, substructure and kinetics of structural transformations depending on the technological conditions of evaporation of thin films of a GaSb-GeTe system were studied by electronography (EG-100) and transmission electron microscopy (UEMB-100K) methods.

The temperature of the substrate supported in a precipitation process of films has a dominant effect on the structure formation of the explored films. As the electronography investigations showed, the films of all the investigated compositions of the GaSb-GeTe system obtained at room temperature were amorphous. The GaSb threefold coordination in the distribution of the proximate atoms is observed in amorphous films. The atoms of Ge are surrounded, on average, by two Ge atoms at a distance of 0.244 nm and two Te atoms at a distance of 0.259 nm, the Te atoms are surrounded by two Te atoms at a distance of 0.259 nm in the amorphous films of GeTe. A continuous decrease in the averaged area at the first coordination maximum determined from the radial distribution curve (from 2.77 units for a-GaSb to 2.44 for a-GeTe), as well as a linear change of the nearest interatom distance (from 0.272 nm for a-GaSb to 0.255 nm for a-GeTe) with the increasing GeTe concentration, witnesses the formation of an alloyed structure in the films of the investigated system.

The electrical conductivity of GaSb films at temperatures above the room temperature is determined by an activation mechanism of conductivity with the activation energy 0.32 eV and at low temperatures it becomes hopping conductivity in localized states around the Fermi level. The density of the localized states at the Fermi level is near $4 \cdot 10^{18}$ $\mathrm{cm}^{-3}\mathrm{eV}^{-1}$. With an increase in the GeTe concentration in the films, the density of the localized states at the Fermi level decreases and the activation conductivity becomes dominated with an increase in the activation energy up to 0.35 eV. With the growing GeTe concentration, the conductivity of the amorphous films measured at room temperatures sharply decreases.

Obtaining of Amorphous-Nanostructure State by Partial Crystallization of Amorphous Alloys Based on Cobalt

V. I. Lysov, T. L. Tsaregradskaya, O. V. Turkov, G. V. Saenko

Taras Shevchenko National University of Kyiv
64/13, Volodymyrska Street, City of Kyiv, 01601 Ukraine

Great attention has been paid to alloys with an amorphous structure associated with the possibility of acquiring specific properties in the amorphous-nanocrystalline state. Amorphous-nanocrystalline alloys are a new class of materials obtained as a result of intensive research of nanotechnology and advanced amorphous and nanocrystalline materials. In terms of physical properties, biphasic amorphous-nanocrystalline materials exceed the properties of both nanocrystalline and amorphous materials, creating a significant synergistic effect. The theory of a high-temperature stability of an amorphous alloy has the following areas of practical application: an increase in the thermal stability of amorphous alloys by heat treatment in the temperature range where crystalline germs can be dissolved in the amorphous phase ($\Delta\mu_i < 0$); and obtaining the amorphous-nanocrystalline state from the initial amorphous state by isothermal annealing at temperatures which will be controlled by the crystal growth of embryos that are ($\Delta\mu_i > 0$) [1]. Based on the analysis of the theory of high thermodynamic stability of amorphous alloys we proposed a method for the amorphous-nanocrystalline state from the initial amorphous state by isothermal annealing at temperatures where the controlled growth froze the crystallization centers ($\Delta\mu_i > 0$). According to the researched object, the selected multicomponent amorphous alloys were based on a basic binary Co-B system. The main characteristic of the thermal stability of amorphous alloys begins in intensive crystallization temperature, which is determined using highly sensitive dilatometer techniques. The table shows the beginning intensive crystallization temperature T_k by initial alloys, the temperature of heat treatment $T_{annealing}$, the part of the crystalline phase X in the samples performed after heat treatment and the relative change of the microhardness between the initial samples and the samples after heat treatment $(H_{an} - H_0)/H_0$.

Amorphous alloy	T_k [°C ±5°C]	$T_{annealing}$ [°C]	X	$((H_{an} - H_0)/H_0) \cdot 100$
$Co_{84}Fe_{5.3}Si_{8.5}B_{2.2}$	519	485	0.30	21.4
$Co_{72.5}Ni_{12}Fe_{5.5}Si_{6.4}B_{3.6}$	551	515	0.29	22.9
$Co_{83.85}Fe_{5.7}Si_{7.85}B_{2.6}$	560	500	0.31	23.7
$Co_{67}Fe_3Cr_3Si_{15}B_{12}$	458	420	0.17	15.7
$Co_{55}Fe_5Ni_{14}Si_{16}B_{10}$	529	500	0.20	14.6

It was established that the part of the crystalline phase in the obtained material was $X = (0.17 \div 0.31)$, while the increase in the microhardness was $(15.7 \div 23.7)\%$

compared to the original amorphous state. This fact can be explained by the growth of frozen crystallization centers in the samples and the formation of the amorphous-nanocrystalline state.

References

[1] Lysov V I, Tsaregradskaya T L, Turkov O V, Saenko G V 2014 *J. Phys. Chem.* **A8** (12) 1981

The Theory of Waves in a Context – My Graphic Art

A. Marcinkowski

Visual Arts Department, Academy of Art in Szczecin
Pl. Orła Białego 2, 70-562 Szczecin, Poland

The paper will present the results of studies on the influence of the theory of waves on my current printmaking. I think that although it has been quite a well-known problem for physicists or mathematicians, artistic creativity is fundamentally new for them. In this paper I will present the contemporary phenomena from the scientific point of view – the cultural influence on the formation of my artistic work. This is a basic problem which has been essential in my recent creative activities.

The target of my research is to show the impact of modern scientific issues relating to radio, television, marine, light waves in the context of my current graphic art.

Materials and Methods: presentation of my recent graphic artwork from the exhibition entitled *Fluctus* and presentation of selected materials presenting pictures of waves. Another element will describe my planned next exhibition under the same title which is to be presented in the Japanese gallery CASO in Osaka in 2017.

The purpose of the paper is to demonstrate that the wave to me is synonymous with the contemporary reality.

Electronic Properties of Nanostructured Heat-Resistant Metals

V. I. Marenkov

Odessa I.J.Mechnikov National University
Dvoryanska 2, 65026 Odesa, Ukraine

Modern nanostructured heat-resistant metals (NHRMs) are used in modern high-temperature technologies aimed at creating sensors for space technology for the study of plasma objects by introducing into their volume foreign nanoscale inclusions that form a multiply connected 3D structure in the bulk of the base metal (BM) [1]. The dynamic equilibrium of the electronic subsystems of the BM matrix and the nanocluster (Nl) results in a redistribution of the effective local carrier density both in the volumes of individual NIs and in BMs, which ultimately changes the effective level of the electrochemical potential of the structure carriers as a whole [2]. The development of the foundations of the theory and calculation of the local Fermi level of carriers in nano-structured heat-resistant metals (NHRM) is one of the topical problems of high-temperature electronics. Typically, the NHRM element is a single-bonded metal matrix with an embedded subsystem of NIs of other materials (metals, high-temperature semiconductors or nanosized warps-fill volume defects in the form of pores of a certain geometry regularly or randomly distributed in the sample). The presence of the NIs-structure embedded in the BM changes its electrophysical properties which are determined by the local redistributed carrier density in the sample volume, that is, in the final analysis, by the averaged level of the electrochemical potential of the carriers and by the parameters of local thermodynamic equilibrium (LTE)). Known methods of accounting for the quantum-size effects in NIs contain many adjustable parameters and, most importantly, assume the Fermi level of F electrons n the sample to be known, which makes it difficult to implement them for the use in applications where F is not a known function [3,4]. At the same time, the local values of F and ts that change "along the volume", due to the action of local electric fields in the sample, are of primary interest for the development of sensitive elements of nano sensors. Within the given "plasma" framework, the electrochemical potential F depends only on the electronic and dielectric constants of BM and NI, and on the concentration and geometric properties of NI subsystem, which are determined from the experiments. This gives new opportunities in the technologies of sensor development with the help of NHRMs.

In the present work the distribution of the local Fermi level for the carriers in the sample volume is proposed for the samples with planar, cylindrical or spherical defects of volume filling (DVFs), based on the proposed statistical plasma approach for the description of electrophysical properties of nanostructured materials. The influence of the determining parameters of nanostructure (electronic and dielectric characteristics of BM, geometry, concentration and size of NI) on the level of electrochemical potential

of carriers and the distribution of local electric fields in the vicinity of DVFs is studied. The main point of the proposed statistical approach is the concept of a statistical cell of the quasi neutrality of the sample – the smallest instantaneous electrically neutral region of the volume of the NHRM isolated by the simply connected element of the surface Π of the extreme of the local self-consistent potential of the system, completely containing the volume of isolated Nl (DFV). Statistical averaging of the local parameters over the ensemble of cells for DPVs gives the effective values of the electronic properties of the sample. For a number of heat-resistant metals: niobium, tantalum, rhenium, etc., containing subsystems of identical DFVs, complex computer calculations of the functional dependences of effective electronic properties in the region of thermodynamic parameters characteristic of applications were carried out. The application of the new results obtained to solve the problems of telediagnosis of heterogeneous plasma formations in the atmosphere and in space is analyzed, based on the general formulas [5].

References

[1] Marenkov V I 2003 *Journal of Molecular Liquid* **05** (2) 299
[2] Marenkov V I 2011 *Nanomaterials: Applications & Properties* (NAP-2011) 82
[3] Marenkov V I 2015 *The Influence Cylindrical Nano Defects Filling Volume on Heat-Resistant Metal Thin Pirns Effectve Electronic Characteristics*. In Bk: *Physics and Nano technology of Thin Films and Nanosystems XV-International Conference* (ICPTTFN-XV). – Conference Proceedings – May 11–16, 2015, Ivano-Frankivsk, Ukraine, 34
[4] Marenkov V I 2017 *Electrochemical Potential of Charge Carriers in Nanostructured Films High-Temperature Metals with a Cylindrical Defects Filling Volume*. In Bk: *Physics and Nanotechnology of Thin Films and Nanosystems. – XVI—International Conference dedicated to memory Professor Dmytro Freik* (ICPTTFN-XV). – Conference Proceedings. – May 15–20, 2017, Ivano-Frankivsk, Ukraine, 50
[5] Marenkov V I 2014 *Ukrainian Journal of Physics* **59** (3) 257

Ultrafine β-FeOOH: Synthesis, Optical and Magnetic Properties

L. Mokhnatska[1], A. Hrubiak[2], V. Kotsyubynsky[1], V. Moklyak[2]

[1] *Faculty of Physics and Technology, Vasyl Stefanyk Precarpathian National University Shevchenko 57, 76025 Ivano-Frankivsk, Ukraine*

[2] *Institute of Metal Physics, National Academy of Science Ac. Vernadsky Av. 36, 03142 Kiev, Ukraine*

Iron oxides and oxyhydroxides, in particular akaganeite β-FeOOH, have been of a great scientific and technological interest due their low cost, being environmentally friendly, good stability as pigments, catalysts, sorbents and ion-exchange materials. The obtaining of ultrafine akaganeite with a significant surface area is an important scientific problem. The particle size and morphology determine the electronic properties of nanodispersed β-FeOOH and specify the successful use of materials. The iron oxyhydroxides β-FeOOH with a tunnel structure and rod-like morphology were synthesized by controlled precipitation. Three systems (F1, F2 and F3) were obtained at a different molar concentration of $FeCl^3{\cdot}6H_2O$ in the initial mixture (0.1 M, 0.37 M and 0.55 M, respectively). All the samples were monophase β-FeOOH (XRD and Mössbauer spectroscopy data). The Mössbauer spectra of all β-FeOOH samples are characterized by the presence of a dominating doublet component which corresponds to absorption by the nucleus of tetrahedral coordinated ions Fe^{3+} in the high-spin state. The formation of a doublet component is a result of size effects and superparamagnetism phenomena. For the spectra obtained at room temperature (293 K) the transition from a magnetically ordered to superparamagnetic state occurred for particles with sizes smaller than 25 nm (spherical approach) due to the comparatively low values of magneto-crystalline anisotropy (about $2.1 \cdot 10^3$ J/m^3). This result is in good agreement with the XRD data about average sizes of CSR. All experimental spectra are a superposition of the two doublets with a close isomeric shift (about 0.35–0.37 mm/s) and different quadrupole splitting (of about 0.6 and 1.1 mm/s). The presence of two doublets can be explained by the difference in near surroundings of ^{57}Fe nuclei located in non-equivalent crystal positions in the inner and outer parts of sintered β-FeOOH particles which form a mesoporous grid [1].

The ratio between relative areas of doublets depends on the molar concentration precursors for all samples and has the minimum value for sample F1. The magnetic component of the Mössbauer spectra is very broad only for sample F1, hence, the average particle size is close to 20–25 nm. This result is confirmed by direct observation by a TEM: sample F1 consists of ellipsoidal agglomerates with about 40×200 nm in size. Agglomerates were observed for sample F3, too. At the same time sample F2 is characterized by separate particles with the average sizes of not more than 30 nm. The specific surface areas for systems F1, F2 and F3 were 138, 143 and 190 m^2/g.

The obtained materials have direct optical band gaps – 2.8, 3.0, 2.7 eV for samples F1, F2 and F3, respectively. Thus, the band gap values for F1, F2 and are higher than for the bulk akaganeite (E_g about 2.0–2.1 eV) as a result of the quantum confinement effect.

The CVA curves of the β-FeOOH electrode (1 M Li_2SO_4 electrolyte, scan rate of 1–20 mV/s, potential window of -0.8–0.0 V vs. Ag/AgCl) consist of redox peaks which corresponds to the surface faradic reactions β-FeOOH+OH^- $\rightarrow$ β-FeOOH+H_2O+e^-. For all systems the specific capacitance decreases with the scan rate increasing which is caused by diffusion of electrolyte ions limiting at high scan rates. The Li^+ diffusion coefficients (calculated from CVA according to [2]) are in the range $2 \cdot 10^{-15}$–$3 \cdot 10^{-13}$ cm^2/s, hence these materials are promising for electrochemical application based on fast reversible redox processes.

References

[1] Kotsyubynsky V, Ostafiychuk B, Moklyak V, Hrubiak A 2015 *Solid State Phenomena* **120** 126

[2] He P, Zhang X, Wang Y, Cheng L, Xia Y 2008 *J. Electrochem. Soc.* **144** 150

Synthesis of a Nanosized Powder with a Perovskite-like Structure ($LaCoO_3$)

M. Mokhnatskyi, I. P. Yaremiy

Faculty of Physics and Technology, Vasyl Stefanyk Precarpathian National University
Shevchenko 57, 76025 Ivano-Frankivsk, Ukraine

Nowadays the basic task of physical material science is developing and searching for new materials and finding new simpler and cheaper methods of synthesizing already known materials. Perovskite-type oxides ABO_3 have been widely used as a heating element, a solid oxide fuel cell interconnector, a catalyst, negative temperature coefficient thermistor materials. Some of those oxides were found to electrochemically repeat the hydrogen charge and discharge in alkaline solutions[1].

A Perovskite-like material was synthesized in two stages. The first stage was a sol-gel method with auto burning and the second stage was annealing. The initial materials for the sol-gel synthesis in the first stage were nitrate crystal hydrates $La(NO_3)_3 \cdot 6H_2O$, $Co(NO_3)_3 \cdot 6H_2O$ and citric acid as complex formation. Reagents dissolved in distilled water and mixed. 10% ammonia solution was then added into the resulting solution to establish the level of pH to 7. The prepared solution dried with access to air in an oven at 140°C for a day. After that the resulting xerogels were heated up to a temperature of 230°C, auto-combustion was activated at this temperature. The structure of the material obtained after auto-combustion was checked by an X-ray diffractometer (Figure 1).

Figure 1 shows that the synthesized material is similar to amorphous. In the second stage amorphous powder was annealed at different temperatures and each annealing

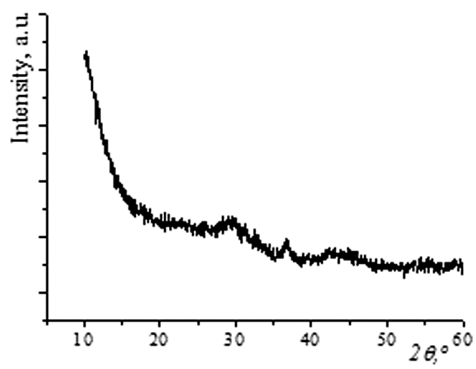

Figure 1: Diffraction of amorphous synthesized perovskite $LaCoO_3$

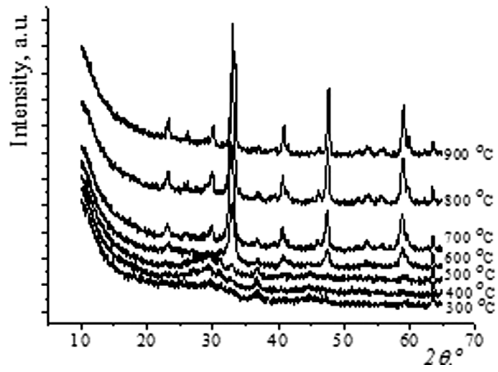

Figure 2: Annealing $LaCoO_3$ with different temperatures

was carried out within 1 hour. Figure 2 shows a change in the diffraction pattern with temperature. A perovskite-like structure $LaCoO_3$ appears at the annealing temperature of 600°C, but this structure is not homogeneous. Homogeneous perovskite-like complex oxide $LaCoO_3$ was obtained at the annealing temperature of 900°C.

References

[1] Song M, Chen Y, Tao M, Wu C, Zhu D, Yang H. 2010 *Electrochimica Acta* **55** (9) 3103

3D Triboelectric Nanogenerator Based on Ferroelectric Powder Internal Motion

A. Molnar[1], D. Gal[1], H. Ban[1], V. Gerasimov[2]

[1] *Department of Physics of Semiconductors, Uzhhorod National University Voloshina 54, Uzhhorod, 88000, Ukraine*

[2] *Faculty of Economics, Management and Engineering, Mukachevo State University Uzhorodskaya 26, Mukachevo, 89600, Ukraine*

The massive development of the world electronic technology follows a general trend of miniaturization, portability and functionality. The development of mobile phones is a typical example of miniaturization, from the transistors based huge-size machine, to solid state MOSFET based handhold cell phones or smart watches with communication functionality. Such small size electronics operates at ultralow power consumption, making it possible to be powered by the energy harvested from our living environment. New technologies that can harvest energy from the environment as sustainable self-sufficient micro power sources are a newly emerging field of nano-energy, which is about the applications of nanomaterials and nanotechnology for harvesting energy for powering micro- or nano-systems. We have mainly utilized two physical effects for harvesting small-magnitude mechanical energies: the piezoelectric effect and the triboelectric effect. Since the former is described quite well in the literature, we will consider here only the second type of transducers [1].

In this work, we demonstrate a combined triboelectric-piezoelectric generator which uses the ferroelectric $Sn_2P_2S_6$ powder as an active material. If triboelectrically or piezoelectrically charged particles can move freely in any direction within suitably placed electrodes, it will be possible for an energy harvester to generate electrical energy regardless of the direction of movement due to its inherent freestanding feature [2].

A generator-cell consists of a cube made of an insulator, opposite inner sides which are coated with nanostructured aluminum or copper electrodes. 20% of the cell contains the $Sn_2P_2S_6$ ferroelectric powder (with the particle size of 50–100 microns). The minimum size is limited by the piezoelectric parameters of the particles. 3 pairs of electrodes are connected to an AC-DC converter, and then to a voltage driver and an energy storage device (battery or supercapacitor). In the presence of external vibrations, powder particles rub against the electrodes. The electric current is generated due to the triboelectric effect. Additional charge on the surface of ferroelectric particles is accumulated thanks to the piezoelectric effect. The correct orientation of polarized particles is realized automatically due to electrostatic interactions with the charged electrodes.

The fluid-like characteristic of the powder removes restrictions on the geometric design of the container. There is a possibility to create generators with various forms:

cube, sphere, cylinder, tube. The size of the device may vary from $5 \times 5 \times 5$ mm^3 (or smaller) to $0.5 \times 0.5 \times 0.5$ m^3 (or bigger).

The main advantages of the proposed generator: waterproof, insensitive to the direction of motion, highly efficient, durable, scalable.

References

[1] Zhonglin W, Long L, Jun Ch, Simiao N, Yunlong Z 2016 *Triboelectric Nanogenerators (Green Energy and Technology)* Springer 517

[2] Daewon K, Yura O, Byeong-Woon H, Seung-Bae J, Sang-Jae P, Yang-Kyu Ch 2016 *ACS Nano* **10** (1) 1017

Thermodynamic Properties of Superionic Phase $Ag_4HgSe_2I_2$ Determined by EMF Method

M. Moroz[1,2], F. Tesfaye[1], M. Prokhorenko[3], O. G. Mykolaychuk[4], O. Reshetnyak[5]

[1] *Johan Gadolin Process Chemistry Centre, Laboratory of Inorganic Chemistry Åbo Akademi University Piispankatu 8, 20500 Turku, Finland*

[2] *Department of Chemistry and Physics National University of Water and Environmental Engineering Soborna 11, 33028 Rivne, Ukraine*

[3] *Department of Cartography and Geospatial Modeling, Lviv Polytechnic National University Bandera 12, 79013 L'viv, Ukraine*

[4] *Department of Metal Physics, Ivan Franko National University of Lviv Kyrylo i Mephodiy 8, 79005 L'viv, Ukraine*

[5] *Department of Physical and Colloid Chemistry, Ivan Franko National University of Lviv Kyrylo i Mephodiy 6, 79005 L'viv, Ukraine*

The overall progress of renewable energy harvesting in materials science is largely associated with the discoveries of new solid-state electrolytes with purely ionic and mixed (ionic-electronic) conductivity. Solid electrolytes are essential components of the new type of batteries, fuel cells, supercapacitors, and functional air pollution sensors [1,2]. The optimization technology of synthesis of new multicomponent inorganic materials, in particular superionic compounds, is impossible without a preliminary analysis of the thermodynamic properties of intermediate phases.

Triangulation of the Ag-Hg-Se-I system in the vicinity of the quaternary phase $Ag_4HgSe_2I_2$ was performed by differential thermal analysis, X-ray diffraction and electromotive force (EMF) methods. The spatial position of the phase region $Ag_4HgSe_2I_2$-Se-HgI_2 regarding the figurative point of silver was used to write the chemical reaction of a formation of $Ag_4HgSe_2I_2$. The EMF measurements were carried out by applying electrochemical cells: (−) C | Ag | Ag_2GeS_3 glass | $Ag_4HgSe_2I_2$, HgI_2, Se | C (+) and (−) C | Ag | Ag_2GeS_3 glass | $Ag_4HgSe_2I_2$ | C (+), where C is graphite and Ag_2GeS_3 glass is the purely Ag^+ ion fast conducting electrolyte. The assembly of the concentration chains and the method of carrying out measurements are described in detail elsewhere [3]. The linear dependencies of the EMF of the electrochemical cells on temperature were used to determine the standard thermodynamic values of $Ag_4HgSe_2I_2$ for the first time:

$$\Delta_f G^\circ_{Ag_4HgSe_2I_2}[\mathrm{kJ\,mol^{-1}}] = -(194.2 \pm 0.2) - (34.8 \pm 0.5) \cdot 10^{-3} T[\mathrm{K}], \quad 298 \le T[\mathrm{K}] \le 410$$

The activity of silver in a quaternary compound was also determined. Furthermore, the superionic properties of $Ag_4HgSe_2I_2$ were characterized.

References

[1] Funke K 2013 *Sci. Technol. Adv. Mater.* **14** 043502 DOI:10.1088/1468-6996/14/4/043502

[2] West A R 2014 *Solid State Chemistry and its Applications*, 2nd Edition, John Wiley & Sons

[3] Moroz M V, Prokhorenko M V, Demchenko P Y, Reshetnyak O V 2017 *J. Chem. Thermodyn.* **106** 228 DOI:10.1016/j.jct.2016.12.004

Structural Aspects of Disorder-Order Transition in Metallic Liquids

S. Mudry

Physics of Metals Department, Ivan Franko National University of Lviv
Kyrylo i Mephodiy 8, 79005 L'viv, Ukraine

It is well known that liquid metallic alloys reveal a short range order in the atomic arrangement contrary to solid ones, whose atoms show a large scale periodicity in distribution. It follows from the results of numerous diffraction studies, measurements of physical properties and computer simulation investigations that the short range order structure is dependent on many thermodynamic parameters, but it is most sensitive to the temperature and composition. In case of binary or more complex alloys the total short range order consists of a topologic short range order and a chemical one. Each of them depends on ordering processes and is related to the thermodynamic characteristics, first of all to entropy, which is a direct measure of the ordering degree. Unfortunately, there are only few works in which the relation between the ordering processes in metallic liquid systems are studied combining the thermodynamic and structure characteristics.

We have investigated liquid metals and metallic binaries with different kind of phase diagrams in which the formation of atomic solutions, eutectic phases, intermetallics or two immiscible phases, coexisting within some temperature and concentration range, occurs. The results of X-ray diffraction studies allowed us to point out a conclusion about the existence of clusters of a different kind, due to which the degree of ordering increases. We compared the values of entropy which were maximal for liquid solutions and minimal for melts with chemically ordered clusters with the parameter of ordering obtained from the diffraction data.

Structure Transformation in $Fe_{73.5}Nb_3Cu_1Si_{15.5}B_7$ Amorphous Alloy Induced by Laser Radiation

Yu. Nykyruy, S. Mudry

Physics of Metals Department, Ivan Franko National University of Lviv
Kyrylo i Mephodiy 8, 79005 L'viv, Ukraine

An amorphous structure is metastable and it transforms into a crystalline structure under heat treatment. Laser irradiation also heats the alloy, but the heating/cooling rate is very high, hence the crystallization process occurs under nonequilibrium conditions that depend on the spatiotemporal and energy parameters of the laser beam. The non- equability may change the crystallization mechanism resulting in the formation of nontypical or even some new phases, especially for a multicomponent alloy. For the time being, the laser induced crystallization process has not been studied sufficiently enough to predict structural changes, and thus the properties of amorphous-crystalline materials. All this determines the aim of our research.

An amorphous $Fe_{73.5}Nb_3Cu_1Si_{15.5}B_7$ alloy was obtained by rapid cooling from a melt in the form of a ribbon with about 25 μm in thickness and about 15 mm in width. The ribbon was irradiated by a laser with a wavelength of 1.06 μm, power – 42 W and a Gaussian distribution of the radiation intensity. During irradiation a sample of the ribbon was placed at a distance from the focal plane of the lens so that the size of the laser spot on the surface of the ribbon was about 10 mm. The duration of the exposure changed within the interval 0.25–0.70 s.

The structure of the irradiated samples was studied using the X-ray diffraction method (XRD) and a DRON-3 diffractometer (Co-K_α radiation, $\lambda = 1.7902$ Å). Phases that crystallize at laser irradiation were determined by defining the position of diffraction peaks. The structural changes of the irradiated surface were studied using a scanning electron microscope.

As a result of laser irradiation of the amorphous alloy $Fe_{73.5}Nb_3Cu_1Si_{15.5}B_7$ by continuous laser irradiation with a power of 42 W and the exposure duration of about 0.55–0.70 sec. a two-component nanocrystalline alloy with α-Fe(Si) and H-hexagonal phases (hexagonal phase, rhombohedral distortion of α-Mn structure) were formed.

Al-Cu-Fe System Alloy Structure Formation at Crystallization

Z. Oliynyk, A. Korolyshyn

Physics of Metals Department, Ivan Franko National University of Lviv
Kyrylo i Mephodiy 8, 79005 L'viv, Ukraine

Intermetallic compounds with a wide homogeneity region, as well as other intermediate phases, are the basis of multicomponent alloys with different functional characteristics, depending on the type of these phases and the nature of the alloying elements. But in order for their use to be as extensive and effective as possible, such systems should be investigated not only in the solid but also in the liquid state. In this plan, the actual issues of the relationship between the specific structure of non-stoichiometric solid alloys and the short range order in the liquid phase and the thermodynamic conditions of their crystallization arise.

The high-temperature X-ray diffraction method was used to study the structure of the melts of a quasi-binary Al_2Cu-Fe system at various temperatures. The structural factors and pair correlation functions were analyzed.

The prepeak (*i.e.* an additional maximum at low values of the diffraction vector) on the curves of the structural factors of the Al_2Cu compound indicates that the structural units in the melt correlate at distances larger than the distances to the nearest neighbors surrounding the atom. Since the short-range order corresponds to the local environment of the atom, the so-called medium-range order corresponds to correlations outside the nearest environment of the atom. The asymmetry of the second maximum of a structural factor is usually associated with the presence of an icosahedral atomic arrangement in the melt.

Experimental structural factors of the melting of the Al_2Cu compound with the addition of 5 to 20 at.% Fe have a precession in the vicinity of 11–21 nm^{-1} and an influx at the second maximum on the right side. Both features of the SF disappear, when heated.

The prepeak on the SF indicates a chemical arrangement in the melt, which correlates with the formation of the phase structure of Al_7Cu_2Fe at temperatures close to the liquidus line.

The asymmetry of the second SF maximum indicates the presence of icosahedral polytetrahedral clusters in the melt, from which the formation of the nuclei of quasicrystals occurs.

Nanoporous Carbon as Electrode Material for Electrochemical Capacitors

B. K. Ostafiychuk, I. I. Budzulyak, B. Rachiy, A. Kachmar, R. Lisovsky, V. Mandzyuk

Faculty of Physics and Technology, Vasyl Stefanyk Precarpathian National University Shevchenko 57, 76025 Ivano-Frankivsk, Ukraine

The problem of the porous structure formation in nanoporous carbonaceous materials (NCM) which are the basis of electrodes of electrochemical capacitors (EC) is still relevant both in scientific and in applied terms. NCM are not only the basis of classical EC, which operates on the principle of charge/discharge of the double electric layer, but they are also practically an integral part of devices of hybrid and pseudocapacitors. The porous structure, formed in the NCM in different ways, determines the possibilities of their application in charge accumulation devices. In particular, the pore size distribution and the surface area are the most important characteristics, without which it is impossible to select one or another electrolyte and to establish the optimal ratio between the internal resistance and the specific capacity of EC [1].

The results of electrochemical studies of NCM as the electrode material for EC have been shown in the work. The NCM were obtained from raw materials of plant origin by carbonization and activation with sodium hydroxide. Carbonated material was activated by sodium hydroxide at a temperature of 600, 700, 800 and 900°C. Carbon was mixed with NaOH and water in the ratio 1:1:1. After activation the material was washed off by hydrochloric acid and hot distilled water to neutral pH.

EC electrodes were formed by pressing the NCM and a conductive additive in the form of lamella on a nickel grid. The formed electrodes were placed in a two-electrode cell with typical size "2525", which was sealed after having been poured with 3 M aqueous KOH as the electrolyte.

The specific capacity characteristics of the obtained EC were studied by galvanostatic cycling at a discharge current of 10–100 mA. The dependence of EC specific capacitance on the thermochemical activation temperature was established on the basis of the analysis of galvanostatic research. It was shown that the NCM activated at 600°C was characterized by a specific capacity of 138 F/g. The activation at 700–800°C allows us to obtain NCM with a capacity of 90–95 F/g. The smallest capacity of 62 F/g is defined for the material activated at 900°C. The capacity value is determined at a discharge current of 50 mA.

An optimal activation temperature (600°C) of the carbon material by sodium hydroxide is established for obtaining NCM with a specific capacity of 140–130 F/g in the range of discharge currents of 10–200 mA.

References

[1] Rachiy B, Budzulyak I, Vashchynsky V, Ivanichok N, Nykoliuk M 2016 *Nanoscale Research Letters* **11** 18

Spectroscopic Properties and Intrinsic Luminescence of Un-Doped Borate Glasses

B. V. Padlyak[1,2], I. I. Kindrat[2]

[1] *Vlokh Institute of Physical Optics, Sector of Spectroscopy*
Dragomanov 23, 79-005 Lviv, Ukraine
[2] *University of Zielona Góra, Institute of Physics*
Division of Spectroscopy of Functional Materials
Szafrana 4a, 65-516 Zielona Góra, Poland

The spectroscopic properties and intrinsic luminescence of un-doped borate glasses with different chemical compositions were investigated using modern spectroscopic equipment and methods including optical absorption, photoluminescence, electron paramagnetic resonance (EPR), and thermally stimulated luminescence (TSL). The un-doped borate glasses with $Li_2B_4O_7$, $LiKB_4O_7$, CaB_4O_7, and $LiCaBO_3$ basic compositions were obtained from corresponding polycrystalline compounds in the air using the technology of borate glasses described in [1].

Three different broad emission bands in the UV – visible spectral range were observed in the un-doped borate glasses under different wavelengths of photoexcitation [2]. The photoluminescence spectra and decay kinetics of the observed emission bands were registered and analysed using the modern time-resolved luminescence technique [3]. The nature and possible mechanisms of intrinsic luminescence in the investigated borate glasses are proposed based on the analysis of the obtained results and the published data.

References

[1] Padlyak B V, Mudry S I, Kulyk Yu O, Drzewiecki A, Adamiv V T, Burak Y V, Teslyuk I M 2012 *Mater. Sci. Poland* **30** 264
[2] Kindrat I I, Padlyak B V, Drzewiecki A 2017 *J. Lumin.* **187** 546
[3] Kubicki A A, Bojarski P, Grinberg M, Sadownik M, Kukliński B 2006 *Opt. Commun.* **263** 275

Physics, Technology and Art

G. J. Papadopoulos

Department of Physics, Solid State Physics Section
National and Kapodistrian University of Athens
Panepistiomiopolis, Zografou, 15784 Athens, Greece

Physics, Technology and Art form three interrelated branches of our civilization, Physics stands at the basis of science which derives from the instinct of curiosity, Art relies on beauty and Technology on survival. Since the conference takes place on the island of Crete where excavation resurfaced a prehistoric civilization, the Minoan, the presentation begins with Archeology and its specialties in common with Physics. Finally, the presentation ends with Science versus Technology.

Electrical Properties of Thin NiO Films Deposited by Spray Pyrolysis

H. P. Parkhomenko, P. D. Maryanchuk

Department of Electronics and Energy Engineering
Yuriy Fedkovych Chernivtsi National University
Kotsyubynsky 2, 58012 Chernivtsi, Ukraine

Thin metal oxide films are of great scientific and practical interest today. Extensive investigations of transparent conducting layers are stimulated by their application in electronics, optoelectronics, and solar energy, as well as by the economic efficiency of using thin films instead of bulk crystals.

Most conducting transparent oxides possess n-type conductivity. However, it is known that nickel oxide (NiO) has p-type conductivity and good optical, electrical and thermoelectric properties, as well as high chemical stability, and is widely used in various devices, especially in the photoelectric technique in the form of transparent layers (windows) for solar cells, antireflection coatings, and photodetectors. Thin NiO films are formed by various chemical and physical methods [1].

Spray pyrolysis is a processing technique considered in the research to prepare thin and thick films, ceramic coatings, and powders. Unlike many other film deposition techniques, spray pyrolysis represents a very simple and relatively cost-effective processing method (especially with regard to the cost of equipment). It offers an extremely easy technique for preparing films of any composition. Spray pyrolysis does not require high-quality substrates or chemicals. The method has been employed for the deposition of dense films, porous films, and for powder production. Even multilayered films can be easily prepared using this versatile technique. Spray pyrolysis has been used for several decades in the glass industry and in solar cell production [2].

Therefore, the aim of the present work was to form thin films by reactive magnetron sputtering and spray pyrolysis and to study their optical and electrical properties.

We used 0.1 M aqueous solutions of nickel chloride $NiCl_2 \cdot 6H_2O$ to deposit thin NiO films by spray pyrolysis. The solution was sprayed on glass substrates by compressed air at a rate of 2.5 mL/min. The temperature of substrates was controlled by a thermocouple system to be ~ 700 K.

We deposited two nickel ohmic contacts on the samples by reactive magnetron sputtering with the use of a mask at a substrate temperature of ~ 373 K to measure the electric resistivity of the samples.

The temperature dependence of the resistivity was measured in the temperature range $T = 300$–420 K. Since the film parameters may vary during these measurements due to irreversible processes, our investigations were performed at both increasing and decreasing temperatures.

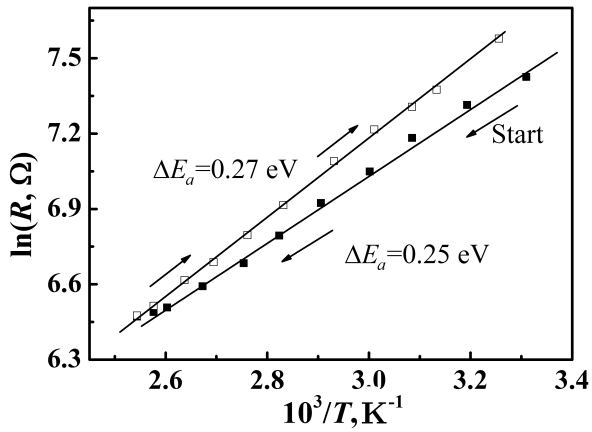

Figure 1: Temperature dependence of resistance of NiO thin films deposited by spray pyrolysis

We determined the activation energies upon increasing ($\Delta E_a = 0.25$ eV) and decreasing ($\Delta E_a = 0.27$ eV) temperatures from the slope of the straight portions of dependences $\ln R = f(10^3/T)$.

References

[1] Parkhomenko H P, Solovan M N, Mostovoi A I, Orletskii I G, Parfenyuk O A, Maryanchuk P D 2017 *Optics and Spectroscopy* **122** (6) 944
[2] Perednis D, Gauckler L J 2005 *J. Electroceramics* **14** (2) 103

Influence of Hybrid System of Nanofillers Including MWCNTs, Graphene Nanoplatelets and Carbon Black on PET-G Post-Consumer Foils

D. Pawlikowska[1], S. Paszkiewicz[1], I. Irska[1], A. Szymczyk[2], E. Piesowicz[1]

[1] *Institute of Materials Science and Engineering*
West Pomeranian University of Technology
Al. Piastow 17, Szczecin, 70-310, Poland
[2] *Institute of Physics, West Pomeranian University of Technology*
Al. Piastow 48, Szczecin, 70-310, Poland

One of the most currently developing directions of cognitive and applied works is the research on nanocomposites, polymer nanocomposites in particular. Polymer nanocomposites, consisting of polymer matrices and additives are considered to be an important group of relatively inexpensive materials for many engineering applications. Significant improvement in the properties of composites depends mainly on: the size and shape of nanofiller particles, the specific surface area, the degree of development of the surface area and the spatial distribution of nanoparticles in the polymer matrix. Incorporation of three types of carbon nanofillers such as carbon black (CB) (powder type nanofiller -3D), graphene nanoplatelets (GNPs) (plate filler – 2D) and carbon nanotubes (CNT) (fibrous filler / linear 1D) seems to be interesting from the point of view of their impact on the enhancement effect. The aim of this work was to develop novel reinforced and electrically conductive polymer hybrid nanocomposites. Nanocomposites based on post-consumer PETG foils and MWCNTs/GNPs/CBs were prepared by *in situ* polymerization. The morphology of the nanocomposites was examined by electron microscopy (SEM). The relation between the preparation method, the morphology, the mechanical properties and the electrical conductivity was studied. Electron microscopy images revealed that the nanocomposites exhibited well dispersed carbon nanoparticles. It was observed that the incorporation of three different types of carbon nanofiller to PETG resulted in a sharp insulator-to-conductor transition. The low percolation threshold and relatively high electrical conductivity are attributed to a high aspect ratio, a large surface area and a uniform dispersion of the MWCNTs/GNPs/CBs hybrid system in the PETG matrix.

Acknowledgements
This work is the result of the research project GEKON2/O5/266860/24/2016 funded by the National Centre for Research and Development and the National Fund for Environmental Protection and Water Management, Poland.

References

[1] Paszkiewicz S, Pawlikowska D, Szymczyk A, Irska I, Piesowicz E, Jotko M, Lisiecki S, Bartkowiak A, Sieradzka M, Fryczkowski R, Kochmanska A, Kochmanski P, Roslaniec Z

"Improvement of barrier properties of glycol-modified poly(ethylene terephthalate) (PETG) – based nanocomposites containing graphene derivatives forms", *Polimery* (in press)

[2] Paszkiewicz S, Piesowicz E, Irska I, Pawelec I, Szymczy Ak Rosłaniec Z 2016 "Thin polymer films containing carbon nanostructures", *Proceedings of the 2015 International Conference on Advanced Material Science and Engineering AMSE2016*

[3] Paszkiewicz S, Szymczyk A, Špitalský Z, Mosnáček J, Janus E, Rosłaniec Z, 2013 *Polimery* **58** (11–12) 47

COEXISTANCE: Thinking of the Future of Printmaking...

M. Pawłowski

University of Arts
Al. Marcinkowskiego 29, Poznań, Poland

I wonder which communication and transmission tools allow the contemporary man to make the most characteristic statement from the point of view of civilization development. Another way in which the media let us describe the world in the most complete way?

Every epoch presents its own image in its own peculiar way, preferring these media which characterize it the best. Art may be a sign of acceptance of the world or an act of disagreement, a form of contestation. However, it is only this art which bravely derives from the technological development, uses new ideas, as at the time of Leonardo de Vinci and Michael Angelo, and then at the time of the impressionists and the cubists, that becomes the memory of its times, in the major part at least.

These days, it may sound as a banality, we live in a world subjected to the guidelines or even the terror of the digital picture. The transmission which was to serve us – has made us its slaves. The Internet, the computer, the mobile phone, changing our imagination about the outer world, have interfered with the inner human life so deeply that they have accidentally made a structural reconstruction of the human brain. The mind has been functioning differently and the graphic art has changed, as well.

Effect of Carbon Nanotubes on Physical Properties of Sn-Ag-Cu Alloys

Yu. Plevachuk[1], P. Svec Sr.[2], P. Svec[2], O. Tkach[1]

[1] *Department of Metal Physics, Ivan Franko National University of Lviv Kyrylo i Mephodiy 8, 79005 L'viv, Ukraine*

[2] *Institute of Physics, Slovak Academy of Sciences Dubravska cesta 9, 845 11 Bratislava, Slovakia*

Increasingly lead-free solder application in various industries requires further improvement of their properties. The exceptional mechanical and physical properties demonstrated by carbon nanotubes (CNT) combined with their low density have made this new form of carbon an excellent candidate for composite reinforcement. Incorporating them to a solder matrix yields good results for solder joint reliability.

Nanoparticles often possess phase stabilities that differ from those of bulk materials, as a result of their large surface-to-volume ratio. When the size of the nanoparticles is decreased, the eutectic temperature decreases. The Sn–Ag–Cu-based solders (SAC) are chosen by most companies as lead-free solders due to the requirement restricting the use of Pb in the electronic industry. While employing near-eutectic Sn–Ag–Cu alloys in the soldering process involves some disadvantages compared to the Pb–Sn alloys, such as a higher melting point and poor mechanical shock resistance, a number of studies have been related to the improvement of the properties of SAC solders introducing additional nano-sized components. In this work the influence of CNTs on some thermophysical and mechanical properties of Sn–Ag–Cu alloys is reported.

Localized States in Amorphous Metals

G. Ponedilok, M. Klapchuk

Institute of Applied Mathematics and Fundamental Sciences
Lviv Polytechnic National University
Bandera 12, 79013 L'viv, Ukraine

The generalized microscopic Anderson model [1] in the Hartree-Fock approximation (HFA) is used to describe the charged and magnetic states of isolated impurities in structurally disordered systems [2]. The scattering of conduction electrons on the charged impurity is included in the model Hamiltonian. The two-time retarded Green's functions [3] are obtained within the HFA. The system of self-consistent equations for calculating the electronic spectrum, the charged and spin-polarized impurity states is given. The Green's function of localized electrons is obtained in the form:

$$L^{\sigma}_{0,0}(E) = (E - E_{0,\sigma} - \Sigma_0(E) - \Sigma_1(E))^{-1}$$

where $\Sigma_0(E) = \sum\limits_{\mathbf{k}} \dfrac{|\Omega^{\sigma}_k|^2}{E - E_k - \Lambda_0}$, $\quad \Sigma_1(E) = \sum\limits_{\mathbf{k}} \sum\limits_{\mathbf{q}\neq\mathbf{k}} \dfrac{\Omega^{\sigma}_{0,k}\widetilde{\Lambda}_{\mathbf{k},\mathbf{q}}\Omega^{\sigma}_{q,0}}{(E - E_k - \Lambda_0)(E - E_q - \Lambda_0)}$.

The effective potential $\widetilde{\Lambda}_{\mathbf{k},\mathbf{q}}$ has the form of a series in terms of the effective pseudopotential

$$\Lambda_{\mathbf{k}-\mathbf{q}} = \frac{1}{\sqrt{N}} \sum_{1\leq j\leq N} e^{-i(\mathbf{k}-\mathbf{q})\mathbf{R_j}} v(|\mathbf{k}-\mathbf{q}|) + \widetilde{v}_0(|\mathbf{k}-\mathbf{q}|)$$

Here we introduce $v(|\mathbf{k}-\mathbf{q}|)$, $\widetilde{v}_0(|\mathbf{k}-\mathbf{q}|)$ – the Fourier components of local potentials of metal ions and impurity [4], respectively. Both the structural disorder and correlation effects should be taken into account in the self-energy term.

The effective charge $Z_{eff} = |e|(\langle n_{\uparrow}\rangle + \langle n_{\downarrow}\rangle)$ and the local magnetic moment $M = \mu_B(\langle n_{\uparrow}\rangle - \langle n_{\downarrow}\rangle)$ are obtained in the quasi-crystalline case [2]. Graphical representations are given depending on the model microscopic parameters $y = U_0/\Delta$, $x = (E_F - E_0)/U_0$, $z = (U/W)_c$.

The configuration averaged Green's function of localized electrons is obtained. A qualitative analysis of the influence of the metallic host structural disorder on the electronic spectrum, the charged and magnetic impurity states is presented. An additional shift and broadening of the virtual impurity level results from the structural disorder of the impurity environment. The contribution to the broadening of the virtual impurity level at $T = 0$ comes from the scattering processes on the charged impurity and from the structural disorder of the impurity environment as well. This interplay may be relevant to experimental realizations of the "liquid metal+electronegative impurity" system for studying its magnetic properties. The next possible step of exploration of the proposed model can be a study of the Kondo regime taking into account the processes of exchange.

References
[1] Anderson P 1961 *Phys.Rev.* **124** (1) 41
[2] Ponedilok G, Klapchuk M 2013 *Cond. Mat. Phys.* **16** (3) 33705 1
[3] Zubarev D 1960 *Usp. Fis. Nauk* **71** 71
[4] Rudavskii Yu, Ponedilok G, Klapchuk M 2003 *Conden. Matter Phys.* **6** (4(36)) 611

Stability of Structure and Physical Properties of Gd-Fe Films

V. I. Prysyazhnyuk, O. G. Mykolaychuk

Physics of Metals Department, Ivan Franko National University of Lviv
Kyrylo i Mephodiy 8, 79005 L'viv, Ukraine

Films of binary compounds of a Gd-Fe system were obtained by means of thermal vacuum evaporation of a polycrystal mix material of a corresponding composition. The films, 50–60 nanometers in thickness, were evaporated on chips of NaCl crystal, then NaCl dissolved in water. Parts of the films were picked up at once on copper electron diffraction grids. The second series of films were transferred on copper grids, coated with thin collodion films, and in such form stored 3–6 years. Then, recurring research was carried out. The films were condensed on glass-ceramic substrates for electrophysical measurements. The thickness of films changed within the range of 100–200 nanometers. The temperature of substrates had two values 300 and 500 K. An electron microscope UEMV-100K and a high-temperature PRON-2 attachment were used for structural investigations. The angle dependence of atomic factors of electron scattering was considered by gadolinium and iron atoms. All measurements were repeated 3–6 years after the first stage of measuring.

The electron diffraction examinations of the structure of Gd-Fe system films show that the analyzed films are condensed in the amorphous-crystalline state. The structure formation essentially depends on the requirements for condensation of films. The rising substrate temperature leads to magnification of the polycrystalline phase [1].

It is known that the analyzed compounds belong to the class of soft magnetic materials. Some magnetic performance of films and massive samples of the Gd-Fe system were measured. Hysteresis curves and numerical values of a coercive force were obtained for massive and thin film samples. The Curie temperature was also determined for these samples. The effect of the polycrystalline phase formation on the absolute value of the coercive force was studied. The temperature dependences of magnetic saturation and curve magnetization were obtained for films and compounds of the Gd-Fe system [2].

We explored the structure, electrophysical and magnetic properties of films of different compounds of the Gd-Fe system in the period of 3–6 years. A high temporary durability of the physical performance of films of Gd-Fe compounds and the lack of oxidizing action were revealed.

References

[1] Prysyazhnyuk V I, Mykolaychuk O G 2015 *Abstr. book 3-rd International research and practice conference: "Nanotechnology and Nanomaterials" Lviv*, 13
[2] Prysyazhnyuk V I, Mykolaychuk O G 2016 *University Visnyk. Series: Physics* **51** 44

Thermal Expansion Effect on Phonon Localization in Disordered Molecular Crystals

O. Pursky[1], V. Konstantinov[2]

[1] *Kyiv National University of Trade and Economics*
19 Kioto St., Kyiv 02156, Ukraine

[2] *B. Verkin Institute for Low Temperature Physics and Engineering*
National Academy of Science of Ukraine
47 Nauky Ave., Kharkiv 61103, Ukraine

In the present study an attempt has been made to find a thermal expansion effect on phonon localization of simple molecular crystals in orientationally-ordered (OO) and orientationally-disordered (OD) phases. The influence of thermal expansion on heat transfer processes was studied by a modified method of reduced coordinates [1] which permitted separating phonon-phonon and phonon-rotation contributions to the total thermal resistance of simple molecular crystals in isobaric and isochoric cases. A quantitative description of the thermal conductivity is given in the framework of the Debye model under the assumption that the heat is transferred by phonons and "diffusive" modes, and taking into account translation-rotation coupling [2]. The calculations were carried out for the isochoric and isobaric cases, which allowed the influence of thermal expansion on phonon localization to be determined. Based on the results of the studies it is concluded that the thermal expansion brings about an increase in the phonon localization temperature. Also from this analysis, it was found that the transition from strongly to weakly hindered rotation of molecules was accompanied by a decrease in the portion of the thermal energy that was transferred by "diffusive" modes. It was shown that a discrepancy between the temperature dependences of the isobaric and isochoric thermal conductivity in OO phases was mainly governed by the intensity of a phonon-phonon interaction because the phonon-rotational component of thermal resistance weakly depends on thermal expansion. In OD phases of simple molecular crystals the thermal expansion causes a general decrease in the phonon-rotational thermal resistance in comparison with the corresponding values at constant volume. The observed effect can be related to a decrease in the potential barrier that hinders the rotation of molecules due to the thermal expansion.

References

[1] Pursky O, Zholonko M, Konstantinov V 2000 *Low Temp. Phys.* **26** (4) 278
[2] Pursky O, Konstantinov V 2004 *Centr. Eur. J. Phys.* **4** (2) 210

Properties of n-Cyanobiphenyls Mesogene Phases between Graphene Planes – Computer Simulation Study

V. Raczyńska[1,2], Z. Dendzik[1,2], K. Górny[1,2], P. Raczyński[1,2]

[1] *Institute of Physics, University of Silesia*
Uniwersytecka 4, 40-007 Katowice, Poland

[2] *Silesian Center of Education and Interdisciplinary Research, University of Silesia*
75 Pułku Piechoty 1A, 41-500 Chorzów, Poland

Mesogene molecular phases anchored on different substrates are of great interest not only from the point of view of fundamental science but also because of their important potential applications in the design of novel generations of displays and other opto-electronic devices [1]. Features like improved phase stability, selective diffusion patterns and odd-even ordering and activation effects have been observed in n-Cyanobiphenyl mesogene films anchored on the surfaces of carbon and silicon carbide nanotubes [2].

The structure of mesogenes anchored on different surfaces strongly depends on the substrate morphology and homogeneity [3]. One of the most promising substrates is graphene, due to its unique 2D structure and mechanical, electrical and optical properties. The electronic structure of graphene and the presence of two strongly interacting benzene rings in n-Cyanobiphenyls leads to the formation of planar alignment of anchored mesogenes. n-Cyanobiphenyl molecules located between graphene

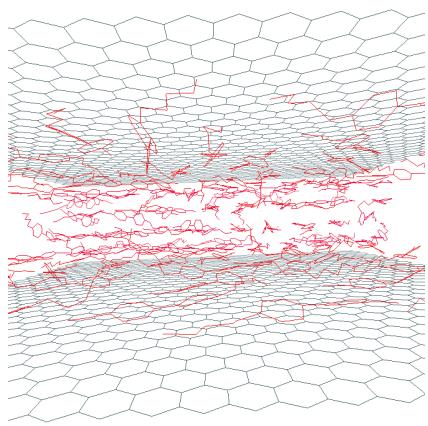

Figure 1: Simulation snapshot of two layered structure of 5-Cyanobiphenyl mesogenes located between graphene planes

sheets form layered structures. The structure and dynamical properties of these phases depend on the number of aliphatic C atoms in the tail of the mesogene molecule, as well as on the distance between the graphene sheets. The ordering effects, stability and dynamical properties of n-Cyanobiphenyl phases were studied using molecular dynamics computer simulations.

References

[1] Rahman M, Lee W 2009 *J. Phys. D: Appl. Phys.* **42** (6) 063001
[2] Górny K, Raczyński P, Dendzik Z, Gburski Z 2015 *J. Phys. Chem. C* **119** (33) 19266
[3] Roscioni O M, Muccioli L, Zannoni C 2017 *ACS Appl. Mater. Interfaces* **9** (13) 11993

Influence of Alloying on Fe Aproximant Phase Content in Ti-Cr-Al-Si-O System

O. A. Rokitska, M. V. Karpets, M. O. Krapivka, V. F. Gorban, S. O. Firstov

I.N. Frantsevich Institute for Problems of Materials Science
National Academy of Sciences of Ukraine
Kyiv, Ukraine

The quasicrystalline phase was discovered for the first time by Dan Schethman in 1984 in an Al-based alloy [1]. Later, quasicrystals and their approximants were also found in Ti-based systems. Alloys of the Ti-Me(Cr, Mn, Fe)-Si-O system were investigated in [2]. The authors have determined that up to 20 at.% of oxygen is required to stabilize the 1/1 approximant phase in the Ti-Cr-Si-O system, while only 4 at.% is required for Ti-Fe-Si-O. XRD showed not only the 1/1 approximant but also indicated two phases – Cr_2Ti (C14) and α-Ti. Two intermetallic phases – TiFe and Ti_2Fe are formed in Ti-Fe-Si-O systems other than $1/\alpha$ (TiCrSi). In this case, α-Ti is initially crystallized in alloys with chromium, and there is an approximant phase in alloys with iron. However, the effect of iron doping on the phase composition and properties of the Ti-Cr-Si-O alloys has not been found in the literature.

Therefore, the purpose of the study is to determine the effect of iron on the change in the phase composition of Ti-Cr-Al-Al-Si-O alloys in cast and annealed states.

The alloys were prepared by arc melting in an atmosphere of high-purity argon. The samples were annealed for 3 hours at 800°C in a vacuum oven. The phase composition of alloys was investigated by X-ray diffraction (DRON-UM1) in monochromatic CuKα radiation. The data of the diffractometric experiment was processed using a program for a full-spectrum analysis of X-ray spectra from a mixture of polycrystalline phase components of PowderCell 2.4. In a full-profile analysis of diffraction patterns, the crystallographic texture was taken into account under the March-Dollase texture model [3].

The X-ray diffraction studies have shown formation of the 1/1 approximant α(TiCrSi) with a cubic crystal lattice and Cr_2Ti (C14) Laves phase with hexagonal crystal lattice in both alloys. In addition, the amount of the approximant phase in the $Ti_{60}Cr_{30}Al_3Si_2{\cdot}(SiO_2)_5$ alloy is 74% wt, and its amount increases to 84% wt. in the alloy in which the chromium part is replaced by iron. The lattice parameter $1/1\alpha$ (TiCrSi) in the $Ti_{60}Cr_{30}Al_3Si_2{\cdot}(SiO_2)_5$ alloy in the initial state is $a = 1.3144$ nm, and Cr_2Ti – $a = 0.4295$ and $c = 0.8026$, respectively. The addition of 10 at.% Fe reduces the approximant lattice parameter to $a = 1.3135$ nm, with parameter a of the Laves phase Cr_2Ti increasing to 0.4938 nm, and parameter c decreases to 0.7995 nm. Since Fe and Cr have similar values of the atomic radii (0.126 and 0.128 nm, respectively), iron isomorphically replaces chromium in the lattice of the approximation phase, which leads to a decrease in its lattice parameter as compared to the alloy

$Ti_{60}Cr_{30}Al_3Si_2{\cdot}(SiO_2)_5$, which does not contain Fe in the composition. The phase composition in both alloys does not change after annealing at 800°C – there is only a change in their quantitative ratio. The amount of the approximation phase increases only to 79% wt in the $Ti_{60}Cr_{30}Al_3Si_2{\cdot}(SiO_2)_5$ alloy, and its amount sharply increases to 97% wt in the $Ti_{60}Cr_{30}Al_3Si_2{\cdot}(SiO_2)_5$ alloy, indicating the stabilizing effect of Fe. In addition, an annealed iron alloy exhibits a texture that manifests itself in the inconsistency of experimental intensities – the $1/1\alpha$ (TiCrSi) approximant exhibits a texture in the direction [600] with the coefficient $\tau = 0.58$ and Cr_2Ti in the direction [004] with the coefficient texture $\tau = 0.40$. The opposite dependence of the change of the phase lattice parameter is observed after annealing in the alloys. Thus, the parameter of the $1/1\alpha$ (TiCrSi) approximant lattice parameter (TiCrSi) in an iron-free alloy increases to $a = 1.3150$ nm with a simultaneous decrease in both values of the Cr_2Ti (C14) parameters to $a = 0.449$ and $c = 0.7998$ nm. Conversely, in the alloy $Ti_{60}Cr_{30}Al_3Si_2{\cdot}(SiO_2)_5$, there is a significant decrease in the approximant phase lattice period to $a = 1.3118$ nm and an increase in the Laves phase Cr_2Ti (C14) to $a = 0.5001$ and $c = 0.8220$ nm.

References

[1] Shechtman D, Blech I, Gratias D, Cahn J 1984 *Phys. Rev. Lett.* **53** 1951
[2] Croat T K, Kelton K F, Holland-Moritz D 1999 *J. Mat. Res.* **14** 4208
[3] Dollase W A 1986 *J. Appl. Cryst.* **19** 267

Mechanism of Generation of Donor-Acceptor Pairs in *n*-ZrNiSn Semiconductor Heavily Doped by Ga Acceptor Impurity

V. V. Romaka[1], V. Krayovskyy[1], L. P. Romaka[2], Z. Rykavets[1], Yu. Stadnyk[2], A. Horyn[2]

[1] *Lviv Polytechnic National University*
Bandera 12, 79013 L'viv, Ukraine

[2] *Ivan Franko National University of Lviv*
Kyrylo i Mephodiy 6, 79005 L'viv, Ukraine

Thermoelectric materials based on *n*-TiNiSn and *n*-ZrNiSn intermetallic semiconductors have a high efficiency of transformation of the waste heat into electrical power. However, uncontrolled changes in the crystal and electronic structures during optimization of the characteristics by doping affect their thermoelectric properties and limit extensive application of these materials. The crystal and electronic structures, electrokinetic, and magnetic characteristics of *n*-ZrNiSn doped by Ga acceptor impurity were investigated to resolve this problem.

The XRD and EPM analyses showed that all samples of $ZrNiSn_{1-x}Ga_x$ up to $x = 0.15$ were single-phase and in agreement with the thermodynamic calculations that predicted maximum Ga solubility of $x = 0.4$ at 1073 K. The concentration dependence of the lattice parameter is nonlinear and reflects effects of local amorphisation. It was found that partial substitution of Sn ($5s^2 5p^2$) by Ga atoms ($4s^2 4p^1$) in the 4*b* crystallographic site generated simultaneously both structural defects of an acceptor (Ga atoms in 4*b* site) and donor nature (vacancies in 4*b* site). Such doping leads to an increase in the compensation degree of the semiconductor and a shift of the Fermi level from the percolation level of the conduction band to the center of the band gap. At $x(\mathrm{Ga}) \approx 0.025$ the Fermi level crosses the center of the band gap and at $x(\mathrm{Ga}) \approx 0.05$ enters the percolation level of the valence band (Anderson transiotion). The modeled distribution of atoms in the crystal structure of $ZrNiSn_{1-x}Ga_x$ showed that the speed of the movement of the Fermi level ε_F, obtained from the band structure calculations was in agreement with the experimental data extracted from $\ln \rho(1/T)$ dependencies. The change of the Seebeck coefficient sign from negative to positive reflects the change of the main charge carriers from electrons to holes. The magnetic susceptibility of samples shows that all of them are Pauli paramagnets. However, at $x > 0.03$ the $\chi(x)$ dependence keeps constant up to $x = 0.15$ and confirms the formation of donor-acceptor pairs.

The results are explained within the Shklovskiy-Efros model of heavily doped and compensated semiconductors.

Radiation-Induced Changes of Physical Properties of a-GeSe Thin Films

R. Romanyuk

Faculty of Physics, Ivan Franko National University of Lviv
Kyrylo i Mephodiy 8, 79005 L'viv, Ukraine

Complex investigations with the aim to make clear the physical features of localized states being formed in the mobility gap of GeSe amorphous films due to a high-energy electromagnetic irradiation were carried out. The temperature region of the GeSe amorphous structure existence was determined. The peculiarities of the low order of amorphous thin films in dependence on the preparation of the technology and the influence of gamma-irradiation were studied. The topology and micro-local features of the formation process of disordered structure GeSe films were established using the method of analysis of experimental scattering curves as well as model interpretation of the radial distribution function of atomic density.

The thin films under investigation (thickness near 0.3–1.2 μm) were obtained using the method of discrete evaporation of a fine-dispersive mixture on the surface in vacuum (10^{-4} Pa) from fresh cleaved NaCl, glass-ceramics and quarts at 293–450 K. It was established that γ-irradiation (1.25 MeV) with a dose of $10^4 - 10^5$ Gy caused changes in the electro-physical properties of GeSe amorphous films, in particular, a decrease in the specific resistance and appearance of the jump mechanism of conductivity on localized states near the Fermi level. The gamma-irradiation of GeSe films caused a low-energetic shift of their fundamental optical absorption edge and increased the refraction index, while the energy gap and steepness of the Urbach edge were decreased. It was established that the form and position of the main diffusion maximum, studied by the X-ray method, did not change after γ-irradiation [1]. It was shown that crystalline processes in irradiated amorphous condensates became more denominated in comparison with the non-irradiated ones.

Low-energy irradiation (a non-focus electron beam with the energy 35 keV) stimulated a more ordered structure of GeSe films with amorphous phase conservation as it led to increasing the mobility gap and decreasing the electro-conductivity of films.

Radiation-induced changes of the physical properties in amorphous GeSe thin film are explained in the framework of radiation defect-formation processes as results of destruction-polymerization transformations. The main topological reactions of formation of centers of radiation defects as well as a model of energy gap transformation under irradiation with a provision for peculiarity reconstruction spectra of localized states were proposed.

References

[1] Romanyuk R R 2014 *Physics and Chemistry of Solid State* **15** 92

AlN Films Grown on Flexible Polymeric Substrates

E. Rudenko[1], I. Korotash[1], D. Polotskiy[1], Z. Tsybrii[2], F. Sizov[2]

[1] *Institute for Metal Physics NAS of Ukraine*
03142 Kyiv, Ukraine
[2] *Institute of Semiconductor Physics, NAS of Ukraine*
03028 Kyiv, Ukraine

Nanostructured aluminum nitride (AlN) film coatings were obtained using hybrid helicon-arc ion-plasma deposition. Combining the magnetic-filtered arc plasma deposition technique with treatment in radiofrequency (RF) plasma of helicon discharge allows the deposition of AlN coating layers on flexible substrates (polymeric Teflon, Mylar) and significantly increases the deposition rate and adhesion of coatings. Studies of the spectral properties of AlN films (infrared reflection and transmission spectra) within the range from to two to twenty-five microns were carried out. The obtained composite structures (AlN coatings on Teflon and Mylar thin layer substrates), due to a high thermal conductivity of AlN, could be used as efficient blocking structures in the infrared spectral range ("infrared stealth") withdrawing the heat from filters warmed by IR radiation or considerably blocking the IR radiation from bodies heated to T less than three hundred fifty K. A simulation of thermal fields of film structures with different values of thermal conductivity (from twenty five hundred to two hundred W/m K) with different values of thermal irradiation and various temperature values of the thermal screen was carried out.

Electronic Structure and Physical Properties of Ag_2XS_3 ($X =$ Si, Ge, Sn) Ternary Semiconductors

M. Rudysh[1,2], M. Brik[1,3,4], M. Piasecki[1], P. Shchepanskyi[1,2], V. Stadnyk[2]

[1] *Institute of Physics, Jan Dlugosz University*
Armii Krajowej 13/15, 42-201, Czestochowa, Poland

[2] *Faculty of Physics, Ivan Franko National University of Lviv*
Kyrylo i Mephodiy 8, 79005 L'viv, Ukraine

[3] *College of Mathematics and Physics*
Chongqing University of Posts and Telecommunications
2 Chongwen Road, Nan'an District, Chongqing 400065, P. R. China

[4] *Institute of Physics, University of Tartu*
W. Ostwald 1, 50411 Tartu, Estonia

Chalcogenide crystals are promising nonlinear optical materials for the middle infrared range. Currently, ternary chalcogenides such as $AgGaS_2$, $AgGaSe_2$ and $CdGa_2S_4$ are widely adopted as materials for converting the laser average infrared range. Attempts to amplify the nonlinear properties of ternary chalcogenides among $AgGaS_2$, $AgGaSe_2$ and $AgGaTe_2$ to enhance the ability of crystals to convert the laser radiation are also known. In addition to those presented, it is important to extend the number of functional materials that will be useful for practical application as active elements in photovoltaics and optoelectronics.

This work is devoted to the study of the electronic structure and related properties of Ag_2XS_3 (where $X =$ Si, Ge, Sn) ternary semiconductors using computational methods based on the density functional theory (DFT). The electronic structure of titled compounds is calculated using the DFT/LDA and DFT/GGA methods. The electronic bandgap values, the genesis of electronic levels are established. The optical spectra are calculated and discussed using electronic structure data. All the theoretically calculated data is compared with the available experimental data.

Fractal Geometry in Architecture

J. Rybicki[1], J. S. Rybicki[2], A. Rybicka[1]

[1] *Department of Solid State Physics, Faculty of Applied Physics and Mathematics*
Gdansk University of Technology
Narutowicza 11/12, 80-233 Gdansk, Poland

[2] *Faculty of History, University of Gdansk*
Wita Stwosza 55, 80–308, Gdansk, Poland

Designs are characterized by historians and scholars as having 'less ornamentation', 'bigger windows', 'denser planning structures', 'industrial detailing', 'richer iconography', 'stronger horizontal lines' and 'more articulated social structures'. They are 'more richly textured', 'starkly geometrical', 'tectonically conservative' and 'phenomenally enlivened'.

These examples are typical of the qualitative descriptions.

There is nothing intrinsically wrong with this way of constructing the history and theory of architecture, but there are valuable alternative approaches.

Here a quantitative, mathematical and computational approach to understand the properties of designs and how they relate to each other, is presented.

The method is known as "fractal analysis". It was used to analyze the designs in an ad hoc version in the 80s of the last century, but it has matured and become refined only in recent few years.

The lecture consists of two parts: (1) the fractal method presentation and (2) some examples of the results analysis with discussion.

Catalyst Screening for Improved Hydrogen Reversible Sorption in Magnesium Borohydride

I. Saldan, O. Reshetnyak

Department of Physical and Colloid Chemistry, Ivan Franko National University of Lviv Kyrylo i Mephodiy 6, 79005 L'viv, Ukraine

Magnesium borohydride, $Mg(BH_4)_2$, is one of the most promising hydrogen storage materials though its kinetics and reversibility are still important challenges for the use of the material in fuel cells [1]. Therefore development of effective materials for the improved decomposition/formation of $Mg(BH_4)_2$ is one of the most important problems to solve before its practical application. High valence transition metal carbides, nitrides, oxides or halides have the ability to form bonds with hydrogen in varying stoichiometries. This encourages the fast dissociation into atomic hydrogen or its recombination to hydrogen molecules [2]. In order to improve the hydrogen sorption performance of $Mg(BH_4)_2$, a wide range of approaches has been tried, including high energy reactive ball-milling, preparation of composite materials, dispersion in a porous matrix, and introduction of transition metal (TM) additives. In the present work Ti-, Mo-, Co- and Ni-based additives are studied as a possible catalyst for the $Mg(BH_4)_2$ decomposition in the prepared $Mg(BH_4)_2$–TM composites [3–5]. The obtained experimental results are summarized in a concise review.

References

[1] Li H W, Yan Y, Orimo S I, Züttel A, Jensen C M 2011 *Energies* **4** 185
[2] Barkhordarian G, Klassen T, Borman R 2006 *J. Phys. Chem. C* **110** 11020
[3] Saldan I, Hino S, Humphries T, Zavorotynska O, Chong M, Jensen C M, Deledda S, Hauback B C 2014 *J. Phys. Chem. C* **118** 23376
[4] Zavorotynska O, Saldan I, Hino S, Humphries T, Deledda S, Hauback B C 2015 *J. Mater. Chem. A* **3** 6592
[5] Saldan I, Frommen C, Llamas-Jansa I, Kalantzopoulos G, Hino S, Arstad B, Heyn R, Zavorotynska O, Deledda S, Sørby M, Fjellvag H, Hauback B 2015 *J. Hydrogen Energy* **40** 12286

Refractive Parameters of $K_{1.75}[NH_4]_{0.25}SO_4$ Crystals: Ab Initio Calculations, Experimental Measurements

P. Shchepanskyi[1,2], V. Stadnyk[1], M. Rudysh[1,2], R. Brezvin[1]

[1] *1Faculty of Physics, Ivan Franko National University of Lviv Kyrylo i Mephodiy 8, 79005 L'viv, Ukraine*

[2] *Institute of Physics, Jan Długosz University of Czestochowa Armii Krajowej 13/15, 42-201, Czestochowa, Poland*

Crystals of the $ABSO_4$ group, where A and B are alkali metal cations, are of significant interest due to the ability to face a richness of phase transitions and their ferroelectric, ferroelastic, superionic, optical and other properties. An interesting feature of the $ABSO_4$ group crystals among the optical properties is the possibility of the existence of isotropic points, when the crystal undergoes transition from biaxial to uniaxial or from uniaxial to isotropic states. Such crystals can be used as temperature and pressure sensors [1,2,3].

Despite a number of investigated crystals, a lot of them possess IPs in a spectrum region that is inconvenient for practice and practically all face phase transitions occur at specific temperatures. Hence, a search for new crystals of this group with IPs is required to expand the range of practically important materials for thermometry and pressure sensing.

With respect to the described issue our attention was attracted to the K_2SO_4-$(NH_4)_2SO_4$ system, known to form a continuous series of solid solutions with a general formula $(K_x[NH_4]_{1-x})_2SO_4$, $(0 < x < 1)$. Crystals of this system appear to be mechanically stable, possess a high melting point and have no phase transitions in a wide temperature region for a row of concentration ratios. In this work the first principles calculations of the band energy, density of states and dielectric function of $K_{1.75}(NH_4)_{0.25}SO_4$ single crystals in a *Pnma* structure are performed in the framework of the density functional theory. A general gradient approximation and a local density approximation are used to describe the exchange-correlation interaction. Refractive indices $n(\omega)$ and absorption coefficients $k(\omega)$ are obtained from the spectrum of real and imaginary parts of the dielectric function.

The dispersion of refractive indices and the birefringence of $K_{1.75}[NH_4]_{0.25}SO_4$ crystals are studied experimentally using the immerse and spectroscopic Obreimov methods.

References

[1] Romanyuk M O, Andriyevsky B, Kostetsky O, Romanyuk M M, Stadnyk V 2002 *Cond. Mat. Phys.* **5** 586

[2] Romanyuk M O, Romanyuk M M 2005 *Ferroelectrics* **317** 57

[3] Stadnyk V Y, Brezvin R S, Romanjuk M O 1997 *Functional Materials* **4** (1) 97

Electronic and Refractive Properties of $LiNaSO_4$ Crystals

P. Shchepanskyi[1,2], V. Stadnyk[1], M. Rudysh[1,2], R. Brezvin[1], M. Piasecki[2]

[1] *Faculty of Physics, Ivan Franko National University of Lviv Kyrylo i Mephodiy 8, 79005 L'viv, Ukraine*

[2] *Institute of Physics, J. Dlugosh Academy of Czestochowa Armii Krajowej 13/15, 42-201, Czestochowa, Poland*

Lithium sodium sulfate ($LiNaSO_4$) crystal belongs to the double sulfates family with the general formula $LiMSO_4$ (M = Na, K, Rb, NH_4, etc.), which has very specific electrical properties. The room temperature structure of the crystal is believed to belong to the $P31c$ space group with six molecules in the hexagonal cell (unit cell parameter $a = 7.627$ Å and $c = 9.8579$ Å; and density = 2.527 g/cm^3) [1].

Recently, new studies on $LiNaSO_4$ crystal have demonstrated possible modern applications of this crystal in dosimetry [2] and as a functional layer of intermediate temperature solid oxide fuel cells [3].

Despite great interest in $LiNaSO_4$, electronic and anisotropic optical properties, to the best of our knowledge, are still lacking.

In this work we performed the first principles calculations of the band energy structure, density of states and dielectric function of $LiNaSO_4$ single crystals using the CASTEP code. We discuss the nature and genesis of the main energy bands of the crystal. The refractive indices dispersions and absorption coefficients spectra are obtained from the calculated dielectric functions.

We also grew $LiNaSO_4$ crystals of good optical quality and studied the refractive indices dispersion and birefringence using conventional immerse and spectroscopic methods.

Both the calculations and experimental results are compared with the available data for isostructural crystals of the $ABSO_4$ group.

References

[1] Morosin B, Smith D L 1967 *Acta Crystallographica* **22** 906
[2] Vidya Y S, Lakshminarasappa B N 2015 *Appl. Phys. A* **118** 249
[3] Lv W, Tang Z, Yin Y-M, Yin J, Ma Z-F 2015 *Nano-Micro Lett.* **7** 268

Electron Structure, Magnetic Properties and X-Ray Spectra of $R.E.M_2X_2$ ($M =$ Fe, Ni, Co, Cu; $X =$ P, Si)

I. Shcherba[1], H. Noga[2], B. Jatsyk[3], M. Kovalska[1], S. Senkiv[1]

[1] *Ivan Franko National University*
Kyrylo i Mephodiy 8, 79005 L'viv, Ukraine

[2] *Institute of Technology, Pedagogical University*
Podchorazych 2, 30-084 Krakow, Poland

[3] *Lviv National University of Veterinary Medicine and Biotechnologies*
Lviv, Ukraine

The new ternary intermetallic compounds are interesting as materials for construction of nuclear fuel reactors. The relatively high heat resistance and high neutron absorption cross-section make their application as neutron capture materials very prospective. The investigations of possible application of these compounds for the radio engineering, electronics, computing technology, etc, are in progress. The electric conduction, thermo ionic and magnetic properties are investigated as well. The family of the formula $R.E.M_2X_2$ is one of the numerous families of ternary intermetallic compounds that have been reported in the literature.

High-energy spectroscopy (XES, XAS and XPS) was used to study the electron structure of the investigated new ternary intermetallic compounds. The calculations of electron energy bands $E(k)$ and partial DOS for compounds were performed by the semi relativistic linear muffin-tin orbital method without consideration of spin-orbit interactions. Good agreement was obtained between the experimental and calculated X-ray emission spectra $R.E.M_2X_2$. The L_{III} – absorption spectra Ce and Yb in ternary Ce(Yb)M_2X_2 compounds were obtained at 78 K and 300 K using a tube spectrometer equipped with an RKD-01 co-ordinate detector. The mixed valence state of Ce and Yb was obtained in Ce(Yb)M_2X_2.

The valence band electronic structure of a compound with the $HfFe_2S_2$ crystal lattice type was established for the first time based on X-ray emission spectroscopy measurements. The band structure and the theoretical spectra of X-ray emission bands of atoms located in non-equivalent crystallographic positions were calculated by means of the LMTO method in non-relativistic approximation. A satisfactory agreement between theoretical and experimental data was achieved. ^{57}Fe Mössbauer absorption measurements confirmed iron atoms occupying non-equivalent positions in the crystal lattice.

On the Nature of Eutectic Alloys

P. I. Shevchuk

National Academy of Public Administration, Office the President of Ukraine
Sukhomlynskogo 16, Lviv, Ukraine

The idea of the study of one of the most difficult problems of physics of metals and alloys, such as the nature of interparticle interaction in eutectic alloys belongs to Prof. Yar. Dutchak and was proclaimed by him back in the 70s of the last century. It was quite revolutionary and an alternative to the dominant paradigm, whereby the eutectic structure was seen as a mechanical mixture of [1].

It analyzed the X-ray emission spectra of both simple (Al, Ag, Au) Ge(Si), and complex eutectic transition metals of the iron group with germanium and the Mg-Ga and Mg-Ge systems [2], which showed an anomaly in the spectral changes of parameters inherent to components that make up the alloy. At the same time significant distortion of the spectra and parameters of X-ray abnormalities was observed in non eutectic alloys.

The results of the X-ray study and the study of electronic charge state of atoms eutectic systems (Ag, Au)-Ge (Si) [2] have shown that the spectra of the eutectic composition are not a simple superposition of the spectra of pure components.

Analysis of the Mössbauer spectra captured from the eutectic alloy of Fe Ge cannot interpret them as an additive sum of the spectra of the components. This applies to both forms of the absorption curve γ-rays and fixed values of the fields at the nuclei.

The above is proved by the results of the X-ray and electron diffraction investigations of the eutectic a-Si of the Al-Si system [3]. which also shows that the eutectic range section cannot be considered as a simple additive sum of the spectra of its components.

In summary, it can be assumed that the main reason for the change of the electronic structure of eutectic alloys is the impact of intercrystalline boundaries of the existing phases.

References

[1] Bochvar A A 1956 *Metallurgy*, Metallurhyzdat, Moscow, 449
[2] Shevchuk P I 1977 *Study of the electronic structure of a number of compounds of rare-earth metals and eutectic. The dissertation of PhD in physics and mathematics*, Lviv, 175
[3] Chychko A N 1994 *Solid State Physics* **3** 785

Effect of Hydrogen Treatment on Structure and Phase Formation of Ga-Ni/NiO Metal Matrix Composites

I. Shtablavyi, S. Mudry, O. Kovalskyi, B. Sokoliuk, Yu. Kulyk, V. Plechysty

Physics of Metals Department, Ivan Franko National University of Lviv
Kyrylo i Mephodiy 8, 79005 L'viv, Ukraine

Metal matrix composites have attracted the attention of scientists for a long time due to the possibility of a controlled change of the composite properties for the best results. Currently, many methods of metal matrix nanocomposite synthesis have been developed and many excellent results have been obtained. However, in most cases it is oxide particles or particles of carbides, borides, nitrides, etc. that are used as fillers. Using such fillers makes it impossible to fully utilize all the benefits of composites compared with other materials. In particular, in many cases there is a necessity of partial or total chemical interaction of the filler with the matrix that is not possible, if the abovementioned fillers are used. On the other hand, the introduction of chemically reactive impurities in a matrix, such as metal particles, can lead to the formation of intermetallic phases already at the stage of composite synthesis and deterioration of properties of the final material. In this regard, there is a need to find new methods to control the phase formation in metal matrix composites.

In this work, a new approach to the synthesis of gallium based micro- and nanocomposites with a controlled process of phase formation has been proposed by adding nickel particles coated with nickel oxide and subsequent treatment of the composite in a hydrogen atmosphere. The particles of nickel were obtained by thermal decomposition of nickel oxalate in the air at various conditions. Composites were synthesized by mechanical mixing at a temperature close to the melting point of gallium.

The structure of the composites in the liquid state and the phase composition after crystallization were studied by the X-ray diffraction method. The microstructure of the composites was studied by scanning electron microscopy and the phase formation process was investigated by the differential thermal analysis method.

Molecular Dynamic Simulations of Solid-Liquid Interface in Bi-Ni System

I. Shtablavyi[1], S. Mudry[1], J. Rybicki[2], V. Plechysty[1,2], S. Winczewski[2]

[1] *Physics of Metals Department, Ivan Franko National University of Lviv Kyrylo i Mephodiy 8, 79005 L'viv, Ukraine*

[2] *Department of Solid State Physics, Gdansk University of Technology Narutowicza 11/12, 80-233 Gdansk, Poland*

The technological achievements of recent decades and the development of nanotechnology have opened interesting research trends aimed at the production of functional materials with controlled properties which can be controllably created, maintained over some period of time or changed. Magnetic materials with tailor-made properties, as a particular class of such materials, are in great demand as structural materials for components of devices and machines as well as for production of functional electronic devices.

The area of fundamental and practical problems in this field has significantly expanded in recent years due to the discovery of new effects in magnetic systems and the implementation of nanotechnology (giant magnetoresistance, quantum Hall effect, superparamagnetism) However, new requirements have appeared on the creation of magnetic systems with specific functional properties, such as magnetic fluids, quantum magnetic fluids, thin-film multilayer composites, etc. At the same time there are many problems that make it impossible to determine the physical and chemical bases of synthesis of magnetic composites and formulate the regularities of their properties.

Currently, there are few studies dedicated to the kinetics of processes occurring at the interface of liquid and crystalline phases during the synthesis of such composites. The processes of phase formation, in this case, are quite fast and, accordingly, complicated for investigation. Experimental methods allow us to determine only the result of the interaction of liquid and crystalline phases and do not provide information about the features of this interaction at different instants of time. Furthermore, there are no generalized theoretical methods that would be effective in solving the problem. For this reason, the mechanism and kinetics of phase formation in composites at the liquid matrix – crystal particle interface should be further investigated by computer simulation methods, which would make it possible to obtain information about the regularities of reactions and diffusion processes at the interface.

In this work the kinetics of the interaction and the phase formation processes at the liquid matrix-nanoparticle surface Bi-Ni interlayer were investigated by molecular dynamics simulations. The EAM potentials were used for the simulations. The phase formation mechanism on the boundaries of the magnetic particle (Ni) – the paramagnetic matrix (Bi) and their influence on the physical properties of the material were established as a result of the investigations.

Preparation and Characterization of Carbon Nanotubes–Cu Metal Matrix Composites

I. Shtablavyi[1], S. Prokhorenko[2,3], D. Ploch[3], V. Plechysty[1]

[1] *Physics of Metals Department, Ivan Franko National University of Lviv Kyrylo i Mephodiy 8, 79005 L'viv, Ukraine*

[2] *Department of Measuring Information Technologies, Lviv Politechnic National University Bandera 28a, 79013 L'viv, Ukraine*

[3] *Center for Microelectronics and Nanotechnology, University of Rzeszow Pigonia 1, 35-959 Rzeszow, Poland*

The need for lightweight, high strength materials has been recognized since the invention of the airplane. As the strength and stiffness of a material increases, the dimensions, and consequently, the mass of the material required for a certain load bearing application is reduced. This leads to several advantages in the case of aircraft and automobiles such as an increase in payload and improvement of the fuel efficiency. For this reason, intensive investigations in the field of new materials and composites with improved properties are currently underway. It is known that carbon nanotubes (CNT) is expected to be used in carbon nanotubes-metal matrix composites due to its remarkable mechanical properties, special morphology and size. Many research studies have been dedicated to depositing metals on the nanotube surface to further their incorporation into a composite. However, pure metals would not easily wet the surface of a CNT. Therefore, traditional techniques such as the powder metallurgic process cannot be used to prepare high quality metal matrix-CNT composites.

Among different synthesis technologies it is the electrochemical technology that shows flexibility in preparing metal composites. However, the main challenge for electrochemical techniques is also the dispersion of CNTs in the metal matrix. The natural tendency of agglomeration of CNTs, due to their high surface energy, hinders uniform dispersion and good suspension in the electrolytic bath. This ultimately results in inhomogeneous distribution of CNTs in the metal matrix coating. The most commonly used technique to improve CNT dispersion in the electrolytic bath includes agitation by means of a mechanical stirrer, ultrasonication, and magnetic forces. However, these methods need to be improved. For this reason the present work reports the results of investigations of nanocomposites consisting of a CNT cowered by Cu by means of the electroplating method. The structure and morphology of the obtained composites were studied by the X-ray diffraction method and SEM microanalysis.

Hf-Ni-Al System at 800°C: Crystal Structures and Electrical Properties

O. Shved[1], L. Salamakha[1,2], O. Sologub[2], S. Mudry[1]

[1] *Department of Physics of Metals, Ivan Franko National University of Lviv Kyrylo i Mephodiy 8, 79005 L'viv, Ukraine*

[2] *Institute of Solid State Physics, Vienna University of Technology 8–10 Wiedner Hauptstrasse, 1040 Vienna, Austria*

The ternary Hf−Ni−Al system was investigated by using X-ray diffractions and optical metallographie at first [1] and then by using an additional technique of microprobe analysis [2]. The isothermal section at 800°C was established and nine ternary compounds − HfNiAl (τ_1), $HfNi_2Al$ (τ_2), $HfNi_2Al_5$ (τ_3), $Hf_6Ni_8Al_{15}$ (τ_4), Hf_6NiAl_2 (τ_5), Hf_5Ni_4Al (τ_6), $HfNi_{0,35}Al_{1,65}$ (λ_1), $HfNi_{0,6}Al_{1,4}$ (λ_2) and $Hf_4Ni_{16}Al_5$ (λ_3) − were discovered. However, crystal structures of λ_3 and τ_6 were not found. The structure of the first compound is still unknown and recently the crystal structure of Hf_5Ni_4Al has been reported [3]. All compounds have a permanent composition, except two Laves phases λ_1, λ_2 which have an insignificant homogeneity range. The partial cross sections at 1273 and 1473 K in the Ni-rich area have been build [2].

In the course of the present investigation the formation and crystal structures of seven ternary compounds (τ_1−τ_5, λ_1, λ_2) were confirmed. The Rietveld refinement of their X-ray powder diffraction data was carried out. The majority of our results are in agreement with the data published earlier. It is only the structure type of Hf_6NiAl_2 that is different from the data [1]. It was discovered as Hf_6FeAl_2, unlike previously reported Hf_6CoAl_2.

The τ_2, τ_4, τ_5 and λ_1 compounds were studied by temperature dependent electric resistivity measurements from 4 K to room temperature. The behavior of the electric resistivity of all these compounds characterizes them as metals and allows describing the dependencies by the Bloch-Gruneisen-Mott formula [4]. The electric resistivity of the Laves phase λ_1 was measured at two composition points of the homogeneity range. It was established that the behavior of the electric resistivity in the vicinity of zero depending on the occupation of the 16d position with Al and Ni may have superconductivity or the Kondo effect.

References

[1] Markiv V Ya, Burnashova V V 1969 *Izv. Akad. Nauk SSSR. Metall.* **6** (2) 113
[2] Verbovytskyy Yu, Latka K 2012 *J. Chem. Met. Alloys* **5** 8
[3] Nash P, West D R E 1981 *Met. Sci.* **15** 347
[4] Mott N F 1936 *Proc. R. Soc. Lond*, Part A **156** 368

Josephson Supercurrent in Multilayered Tunnel Junction

P. Shygorin[1], Yu. Skopiuk[1], V. Bozhko[2], B. Venhryn[3]

[1] *Department of Theoretical and Mathematical Physics*
Lesya Ukrainka Eastern European National University
Volya Avenue 13, 43025 Lutsk, Ukraine

[2] *Department of Experimental Physics*
Lesya Ukrainka Eastern European National University
Volya Avenue 13, 43025 Lutsk, Ukraine

[3] *Department of Applied Physics and Nanomaterials Science*
Lviv Polytechnic National University
Bandera 12, 79013 L'viv, Ukraine

In this work we studied the current states in the double-barrier Josephson junction with the SISIS geometry (S – superconductor, I – isolator). The Josephson current through a junction was calculated analytically in the quasiclassical approximation for the microscopic theory of superconductivity. The calculation gives the following expression for the Josephson supercurrent through the SISIS tunnel junction [1]

$$j = \frac{\pi}{4} e \mathrm{v}_F N_F \frac{\Delta D \sin\varphi}{\sqrt{1 - D\sin^2\frac{\varphi}{2}}} \tanh \frac{\Delta\sqrt{1 - D\sin^2\frac{\varphi}{2}}}{2T}.$$

Here $N_F = \frac{3}{4}\frac{n}{E_F}$ is the density of states at the Fermi surface, φ – the phase difference across the junction. The transparency of the junction D is given by the expression

$$D = \frac{8\kappa^4}{(8\kappa^4 + 4\kappa^2 + 1) + (4\kappa^2 - 1)\cos(2p_z d) + 4\kappa\sin(2p_z d)}, \quad \kappa = \frac{p_F}{2m\alpha},$$

where α is a delta-Dirac potential barrier constant.

The value of the supercurrent through the SISIS junction differs significantly from the current in the case of the SIS-junction. The value of the supercurrent has non-monotonous dependence on the distance between barriers, with the presence of resonance peaks (see Figure 1). This is related to the resonant tunneling of Cooper pairs through a double-barrier structure.

When the thickness of the interior superconducting layer (in $\hbar = 1$ units) satisfies the condition

$$p_F d_{\max} = \frac{1}{2}\left(-\operatorname{arctg}\frac{4\kappa}{4\kappa^2 - 1} + 2\pi n\right), \quad n \in N,$$

then the current reaches maximum values.

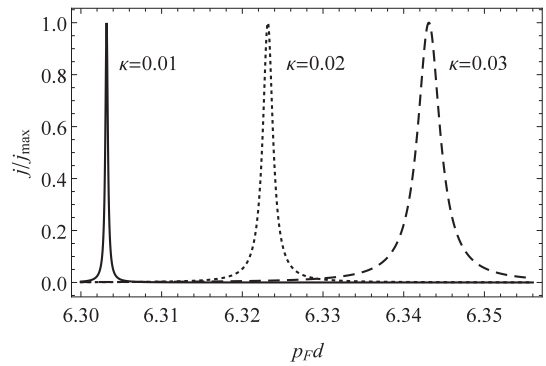

Figure 1: Dependence of current density on the distance between the barriers (interior superconducting layer thickness) at different values $\kappa = \frac{p_F}{2m\alpha}$; for $\kappa = 0.01$ the maximum current (transparency) occurs at $p_F d \simeq 6.30$ (solid line), for $\kappa = 0.02$ at $p_F d \simeq 6.32$ (dotted line), and for $\kappa = 0.03$ we get $p_F d \simeq 6.34$ (dashed line)

Minimum values of the current were observed when

$$p_F d_{\min} = \frac{1}{2}\left(\pi - \operatorname{arctg}\frac{4\kappa}{4\kappa^2 - 1} + 2\pi n\right), \quad n \in N.$$

Typical insulators used for the tunnel junctions (*e.g.* Al_2O_3) are about 10–20 nm in thickness. The barrier height is about 1–5 eV. Hence, the constant α for the delta-Dirac potential is about $(1\text{–}10) \times 10^{-8}$ eV·m. Since the Fermi energy for metals is about 2–10 eV, then the parameter κ takes on the values $(5\text{–}30) \times 10^{-3}$. In the case of $\kappa = 0.01$ the value of the supercurrent would be maximum when $p_F d_{\max} \simeq 0.019$, $p_F d_{\max} \simeq 3.161$, $p_F d_{\max} \simeq 6.303$, $p_F d_{\max} \simeq 9.444$ etc. For the niobium-based junction with $p_F \simeq 2.192 \times 10^{-13}$ kg·ms^{-1}, the thicknesses of the interior superconducting layer that corresponds to the maximum of transparency are $d_{\max} \simeq 1.5$ Å, $d_{\max} \simeq 3$ Å, $d_{\max} \simeq 4.5$ Å, etc.

Another feature of the supercurrent in a double Josephson junction is that it exhibits a non-sinusoidal current-phase relation. The current-phase relation for the SISIS-junction at different values of transparency D is shown in Figure 2.

The value of critical current $j_{\max}$ can be found as an extremum of the supercurrent with respect to the phase difference φ. For the critical values of the superconducting phase difference we find

$$\varphi_{\max} = \arccos\left[1 - \frac{2}{D}\left(1 - x^2\right)\right],$$

where x is a root of the transcendental equation

$$\operatorname{sh}\left(\frac{\Delta}{T}x\right) = \frac{\Delta}{T}\frac{x^2(1-x^2)(1-D-x^2)}{1-D-x^4}.$$

Let us compute the critical current at $T = 2.5$ K for a junction based on niobium with the energy gap $\Delta \simeq 3$ meV, the critical temperature $T_c \simeq 9.5$ K, the density of

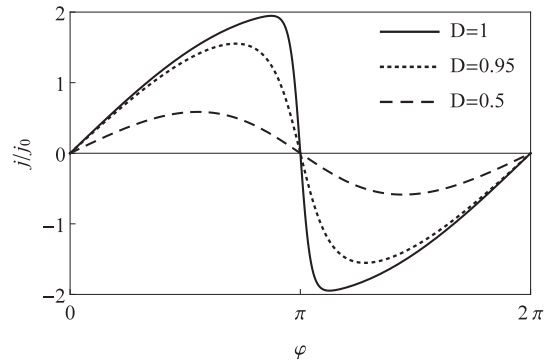

Figure 2: Current-phase relation curves for SISIS-junction at different values of transparency D; the current density is normalized to $j_0 = \frac{\pi}{4} e \mathrm{v}_F N_F \Delta$

states $N_F \simeq 5.56 \times 10^{28}$ m^{-3}, and the Fermi velocity $\mathrm{v}_F \simeq 1.37 \times 10^6$ ms^{-1}. For this case $\Delta/T \simeq 14.2$ and

$$j_0 = \frac{\pi}{4} e \mathrm{v}_F N_F \Delta \simeq 4.59 \ \mu\mathrm{A/m}^2.$$

For the case of perfect transparency, $D = 1$ the root $x \simeq 0.23$ and $\varphi_{\max} = 2.67$, then we have $j_{\max} \simeq 1.94 j_0 \simeq 8.9 \ \mu\mathrm{A/m}^2$. For $D = 0.5$ we obtained $x \simeq 0.84$, $\varphi_{\max} = 1.75$, $j_{\max} \simeq 0.59 j_0 \simeq 2.7 \ \mu\mathrm{A/m}^2$.

In [2] for identifying the behavior of SISIS double-barrier Josephson junctions the skewness S in the current-phase relation has been defined as follows

$$S = \frac{2}{\pi} \varphi_{\max} - 1.$$

The skewness in the current-phase relation of the supercurrent is shown in Figure 3.

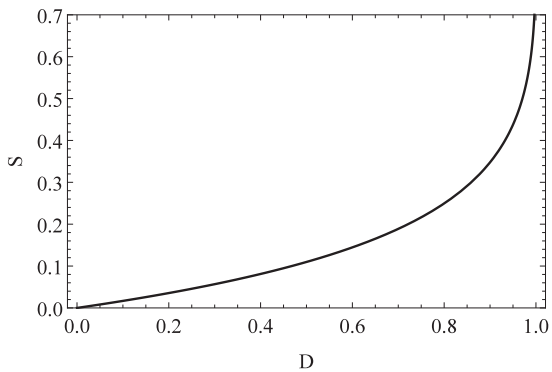

Figure 3: Skewness in the current-phase relation of a SISIS superconducting structure as a function of transparency D

The dependence of the critical current density $j_{\max}$ on skewness S is approximately linear (see Figure 4). The linear increase in the skewness with a critical current was

observed experimentally for Josephson junctions having a graphene barrier obtained by the phase-sensitive SQUID interferometry technique [3].

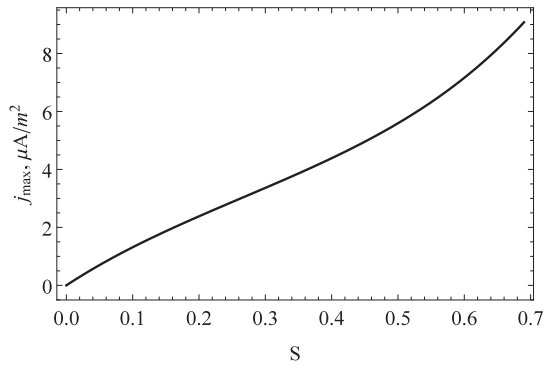

Figure 4: Critical current density $j_{\max}$ versus skewness S plot; the skewness linearly increases with the critical current

References

[1] Shygorin P, Svidzynskyi A, Materian I 2017 *Ukr. J. Phys.* **62** (6) 518
[2] De Luca R 2011 *Phys. Lett. A* **375** (24) 2441
[3] English C, Hamilton D, Chialvo C, Moraru I, Mason N, Van Harlingen D 2016 *Phys. Rev.* **B 94** (11) 115435

Dynamics in Crowded Environments

A. Sikorski[1], P. Polanowski[2]

[1] *Department of Chemistry, University of Warsaw*
Pasteura 1, 02-093 Warsaw, Poland

[2] *Department of Molecular Physics, Technical University of Łódź*
Żeromskiego 116, 90-924 Łódź, Poland

Computer simulation studies of dynamics in two-dimensional systems are presented. The motion of small probe molecules in model disordered systems was studied by means of Monte Carlo simulations. We performed extensive and systematic simulation studies of the two-dimensional fluid motion in a complex crowded environment. In contrast to other works we focused on cooperative phenomena that occur where the motion of particles takes place in a dense system [1]. Our main goal was to answer the following question: How do fluid molecules move in an environment that has a complex structure while the motion of fluid molecules is highly correlated? The lattice model was used and the Dynamic Lattice Liquid algorithm was then employed for these studies [2]. This algorithm can work with the highest possible density where all lattice sites are occupied and it allows taking into account coincidences of elementary molecular motion attempts resulting in local cooperative structural transformations. The following disordered systems were studied: small immobile obstacles, mobile (Brownian) obstacles and polymer chains. Both static and dynamic properties of the model systems were characterized [3,4]. The short- and long-time dynamic behavior of solvent molecules was also described. The influence of the mobility of obstacles, their density, the chain length and the polymer concentration on the mobility and the character of motion of small molecules were studied. The conditions of the appearance of anomalous diffusions and the recovery to the Fickian behavior in such systems were discussed.

Acknowledgements
The computational part of this work was done using the computer cluster at the Computing Center of the Department of Chemistry, University of Warsaw. This work was partially supported by the Polish National Science Center Grant UMO-2013/09/B/ST5/00093.

References

[1] Ben-Avraham D, Havlin S 2000 *Diffusion and reactions in fractals and disordered systems*, Cambridge University Press, chapt. 6
[2] Polanowski P, Pakula T 2003 *J. Chem. Phys.* **118** 11139
[3] Polanowski P, Sikorski A 2014 *Soft Matter* **10** 3597
[4] Polanowski P, Sikorski A 2016 *J. Phys. Chem. B* **120** 7529

A model of Non-Destructive Diagnostics of Inhomogeneously Distributed In-Depth Macrostrains and Microdefects in Functional Materials

O. S. Skakunova, V. B. Molodkin, V. V. Lizunov, S. V. Lizunova, Ye. M. Kyslovs'kyy, O. V. Reshetnyk, T. P. Vladimirova, K. V. Fuzik

G. V. Kurdyumov Institute for Metal Physics, N.A.S. of Ukraine
Ac. Vernadsky Av. 36, 03142 Kiev, Ukraine

A quantum-mechanical model of diffractometry for complex systems with inhomogeneously distributed microdefects of many types and macrostrains of different nature, in particular, for products based on ion-implanted garnets was developed. The instrumental factors as well as both the amplitude mechanism and a more sensitive dispersion mechanism of the influence of structure imperfections and their distribution inhomogeneity on the pattern of multiple radiation scattering were taken into account.

The peculiarities of the essential demonstration of structure inhomogeneities in the scattering pattern were determined analytically. It was shown that this demonstration was caused by colossal (due to the dispersion mechanism) amplification of the influence of inhomogeneities and, at the same time, diffraction conditions on multiple scattering effects.

In particular, the possibility of an additional increase in the informativity of diagnostics of structure inhomogeneities resulting from the dispersion mechanism was theoretically demonstrated and practically implemented. By controlled discrete changes of the conditions and methods of diffraction, the maximum contribution of inhomogeneously distributed macrostrains and microdefects was provided consistently for each of their types both in the scattering pattern and its dependences on continuous changes of other experimental conditions in garnet systems.

Influence of Metal Admixtures on Structure-Sensitive Properties of Sn-Ag-Cu Alloys

V. Sklyarchuk[1], Yu. Plevachuk[1], B. Sokoliuk[1], A. Yakymovych[2]

[1] *Department of Metal Physics, Ivan Franko National University of Lviv Kyrylo i Mephodiy 8, 79005 L'viv, Ukraine*

[2] *Department of Inorganic Chemistry – Functional Materials, University of Vienna Waehringer 42, 1090 Vienna, Austria*

The Sn–Ag–Cu alloys are favorable Pb-free solders widely used in the electronics industry, and a number of studies relating to the improving of the characteristics of those alloys have been carried out. Minor additions of a fourth element comprise a widely employed method to achieve better mechanical properties of the solder joints employing the Sn–Ag–Cu solder. The viscosity and electrical conductivity, as the structure-sensitive transport properties of the liquid state, are important for the modeling of melting and solidification processes. Furthermore, these quantities bring additional information about the influence of a different type of impurities on the structure and physical properties of the metal matrix in the liquid state. The impact of minor Co and Ni impurities on the transport properties of the Sn–3.8Ag–0.7Cu liquid solder were studied based on the viscosity and electrical conductivity measurements. The obtained increase in the viscosity values by minor Co and Ni additions was in agreement with the modeling data using thermodynamic approaches. The behavior of the electrical conductivity was interpreted in the context of the s-d hybridization model.

Structure of CaO-Al_2O_3-SiO_2 Melts

V. E. Sokol'skii[1], D. V. Pruttskov[2], V. M. Busko[2], V. P. Kazimirov[1], O. S. Roik[1], A. D. Chyrkin[1]

[1] *Taras Shevchenko National University of Kyiv*
Volodimirska 64/13, 01601 Kyiv, Ukraine

[2] *ZAO Tekhnokhim*
Nezavisimoy Ukraini 42a, 69037 Zaporozhye, Ukraine

The CaO-Al_2O_3-SiO_2 oxide system is one on the most important slag compositions. Such slags encountered in blast-furnace cast process are used as welding fluxes, etc. The oxide compounds existing in this system such as *e.g.* helenite, anorthite and mullite are well known. However, the data on the CaO-Al_2O_3-SiO_2 melt structure is rather scarce.

Three samples were selected for structural analysis using the X-ray diffraction technique. Two selected compositions of samples 1 and 2 were triple eutectics and sample 3 was a nonvariant point [1].

The general conclusions on the system studied are reduced to the following:

- Silicon and aluminium are tetrahedrally coordinated by oxygen in the studied slag melt. However, a small fraction of aluminium silicon atoms form oxygen octahedrons. The interatomic spacing values for the Si-Si and Al-Al bonds in the melts are in good agreement with the literature data for crystals and other molten oxide systems. The closest environment around the calcium ion Ca^{2+} consists of oxygen atoms, the interatomic spacing being 0.22–0.23 nm. The coordination number for calcium varies from 7.7 to 11.8.

- The interatomic interaction as well as the atom distribution in the considered system cannot be viewed as solely of the fluid type. In our opinion, a heterogeneous mixture consisting of aluminosilicate nanocrystallites immersed in a molten oxide matrix exists in the molten slag of the studied compositions at higher temperatures.

- A model was proposed to describe the structure of such quasi-fluids which contain nanoscale aggregates. The aggregate consists of the oxygen framework containing silicon and aluminium atoms forming a nanocrystallite of the mullite or sillimanite type in the core.

- The tetrahedral voids of the oxygen framework are filled with silicon and partially with aluminium cations. A negligible fraction of the octaghedral voids is occupied exclusively by aluminium ions. The calcium cations are surrounded in turn by surface oxygen of a framework constructing thus the core. The oxygen of the molten slag matrix along with the oxygen of the nanoaggregate framework form the closest environment of the calcium ions building up the particle.

- Three phases were detected in sample 1 annealed at 1873 K and subsequently exposed for 1 h at 1373 K: mullite, silica and $CaSiO_3$. This finding confirms the assumption of the mullite-based structure of the nanocrystalline phase.
- Since the XRD patterns of mullite and sillimanite are quite similar, none of them can be preferred when interpreting the diffraction results. However, mullite might be preferable as it is known to be stable at higher temperatures.

Physics is the Science of the Future

B. Sus[1], V. Synyushko[2]

[1] *Department of Mathematics and Physics*
Military Institute of Telecommunications and Informatization
Moskovska 45/1, 01011 Kyiv, Ukraine

[2] *National Academy of Public Administration, Office the President of Ukraine*
Sukhomlynskoho 16, 79491 L'viv, Ukraine

Physics is both a fundamental experimental science and philosophy. It is one of the most ancient natural sciences and a very important science of the future which contains the answer how to save humanity, and maybe all living beings. Humans should improve themselves in order to survive. Our world, the Sun, and the Earth formed about 5 billion years ago. However, the Sun is not eternal. Thermal nuclear processes will end one day, and the life on the Earth will be impossible. Humanity will look for a solution, and it has already started to work on it, however, in a subconscious way. There is a collective conscience formed. There has been a tremendous development of technology during the past 100 years, radio, TV, computers, cellular phones and more. People have landed on the Moon, reached Mars, and they are developing the nanotechnology now. People could not even imagine this 100 years ago. What will happen in the next 100 years? Physicists will have super-tasks to transfer life beyond the Earth, to different worlds. Adequate technologies will be needed. People will need to learn to develop optimal ways of organization and development of life. Therefore, humanity needs to care for education and science even in the worst conditions because it is the way to solve problems of life and development. It is especially physics that needs to be developed because it is a practical and philosophical science. It is the science of the present and of the future. There many problematic philosophical issues in physics, which were first formulated actually 100 years ago, and have not been not solved still until today. Their solution means future development. Here are some of them:

1. According to the modern understanding, the foundation of the world is the substance called "matter." Matter exists in two forms: substance and field. The substance can be water, stones, sand, celestial bodies, the Moon, the stars. The field could be electrical, magnetic, electromagnetic, gravitational. The electromagnetic field contains electromagnetic waves, *i.e.* light, radio-waves, gamma-rays. It is important that the matter moves perpetually. There is a problematic question whether there is such a movement as a continuous transformation of one kind of matter into another

2. Electromagnetic fields, light, in particular, have a dual nature: waves and particles at the same time. Waves are a dimensional phenomenon, but particles are located in a very certain place in space. How can this happen at the same time?

(Albert Einstein and Leopold Infeld. The evolution of physics. – New York: Simon and Schuster. 1954).

3. Another problem: if light is waves, in what substance are the waves spreading? If light is particles, how do they oscillate?

4. It is known that an electromagnetic wave is the oscillation of electric and magnetic fields, which have energy. When fields oscillate, energy should oscillate too. The problem question: into what does energy transform in the process of oscillation? The energy changes, but it should stay the same as a result of the conservation of energy law!

5. Electromagnetic fields are created by electric charge. What is charge as physical matter?

6. The uniform motion of a particle in quantum mechanics is known as the de Broglie wave. Where is the oscillating movement in the de Broglie wave? What is exactly oscillating?

7. We know two kinds of interaction between two physical bodies, through the substance and by the exchange of particles. Both kinds of interaction produce the repelling of the bodies. However, how to understand the mechanics of gravitational attraction?

We have brought up only a few fundamental questions of a philosophical nature. Future development and direction of understanding of the physical qualities of nature depend a lot on these fundamental questions. The problem is that traditional science addresses only one nature of waves, *i.e.* their propagation in the substance. In reality, there are two different natures of waves: waves as oscillations of the substance (water, air, "ether"), and also it is a flow of particles which have inner oscillations within themselves. In particular, light is the flow of particles (photons), which have inner oscillations: energy-mass-energy-mass [1].

References

[1] Sus B A, Sus B B, Kravchenko O B 2012 *Unusual interpretation of traditional physics problems. The third scientific-methodological edition*, PC "Prosvita", Kyiv

Amino Acids as Growth Inhibitors of Calcium Oxalate Monohydrate Crystals

Y. V. Taranets, O. N. Bezkrovnaya, I. M. Pritula

Institute for Single Crystals, NAS of Ukraine
Nauky Ave. 60, 61001 Kharkiv, Ukraine

The study of crystallization processes in biological fluids is a promising direction of research. It makes it possible to find out mechanisms that can influence the formation of pathogenic crystals. Such a crystal is calcium oxalate monohydrate (COM) which is found in kidney stones. The growth of COM crystals is influenced by various molecules, for example, amino acids, which are present in the human biofluid (urine). They can inhibit and promote the growth of COM crystals [1].

The aim was to study the COM crystallization in vitro in the presence of amino acids – L-aspartic acid (L-asp), L-arginine (L-arg) and L-threonine (L-thr). The model system was close to the physiological conditions [2]: 37°C, the ionic strength of 0.15 M, pH 5.8. The concentration of amino acids was 1–20 mM. The COM powders were investigated by X-ray diffraction, IR-spectroscopy and scanning electron microscopy.

It was found that the molecules of L-asp, L-arg and L-thr amino acids exhibited an inhibitory effect on the growth processes of COM crystals. The crystal size with an addition of amino acids was two times less than that of pure COM crystals. The degree of inhibition increased in proportion to the increase in the concentration of amino acids in the solution. This fact is due to the adsorption of amino acids on the growing faces of COM crystals and blocking the COM molecules of these faces.

References

[1] He J, Lin R, Long H, Liang Y, Chen Y 2015 *J. Colloid Interface Sci.* **454** (1) 144
[2] Ogawa Y, Miyazato T, Hatano T 2000 *World J. Surg.* **24** (10) 1154

Problems of Modeling Structural Phase Transformations in Relaxed Optics

P. P. Trokhimchuck

Department of Theoretical and Mathematical Physics
Lesya Ukrayinka East European University
Voly av. 13, 43025 Lutsk, Ukraine

The problems of modeling laser-induced phase transformations in irradiated matter are very difficult [1]. The creation of laser-induced surface nano- and microstructures may be of a various nature [1]. These structures have various geometrical sizes and physical properties and structural symmetry.

For example, laser-induced nanostructures on silicon have sizes from 15–20 nm (nanosecond pulse Nd-laser irradiation with wavelength 1064 nm [1]) to 2000–3000 nm (series nanosecond eximer KrF-laser irradiation with wavelength 248 nm [2]). Hexagonal nanocolumns 150–200 nm in height were created on a diamond germanium substrate after Nd-laser irradiation (wavelength 532 nm) by the second harmonic of nanosecond pulses [2]. Using femtosecond laser irradiation with wavelength 800 nm the silicon allowed receiving surface nanocolumns 450 nm in height [1].

These results may be modeled and explained on the basis of a cascade model of optical excitation of proper chemical bonds in the regime of saturation excitation [1]. This model allows estimating the intensity of irradiation for the creation of proper solid state structures from the crystal to quasicrystal and amorphous symmetry. For the case of light absorption on stable centers we must have a next chain of transformation of silicon with diamond symmetry: diamond, hexagonal, triclinic, monoclinic, quasicrystals and amorphous. The estimation of the distribution energy for the case of the silicon Nd-laser irradiation by of series of nanosecond pulses confirms this scenario.

The temporal characteristics of irradiation do not have any notable influence for the case of light absorption on unstable and metastable centers. In this case we can use stationary regimes of irradiation. The methods of estimating the energy regimes of irradiation are analogous to the previous case [1]. These concept explains the positive effect of Nd-laser annealing of ion-implanted layers of silicon [1].

Hence, an effective method of modeling the creation of laser-induced nano- and microstructures must be based on the cascade model of step-by-step excitation of the proper chemical bonds in the regime of saturation of the excitation [1].

References

[1] Trokhimchuck P P 2016 *Relaxed Optics: Realities and perspectives*, Lambert Academic Publisher, 250
[2] Pedraza A G, Foulkes M D, Lowndes D H 1999 *Appl. Phys. Lett.* **74** (16) 2422
[3] Trokhimchuck P P 2017 *IJARPS* **4** (2) 37

Magnetic Studies of Nanocrystalline Iron Samples

J. Typek, G. Zolnierkiewicz, N. Guskos

Institute of Physics, West Pomeranian University of Technology
Al. Piastow 48, 70-311 Szczecin, Poland

Five nanocrystalline iron samples with different average sizes (from 20.5 to 35 nm) and different distributions of sizes were synthesized by fusing magnetite with promotors. Magnetisation measurements in the 4–300 K range in field-cooled and zero-field-cooled modes and isothermal (at $T = 2$ K and 300 K) magnetisation in magnetic fields up to 70 kOe provided many magnetic characteristics correlated with very complex morphologies of the samples. The temperature dependences of the χ_{ZFC} and χ_{FC} curves measured in low magnetic fields indicated that the blocking temperature T_B for all our samples was above room temperature, what was expected for strongly agglomerated nanoparticles as was the situation in our samples where strong dipolar interaction acted among nanoparticles. In effect, the system of magnetic nanoparticles was in a blocked state in all our samples in the investigated temperature range. The observed behavior of the χ_{ZFC} and χ_{FC} curves was compatible with a broad distribution of particle sizes which started exhibiting a superparamagnetic regime at different temperatures. The isothermal magnetisation $M(H)$ (at $T = 2$ and 300 K) for all samples showed a narrow hysteresis loop typical for certain ferromagnetic materials. A particular value of M_S was influenced by the following main factors: the magnetite content, the average nanoparticle size and the magnitude of nanoparticle size distribution. The magnetite content in our iron samples was the most important factor determining the M_S value – the higher the Fe_3O_4 concentration the smaller the resulting M_S. Moreover, for smaller nanoparticles the effects of the surface disorder diminishing M_S were more important, thus larger nanoparticles displayed higher M_S than smaller nanoparticles.

Additional magnetic properties of the investigated nanocrystalline powders were obtained by the study of ferromagnetic resonance (FMR) spectra taken at room temperature. The FMR spectrum was analyzed by the decomposition of the observed strongly anisotropic line on three (or four) components representing different magnetic entities. Due to the very complicated morphology of our samples no simple correspondence of these components to specific magnetic units could be established. In general, the most intense low field component might be attributed to smaller, superparamagnetic nanoparticles forming elongated clusters along the applied field and to larger, blocked nanoparticles forming superferromagnetic clusters with their easy axes along the applied field. The other two spectral components could be attributed to the blocked nanoparticles forming clusters of different spatial anisotropy (from nearly spherical to very elongated). The intensity of the FMR line seems to be proportional to the content of the superparamagnetic, small nanoparticles. The morphology and a strong interparticle interaction appear to be the main factors that determine the magnetic characteristics of our samples.

Magnetic Properties of Graphene Oxide/Magnetite Nanocomposites in Concentrated Form and Dispersed in Polymer Matrix

J. Typek, G. Zolnierkiewicz, N. Guskos, A. Szymczyk

Institute of Physics, West Pomeranian University of Technology
Al. Piastow 48, 70-311 Szczecin, Poland

Three samples: a graphene oxide/magnetite ($GOFe_3O_4$) nanocomposite in a concentrated powder form and dispersed in a PTT-PTMO polymer matrix (at 0.3 and 0.5 wt%, samples designated as PTT-PTMO/0.3$GOFe_3O_4$ and PTT-PTMO/0.5GO Fe_3O_4, respectively) were studied by SQUID dc magnetometry in the 2–300 K temperature range in the zero-field-cooled (ZFC) and field-cooled (FC) modes in magnetic fields up to 70 kOe as well as by magnetic resonance spectroscopy, using a conventional X-band Bruker E 500 spectrometer in the 90–290 K range.

The $\chi(T)$ curves showed very similar thermal behaviour of magnetisations in both polymer samples. On the other hand, a comparison of the magnetic susceptibilities of both polymer samples with the $GOFe_3O_4$ sample revealed a significant difference – the polymer samples seemed to display two blocking temperatures, because two shallow maxima could be discerned in the χ_{ZFC} curves, while only one maximum was visible in the χ_{ZFC} curve of the $GOFe_3O_4$ sample. Thus, the procedure of synthesis of polymer samples affected to some degree their magnetic properties producing a bimodial-like distributon of blocking temperatures. A simple explanation of this phenomenon involves the presence of a magnetite-polymer interface that produces a core-shell structure of magnetite nananoparticles. Isothermal magnetisationat $T = 2$ K in magnetic fields up to 70 kOe showed hysteresis loops because at that temperature the samples were in a blocked, ferromagnetic state. The $M(H)$ curve for $GOFe_3O_4$ was analysed as composed from two components: ferromagnetic, saturated below 20 kOe and paramagnetic described by the Langevin function. The saturation magnetisation of the ferromagnetic component was determined to be 99 emu/$g_{(Fe_3O_4)}$ and the paramagnetic moment 2.7 μ_B/Fe. The coercive field was roughly three times and the M_R/M_S ratio was two times larger in the polymer samples in comparison with $GOFe_3O_4$. Enhancement of the coercive field in both polymer samples might be explained by a greater contribution of the shape anisotropy in these samples. A small value of the M_R/M_S ratio in $GOFe_3O_4$ might indicate a smaller size of magnetic clusters in comparison with the polymer samples.

The spectra registered by magnetic resonance were regarded as FMR (ferromagnetic resonance). All the registered FMR spectra were dominated by an intense, broad and asymmetrical line, reflecting very complex spatial arrangements of magnetic particles and a broad range of different interactions in which they were involved. The

spectra were decomposed on components described by two Gaussian lineshape functions. As a result of fitting the values of the resonance field, the linewidth and amplitude of each component were obtained at specific temperatures. A different splitting of the two components in polymer as compared to $GOFe_3O_4$ samples (large for the former and small for the latter) and a different shift of the split components from the magnetic field H_{r0} corresponding to $g = 2$ (no internal field, superparamagnetic case) was observed in both types of the samples. The reasons for these differences should be searched in morphological differences between $GOFe_3O_4$ and both polymer samples. A large shift of the resonance line from H_{r0} in $GOFe_3O_4$ could be explained by an agglomeration of magnetite nanoparticles in that sample and a large split of two components in both polymer samples by a significant contribution of the surface energy due to a strong polymer and magnetite interface. The temperature dependence of the normalized (at RT) integrated FMR intensities I_{FMR} (calculated as the sum of two components) showed some very interesting behaviour. Initial cooling from RT caused a slight increase in I_{FMR}, but near 260 K a very rapid drop in the FMR intensity was observed for all the three samples. The magnitude of this decrease was slightly smaller for $GOFe_3O_4$ (40% drop) than for both the polymer samples (60% drop). This might be explained by a relatively more intense FMR spectrum of the latter samples at high temperatures in comparison to the $GOFe_3O_4$ sample. On further cooling the I_{FMR} curve levelled down and below 120 K started to slowly increase with a temperature decrease. This increase was probably correlated with an increase in magnetisation with the temperature decrease observed in the SQUID magnetisation studies.

Spectral Sensitization of Heterophase Microsystems "CaF_2-Core-AgBr-Shell" by Dyes

A. V. Tyurin, S. A. Zhukov, A. Yu. Akhmerov, V. P. Churashov

Scientific Research Institute of Physics, Odessa National I. I. Mechnikov University
Pastera 27, 65082 Odessa, Ukraine

The spectral sensitization technology of heterophase "nonsilver core – silver haloid shell" microsystems that allows fixing a dye at both molecular and/or J-aggregated stages on the internal as well as external surfaces of a light sensitive shell has been proposed. The creation of heterophase "nonsilver core – dye – silver haloid shell – dye" microsystems is proved by the results of the spectrosensitometric and luminescence characteristics including the depth and surface development of the exposed layers.

It has been shown that a J-aggregated dye disposed on the internal surface of an AgBr shell by comparison of the same on the external shell surface extends the spectral sensitivity area in the long wave region due to the absence of interaction of the dye molecules and J-aggregates under light excitation. The silver haloid shell spatially separates not only the J-aggregated and molecular phases of the dye but even different dye sensitizers the mutual appliance of which leads to desensitization of the emulsion. Anionic dye interaction with the core also essentially changes the relaxation nature of the dye photoexcitation in the investigated microsystems. As a result, a concentration of neutral silver clusters on the external AgBr – shell surface decreases and a most significant change is achieved at the emulsion exposure by the light from the J-aggregate dye absorption region.

Effect of Changing Isovalent Binary Alloys Parameters on Sizes of Regions with Homogeneous Magnetization

M. V. Ushakov[1], T. S. Len[2], V. V. Lizunov[3], E. G. Len[3], V. A. Tatarenko[3]

[1] *Taras Shevchenko National University of Kyiv*
Volodymyrska 64, 01601 Kyiv, Ukraine

[2] *National Aviation University*
Kosmonavt Komarov 1, 03058 Kyiv, Ukraine

[3] *G. V. Kurdyumov Institute for Metal Physics, NAS of Ukraine*
Ac. Vernadsky Av. 36, 03142 Kiev, Ukraine

The sizes of regions with homogeneous magnetization of binary b.c.c. alloys with substitutional disorder are investigated in dependence on isovalent alloys parameters changing within the scope of the generalized single-band Hubbard model. The breaking of the translation invariance of the alloys due to the atomic disorder leads to a violation of the electron-hole symmetry, which results in both the threshold character of the antiferromagnetic ordering at half filling and the asymmetry of the magnetic phase diagrams of the alloys relative to the corresponding value of the average electron density per one site [1]. A different advantageous order for filling the Hubbard subbands of the alloy components, A and B, with the increasing average electron density per one site, which is determined by the sign of scattering potential of impurity, in the general case, results in an asymmetry (relative to the point with equal concentrations of alloy components) of the dependences of the magnetic characteristics on the concentration of component A in isovalent alloys [2]. As found in the present work, the dependences of the sizes of regions with homogeneous magnetization on alloy parameters are determined by the corresponding changes of the equilibrium values of the magnetic order parameter. The latter is calculated by the free energy minimization procedure taking into account the changes in the electron density state of the infinite bulk sample. The dependences of the sizes of regions with homogeneous magnetization on the different values of the scattering potential of impurity, the energy parameter of the Coulomb repulsion of electrons with opposite spins at the one site (the rate of electron-electron correlation), the average electron density per one site, and the concentrations of alloy components are investigated. As demonstrated, the asymmetric concentration dependences of localized magnetic moments and charge densities at the lattice site do not influence significantly the concentration dependence of the size of regions on the homogeneous magnetization.

References

[1] Lizunov V V, Len E G, Melnyk I M, Ushakov M V, Len T S, Tatarenko V A 2014 *Metallofiz. Noveishie Tekhnol.* **36** 575
[2] Len E G, Lizunov V V, Len T S, Ushakov M V, Tatarenko V A 2015 *Metallofiz. Noveishie Tekhnol.* **37** 1405

Modeling of Electronic Properties of Stage Ordered Layered Structures Intercalated by Complex Particles

O. V. Velychko, I. V. Stasyuk

Institute for Condensed Matter Physics, National Academy of Sciences of Ukraine
Svientsitskii 1, 79011 L'viv, Ukraine

Layered semiconductors are well known materials investigated for decades. They posses the remarkable feature of easy intercalation in the space between layers without any significant change in volume. There is a technology of stage ordering of a host compound (monochalcogenides of indium and gallium in our case) aimed at better penetration of intercalant particles into the matrix as well as a possibility of intercalation of large molecular groups like oligo-dimethylamino-methacrylate. Such stage ordering is perpendicular to the host layers with a significant increase in the distance between packets (mostly three layers in a packet in the considered case [1].

Changes in the electronic band structure of the stage ordered layered nanohybrid compound of the GaSe-type due to intercalation by some particles (having, in general, a complex electron spectrum) are studied within the model which is a simplified version of the periodic Anderson model. The principal restructuring of the electron spectrum and the respective density of states consist in additional splitting, emergence of a gap (or pseudogap) and appearance of a single impurity band in addition to the main one. Being far enough from the main band, the impurity band degenerates into the impurity level. Approaching each other they hybridize with the reconstruction of the respective edge of the main band.

In the case, when the single-electron energy spectrum of the impurity particle is approximated by the density of states of the model shape, the full spectral density is smeared out. The singularities of the total density of states (DOS) gradually smear out with an increase in the parameter that characterizes the local level broadening degree, the hybridization gap in the energy spectrum disappears, and the three-step structure of density of states near the energy band edge becomes less distinctive. Similar changes in the DOS take place with an increase in the intercalant concentration [2].

The applied approaches greatly simplify the internal energy structure of intercalated particles but they allow obtaining expressions for the electron excitation spectrum and the density of states in an analytic form. The obtained results provide a good qualitative description of the intercalation effect on the electron subsystem of intercalated stage ordered layered crystals.

Knowledge of the total density of states allows calculating the electron quantum capacitance of the considered intercalated layered compounds [3]. In the low temperature limit the frequency dispersion of the DOS determines the field (voltage) dependence of the quantum capacitance, which strongly depends on the localization of the impurity bands, the strength of electron hybridization and the temperature.

References

[1] Grygorchak I I, Matulka D V, Ivashchyshyn F O, Zaichenko O S, Mitina N Ye, Moskvin M M 2012 *Phys. Surf. Eng.* **10** 256
[2] Grygorchak I I, Kostrobiy P P, Stasyuk I V, Tokarchuk M V, Velychko O V, Ivashchyshyn F O, Markovych B M 2015 *Physical processes and their microscopic models in periodic inorganic/organic clathrates*, Rastr-7, Lviv, 285 (in Ukrainian)
[3] Stasyuk I V, Velychko O V 2015 *Math. Mod. Comput.* **2** (2) 191

New Carbon Architectures for Molecular Storage Devices of Electric Energy

B. Venhryn[1], I. Grygorchak[1], S. Mudry[2], P. Shygorin[3]

[1] *Department of Applied Physics and Nanomaterials Science*
Lviv Polytechnic National University
Bandera 12, 79013 Lviv, Ukraine

[2] *Physycs of Metals Department, Ivan Franko National University of Lviv*
Kyrylo i Mephodiy 8, 79005 L'viv, Ukraine

[3] *Department of Theoretical and Mathematical Physics*
Lesya Ukrainka Eastern European National University
Volya Avenue 13, 43025 Lutsk, Ukraine

Carbon is a promising material for electric energy storage devices due to a variety of its allotropic modifications and morphologic types. Carbon electrodes show a good polarizability, are chemically inert, have good thermodynamic stability over a large temperature range, and it is very important that the amphoteric behavior of carbon allows this material to be used both as anode and cathode.

Taking into account the conceptual approaches in the supercapacitor technology the first problem is to reach a high value of the active surface forming the high porosity of the material. Since the initial carbon materials do not have such a large specific surface, the problem arises how to increase this surface, or in other words, how to activate it.

During the activation process sealed pores are opened and the porous structure of the material develops as a result. Changing the kind of the carbon raw material and the conditions of activation (temperature, duration and the type of atmosphere) it is possible to control the volume of pores, their distribution and topology.

It should be also noted that the hydrophilic-hydrophobic properties of carbon materials, which generally depend on their electron structure, are very important for the optimization of porous electrodes.

Thus, a more effective charge and energy accumulating in a double electric layer at the electrolyte- nanoporous carbon boundary is related to the use of new methods of modification of the porous and electron structure.

In this work we present the results of the investigation of various kinds of carbon materials as well as new methods of their modification (intercalative modification, ultrasonic and microwave electromagnetic irradiation, etc.) which allows synthesizing new carbon architectures which can be used to manufacture electric energy storage devices.

Simulation of Resonant Structures by Tools of Supersymmetric Quantum Mechanics

O. M. Voznyak, O. O. Voznyak

Department of Physics and Chemistry of Solids
Vasyl Stefanyk Precarpathian National University
Shevchenko 57, 76018 Ivano-Frankivsk, Ukraine

Proceeding in the direction of miniaturization modern microelectronics has come to the so-called quantum technologies which are based on the use of quantum wells, dots and their complexes. One of the areas of quantum engineering is the creation of cascades of quantum barriers or wells which can be overcome by electrons without reflection. This is the so-called resonance tunneling through quantum barriers, which is possible only at certain electron energy values.

Moving in the direction of further microelectronic miniaturization of systems will lead to the application of such processes in which single wells or barriers will participate. In this case the need arises to consider the so called resonant potentials which can pass through certain energies without reflection. It is the well-known phenomenon of resonance scattering when passing through rectangular potential wells or barriers, but it is also possible during passing through a potential of an arbitrary shape, if it is changing rapidly in some space area.

In this paper, an approach to the investigation of the resonance potentials of an arbitrary form is developed which is based on the representation of the wave function in next form:

$$\psi(x) \sim \exp\left(-\int^x W(x)dx\right),$$

where $W(x)$ – some function which is called superpotential in supersymmetric quantum mechanics, in which we select real and imaginary parts $W(x) = W_R(x) + W_I(x)$, where $W_R(x)$ and $W_I(x)$ – real and imaginary parts of a superpotential

It is known that a complex superpotential leads to a real potential under certain conditions. Thus, by substituting the introduced wave function into a one-dimensional Schrodinger equation and after equating of its real and imaginary parts, we obtain an expression for the wave function

$$\psi(x) = \frac{1}{\sqrt{W_I(x)}} \exp\left(-\int^x W_I(x)dx\right).$$

Now, choosing $W_I(x)$ which satisfies the corresponding boundary conditions on infinity, we obtain the corresponding resonance potentials, which at certain energies are related with the corresponding electron wave number in which the passing of the potential will be without a reflection.

The developed approach was tested on an example of a well-known unreduced Peshl-Teller potential, implemented when selecting $W_I(x)$ in the form

$$W_I(x) = \frac{a^2}{\cosh(ax)^2}\frac{1}{ik - \operatorname{atanh}(ax)} - ik,$$

and some new resonance potentials were obtained.

Electrical Properties of Glasses with Metallic or Semiconducting Nanostructures

L. Wicikowski, L. Murawski

Faculty of Applied Physics and Mathematics, Gdansk University of Technology
Narutowicza 11/12, 80-233 Gdansk, Poland

The reduction in hydrogen is the simplest method to obtain electronic conductivity on a glass surface in silicate and germanate glasses containing lead or bismuth oxide. The reduction process results in a modification of the material structure within a surface-layer (up to 50 μm thick). The modified surface layer consists of a defected continuous silica matrix and neutral heavy-metal atoms, which agglomerate into metallic granules (or nanostructures) inside the layer. When the metal concentration is small and the metal forms nanostructures embedded in an insulating matrix the conductivity is thermally activated with the activation energy of about 0.1 eV. A commonly accepted theoretical model of electrical conductivity in granular metals is based on the process of tunneling of electrons between granules. According to this model, the creation of charge carriers is due to thermal processes leading to the transfer of electrons from one metal granule to a neighboring one. In order to generate a charge carrier, an electron has to be removed from a neutral grain and placed on a neighboring neutral grain. Such process requires energy $W_c = (e^2/d\varepsilon)F(s,d)$, where d is the granule diameter, s is the distance between two granules, ε is the dielectric constant of the matrix, and $F(s,d)$ is a function which depends on the size and distance distribution between granules. Calculations of the activation energy for typical discontinuous metal structures have shown that this value is small, generally below 0.1 eV at room temperature. In this material the conductivity often follows the exponential temperature dependence:

$$\sigma(T) = \sigma_0 \exp[(-T_0/T)^n]$$

where n is usually in the range $0.2 \leq n \leq 1$ and depends on the mechanism of conductivity. This is consistent with the results of dc conductivity measurements in reduced bismuth containing glasses.

Similar behaviour can be observed in glasses containing semiconducting nanostructures. We have found that the conductivity in nanocrystallized V_2O_5-TeO_2 glasses increases several orders in magnitude and the activation energy is low as in the case of granular metals. Recently, Garbarczyk et al. [1] have published several papers presenting the results of conductivity in some nanocrystallized glasses ($90V_2O_5$-$10P_2O_5$, Li_2O-FeO-V_2O_5-P_2O_5). An increase in conductivity by a factor up to 10^3 and 10^9 has been observed in these glasses as a result of nanocrystallization.

References

[1] Garbarczyk J E, Pietrzak T K, Wasiucionek M et al. 2015 *Solid State Ionics* **272** 53

Tight-Binding Molecular Dynamics Studies of Icosahedral Short-Range Order in Liquid Copper

S. Winczewski[1], J. Dziedzic[1,2], J. Rybicki[1,3]

[1] *Faculty of Applied Physics and Mathematics, Gdansk University of Technology Narutowicza 11/12, 80-233 Gdansk, Poland*

[2] *School of Chemistry, University of Southampton Highfield, Southampton SO17 1BJ, UK*

[3] *TASK Computer Center, Gdansk University of Technology Narutowicza 11/12, 80-233 Gdansk, Poland*

The results of molecular dynamics simulations of liquid copper will be presented. In our approach, to describe the interactions of copper atoms, we used the NRL Tight-Binding method [1,2], known to be able to correctly capture the relevant electronic effects and reproduce the behavior of an element above the liquidus temperature [3]. This was confirmed by comparing our predictions (*e.g.* pair correlation functions, angular distribution functions, structure factors) with other theoretical studies [4,5,6] and the available experimental data [7]. We proposed a new approach to the structure analysis of disordered systems, combining the Voronoi analysis [8] with the bond-orientational order analysis [9,10,11]. The proposed technique was successfully applied to characterize the structure of liquid copper and elucidate the role played by ideal and defective icosahedra.

Acknowledgements

We acknowledge the support of the Polish Ministry of Science and Higher Education (Grant No. IP2012 043972) and of the TASK Academic Computer Centre (Gdansk, Poland). This research was also supported in part by the PL-Grid Infrastructure (Grant No. POIG.02.03.00-00-096/10).

References

[1] Cohen R, Mehl M, Papaconstantopoulos D 1994 *Phys. Rev.* **B 50** 14694
[2] Mehl M, Papaconstantopoulos D, Kioussis N, Herbranson M 2000 *Phys. Rev.* **B 61** 4894
[3] Dziedzic J, Rybicki J 2008 *J. Non-Cryst. Solids* **354** 4316
[4] Ganesh P, Widom M 2006 *Phys. Rev.* **B 74** 134205
[5] Di Cicco A, Trapananti A 2007 *J. Non-Cryst. Solids* **353** 3671
[6] Celino M, Rosato V, Di Cicco A, Trapananti A, Massobrio C 2007 *Phys. Rev.* **B 75** 174210
[7] Eder O J, Erdpresser E, Kunsch B, Stiller B, Stiller H, Suda M 1980 *J. Phys. F: Met. Phys.* **10** 183
[8] Voronoi G 1908 *J. Reine Angew. Math.* **134** 199
[9] Steinhardt P J, Nelson D R, Ronchetti M 1981 *Phys. Rev. Lett.* **47** 1297
[10] Steinhardt P J, Nelson D R, Ronchetti M 1983 *Phys. Rev.* **B 28** 784
[11] Mickel W, Kapfer S C, Schroder-Turk G E, Mecke K 2013 *J. Chem. Phys.* **138** 044501

Central-Force Decomposition of Spline-Based Modified Embedded Atom Method Potential

S. Winczewski[1], J. Dziedzic[1,2], J. Rybicki[1,3]

[1] *Faculty of Applied Physics and Mathematics, Gdansk University of Technology Narutowicza 11/12, 80-233 Gdansk, Poland*

[2] *School of Chemistry, University of Southampton Highfield, Southampton SO17 1BJ, UK*

[3] *TASK Computer Center, Gdansk University of Technology Narutowicza 11/12, 80-233 Gdansk, Poland*

Central-force decompositions are fundamental to the calculation of stress fields in atomic systems by means of Hardy stress [1,2]. We derive expressions for a central-force decomposition of the spline-based modified embedded atom method potential [3]. The expressions are subsequently simplified to a form that can be readily used in molecular-dynamics simulations, enabling the calculation of the spatial distribution of stress in systems treated with this novel class of empirical potentials. We briefly discuss the properties of the obtained decomposition. To demonstrate the practicability of the derived expressions, we apply them to calculate stress fields due to an edge dislocation in bcc Mo, comparing their predictions to those of linear elasticity theory.

Acknowledgements
We acknowledge the support of the Polish Ministry of Science and Higher Education (Grant No. IP2012 043972) and of the TASK Academic Computer Centre (Gdansk, Poland). This research was also supported in part by the PL-Grid Infrastructure (Grant No. POIG.02.03.00-00-096/10).

References

[1] Hardy R J 1982 *J. Chem. Phys.* **76** (1) 622
[2] Murdoch A I 1983 *Q. J. Mech. Appl. Math.* **36** 163
[3] Lenosky T J, Sadigh B, Alonso E, Bulatov V V, de la Rubia T D, Kim J, Voter A F, Kress J D 2000 *Modelling Simul. Mater. Sci. Eng.* **8** (6) 825

Interatomic Potential Suitable for the Modeling of Penta-graphene: Molecular Statics/Molecular Dynamics Studies

S. Winczewski[1], M. Y. Shaheen[2], J. Rybicki[1,3]

[1] *Faculty of Applied Physics and Mathematics, Gdansk University of Technology Narutowicza 11/12, 80-233 Gdansk, Poland*

[2] *Faculty of Engineering Technology, University of Twente Drienerlolaan 5, 7522 NB Enschede, The Netherlands*

[2] *TASK Computer Center, Gdansk University of Technology Narutowicza 11/12, 80-233 Gdansk, Poland*

We test the potentials available for elemental carbon, with the scope to choose the potential suitable for the modeling of penta-graphene, the latest two dimensional carbon allotrope [1]. By using molecular statics and molecular dynamics simulations we show that there is only one potential – namely the Tersoff-type potential proposed by Erhart and Albe in 2005 [2] – which is able to correctly describe all the important features of penta-graphene. We show that this potential gives structural, mechanical and energetic parameters which are in accordance with the previously reported ab initio results.

Acknowledgements

We acknowledge the support of the Polish Ministry of Science and Higher Education (Grant No. IP2012 043972) and of the TASK Academic Computer Centre (Gdansk, Poland). This research was also supported in part by the PL-Grid Infrastructure (Grant No. POIG.02.03.00-00-096/10).

References

[1] Zhang S, Zhou J, Wang Q, Chen X, Kawazoe Y, Jena P 2015 *PNAS* **112** 2372

[2] Erhart P, Albe K 2005 *Phys. Rev.* **B 71** 035211

Surface Plasmon Resonance and Oscillation Spectroscopy for Cancer Diagnostics

R. Wojnarowska-Nowak[1], O. Shynkarenko[2], J. Polit[1], S. Nowak[3], S. Prokhorenko[1], E. M. Sheregii[1]

[1] *Centre for Microelectronics and Nanotechnology, University of Rzeszow Pigonia 1, 35-959 Rzeszow, Poland*

[2] *V. Lashkaryov Institute of Semiconductor Physics National Academy of Sciences of Ukraine Prospect Nauki 41, 03028 Kiev, Ukraine*

[3] *Department of Animal Physiology and Reproduction Institute of Biotechnology, University of Rzeszow Werynia 502, 36-100 Kolbuszowa, Poland*

Nanotechnology influences various areas of researches, including medicine [1,2]. The discovery of surface plasmon resonance (SPR) phenomena has given the chance to begin development of modern diagnostic methods, such as optical biosensors. Due to highly sensitive SPR sensors it became possible to find biomolecules rapidly. This, in turn, helps to collect a lot of important information about the presence and structure of specific molecules using optical spectroscopic methods as SPR, Raman spectroscopy, Surface Enhanced Raman Spectroscopy (SERS) and Fourier Transform Infrared Spectroscopy (FTIR). This information allows to find new markers which can be used in diagnostics of cancer.

In the presented work, the surface plasmon resonance phenomenon excited on gold nanofilm was used for a difference research in structure of blood cells of healthy and cancer patients. Blood serum was analysed with use of the mentioned oscillatory spectroscopy methods.

References

[1] Wojnarowska R, Polit J, Broda D, Gonchar M, Sheregii E M 2015 *Appl. Phys. Lett.* **106** 103701

[2] Wojnarowska-Nowak R, Polit J, Zięba A, Stolyarchuk I D, Nowak S, Romerowicz-Misielak M, Sheregii E M 2017 *Opto-Electronics Review* **25** 137

Electrochemical Properties of Hydrothermally Synthesized Composite Alpha-$Ni(OH)_2$/C

L. Yablon, I. I. Budzulyak, B. K. Ostafiychuk, O. Hemiy, O. Morushko

Faculty of Physics and Technology, Vasyl Stefanyk Precarpathian National University Shevchenko 57, 76025 Ivano-Frankivsk, Ukraine

Nickel hydroxide is of particular interest because it is a cheap and available electrode material. It is known that nickel hydroxide has two major polymorphic modifications: alpha- and beta-$Ni(OH)_2$. Beta-phase $Ni(OH)_2$ is isostructural to brucite $Mg(OH)_2$. The alpha-phase has a high theoretical capacity, but it is unstable in alkaline and quickly transforms into stable beta-$Ni(OH)_2$ [1].

We obtained the nickel hydroxide and the composite with nanoporous carbon materials (NCM) by the hydrothermal method using nickel nitrate as a major precursor. The NCM were dispersed by ultrasound in distilled water for 25 minutes or 2 hours, or exposed to laser irradiation for 3 min.

SEM images showed that the particles of hydrothermally obtained alpha-$Ni(OH)_2$ were microspheres 2.5 microns in diameter. In the composite, microspheres enter the pores of the carbon covering the surface.

Electrochemical studies were conducted using a three-electrode cell in which alpha-$Ni(OH)_2$ and composite alpha-$Ni(OH)_2$/C were used as working electrodes. There were two anodic peaks at 0.3 and 0.35 V for alpha-$Ni(OH)_2$. The presence of these peaks indicates that during anodic oxidized alpha-$Ni(OH)_2$, a system with two separate phases was formed. These phases are at different potentials and are likely alpha- and beta-$Ni(OH)_2$. In the cathode region, the peak did not split so the kinetic properties of restoring the two phases are identical. During cycling the anodic current peak is shifted toward the positive potential (from 0.37 to 0.44 V), what is probably the cause of the process of transition to a stable beta-phase. As the alpha-phase is thermodynamically unstable, the conversion to the beta-phase or the mixed phase is an energetic favorable process. Thus, the most likely interfacial transformation caused the by two distinct processes: the transition to beta-$Ni(OH)_2$ in a concentrated solution of KOH and electrochemical cycling between oxidized and reduced states. For composite alpha-$Ni(OH)_2$/C there is one peak only which is responsible for the alpha-phase. We can therefore say that the addition of carbon improves the stability of alpha-$Ni(OH)_2$ in the cycling. Composite alpha-$Ni(OH)_2$/C dispersed by ultrasound for 2 hours demonstrates the highest specific capacitance (310 F/g, at speed scanning of 1 mV/s).

Hence, the input of carbon into a nickel hydroxide structure and ultrasound successfully stabilize alpha-$Ni(OH)_2$ in alkaline environments and increase the conductivity of composite materials and devices are formed on their basis accordingly.

References

[1] Hemiy O, Yablon L, Budzulyak I, Budzulyak S, Morushko O, Kachmar A 2016 *J. Nano- and Electronic Physics* **8** (4) 04074

X-Ray Diffraction Study of Liquid Ternary Al-Fe-Ge Alloys

O. Yakovenko, V. P. Kazimirov, O. S. Roik, V. E. Sokol'skii

Chemical Department, Taras Shevchenko National University of Kyiv
Volodymyrska 64, 01601 Kyiv, Ukraine

An X-ray diffraction study of liquid Al-Fe-Ge alloys in a wide temperature range was carried out along two cross sections parallel to one of the concentration triangle sides, with the contents of 20 and 55 at.% Al using monochromatic Mo-K_α radiation. The difference in interatomic interactions in the boundary binary Al-Fe, Al-Ge, Fe-Ge melts was taken into account during selection of compositions. It allowed estimating their influence on the formation of the structure of liquid ternary alloys. The maximum value of the enthalpy of mixing (ΔH_{max}) binary melts (in absolute value) being -21 kJ/mol for Al-Fe, -16 kJ/mol for Fe-Ge and -3.3 kJ/mol for Al-Ge according to the published data was taken as a quantitative characteristic of the energy factor. It points out on the existence of a competition between Al and Ge atoms in the formation of a local atomic structure of ternary melts, especially a local environment of the Fe atoms. The maximum value of the mixing enthalpy (ΔH_{max}) of ternary melts is approximately -20 kJ/mol that indicates a priority role of interatomic interactions in the Al-Fe boundary melts in the formation of the thermodynamic properties of the Al-Fe-Ge melts. For example, the structure factor (SF) and the concentration dependences of first peak positions of the structure factor (S_1) and the pair correlation functions (R_1) of the liquid ternary alloys along the $Al_{55}Ge_{45}$-$Al_{55}Fe_{45}$ cross section

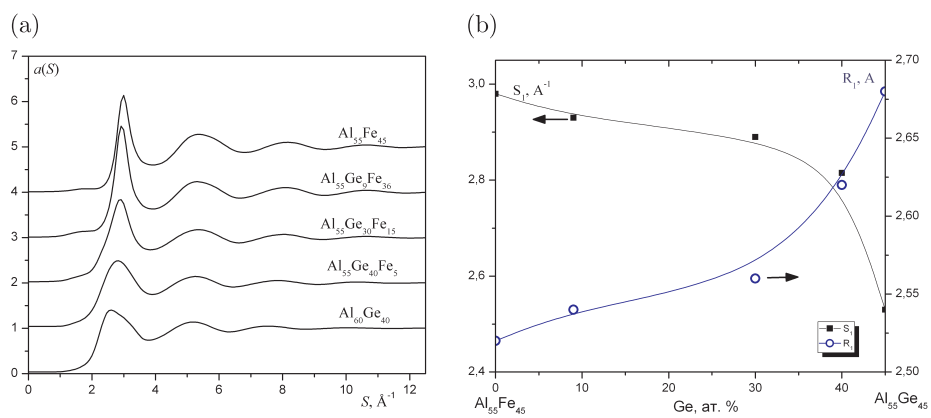

Figure 1: Structure factor curves (a) and concentration dependences of S_1 and R_1 values of liquid Al-Fe-Ge alloys along $Al_{55}Ge_{45}$-$Al_{55}Fe_{45}$ cross section at 1000°C (b)

are shown in Figure 1. As can be seen from Figure 1, the addition of 5 at.% Fe to binary $Al_{55}Ge_{45}$ leads to noticeable changes in the form and position of the first peak of the SF, thus, to a decrease in the R_1 value.

This tendency remains with further replacement of germanium by iron that leads to noticeable negative deviations of the concentration dependences of R_1 from the additive behavior in the range $Al_{55}Ge_{45}$-$Al_{55}Ge_9Fe_{36}$. It is also consistent with the concentration dependence of the R_1 value of the binary Al-Fe liquid alloys due to the priority of heteroatomic interactions in the formation of the local atomic structure. It has been found that the structure factor of the liquid ternary alloys with $\geqslant 15$ at.% Fe has a weak prepeak at low Q values (1.8 Å). According to the literature, the presence of a prepeak on the SF is a structural feature of liquid Al-Fe alloys. There are microgroups of germanium atoms in liquid ternary alloys with the content of 40–30 at.% Ge (Figure 1a) that is manifested by a shoulder on the low-Q side of the first peak of the SF which is in agreement with the position of the first peak of the SF of liquid germanium. Similar changes in the structure factor and the pair correlation function are also characteristic for ternary melts along the $Al_{20}Fe_{80}$-$Al_{20}Ge_{80}$ cross section. The obtained results indicate the priority role of interatomic interactions in Al-Fe pairs in the formation of the local atomic structure of liquid Al-Fe-Ge alloys at 1000°C.

Reinforced Sn-Ag-Cu Solders: Metal Nanoinclusions Versus Alloying Elements

A. Yakymovych, H. Ipser

Department of Inorganic Chemistry – Functional Materials
Faculty of Chemistry, University of Vienna
Althanstr. 14, A-1090 Vienna, Austria

Although considerable research has been performed to investigate the impact of nanoinclusions on the commercial Sn-Ag-Cu (SAC) alloys and considerable improvements of the microstructure and of various properties have been reported, manufacture and application of nanocomposite SAC solders appear to be still in the distant future. In fact, there are many open questions related to the long time behavior of nanoparticles in the bulk Sn-based matrix. One of the major points is whether metal nanoparticles will be stable inside a metal matrix, or whether their high chemical activity will lead to dissolution, changing the microstructure and properties of the solder.

A key issue discussed in the current study is the examination of the impact of adding metals into SAC solder either in the bulk or nanosized form. Measurements of various thermophysical and thermodynamic properties, supported by structural studies in the liquid state, were performed to discover the changes in the behavior of the liquid Sn-3.8Ag-0.7Cu and Sn-3.0Ag-0.5Cu solder alloys caused by minor metal additions, namely Co and Ni up to 5 wt. Furthermore, the reliability of Cu/nanocomposite solder/Cu joints was studied based on microstructural analysis and tests of various mechanical properties, such as shear strength and microhardness.

Acknowledgements
The authors want to acknowledge the financial support for this study from the Austrian Science Fund (FWF) under projects Nos. P 26304 and P 27049.

Effects of Al Additions and Annealing Treatment on CoCrFeNi Alloy Microstructure

A. Yakymovych, H. Ipser

Department of Inorganic Chemistry – Functional Materials
Faculty of Chemistry, University of Vienna
Althanstr. 14, A-1090 Vienna, Austria

The high-entropy alloys (HEAs) form simple Bravais lattice structures, such as face-centered cubic (FCC) and/or body-centered cubic (BCC) while they contain at least five pure components with a more or less equiatomic composition. This unique internal structure leads to unexpected characteristics which could not be obtained from any single component. The addition of Al to the multi-component solid CoCuFeNi solution in order to produce HEA leads to a phase decomposition with the formation of Al-rich and Al-poor phases. Furthermore, as-solidified Al-containing HEAs show the formation of Al-Co (Al-Ni) intermetallic compounds (IMCs). The above-mentioned structural transformations should certainly have an impact on the physical and chemical properties of HEAs.

The goal of this study is to investigate structural changes in CoCuFeNi alloys with increasing the content of Al up to an equiatomic composition. For this purpose, high-entropy $Al_xCoCrFeNi$ alloys ($x = 0$; 0.2; 0.4; 0.6; 0.8; 1) were prepared using an arc-melting furnace. The microstructure and phase composition were investigated based on scanning electron microscopy (SEM) and X-ray diffraction analysis. Furthermore, parts of the samples were subsequently heat treated at 1273 K and 1073 K for two and six days, respectively. The annealed samples were investigated to study the evolution of the phase composition and microstructure after heat treatment.

Optical Properties of Layered Compounds $TlGaSe_2$–ZnSe

O. V. Zamurueva, G. V. Macknovetsc, G. L. Muronchyk,
L. V. Piskach, Y. S. Suchyk

Department of Experimental Physics and Information Technologies
Lesya Ukrainka Eastern European National University
Volya Avenue 13, 43025 Lutsk, Ukraine

Semiconductors with a layered crystalline structure occupy a special place among a large number of new semiconductor materials. Both scientific and practical interest in similar semiconductors is growing every year [1,2]. Therefore, the expansion of the class of precisely layered semiconductors such as $A^{III}B^{III}C_2^{VI}$, including $TlGaSe_2$, production of perfect crystals, and the further study of the complex of their physical properties, are the current issues in modern solid-state physics.

The investigated compounds were grown by directional crystallization (Bridgman-Stockbarger method) with the percentage content of 98 mol% $TlGaSe_2$ – 2 mol% ZnSe.

The optical absorption coefficients are determined in the temperature range of 100-300 K using the R values at room temperature and provided that the temperature change does not contribute to a large significant change in R [3] (Figure 1). An analysis of these curves shows that the absorption spectra can be described by the formula $\alpha^k = A(h\nu - E_g)$, where $k = 2$ – direct transitions are allowed; $k = 1/2$ – indirect transitions are allowed (Figure 2a,b).

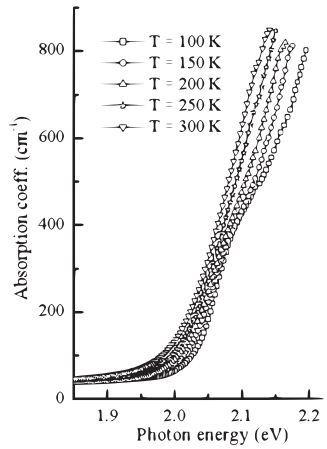

Figure 1: Typical absorption spectra for 98 mol% $TlGaSe_2$ – 2 mol% ZnSe

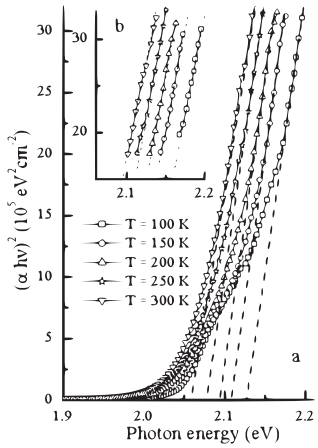

Figure 2: Typical absorption spectra (a) and direct absorption spectra (b) for 98 mol% $TlGaSe_2$ – 2 mol% ZnSe

The width of the forbidden band for indirect optical transitions is less than for direct optical transitions. This change is typical for crystals that have a layered structure [1].

From Figure 1, it is clear that below the strong absorption range the dependence $\alpha = f(h\nu)$ is exponential-like. The region of exponential variation of α with increasing $h\nu$ is called the Urbach's tail [4]. On the exponential part, the dependence $\alpha = f(h\nu)$ is subject to the Urbach rule (Figure 3)

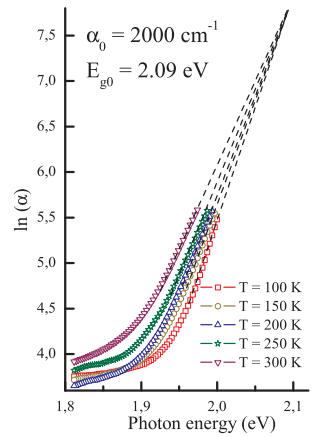

Figure 3: Typical absorption spectra obtained at 100, 150, 200, 250 and 300 K for p-98 mol% $TlGaSe_2$ – 2 mol% ZnSe

The EU growth for the compound with the increasing temperature (Table 1) is associated with an increase in the disorder of the samples and it is determined both by static ("frozen phonons") and by dynamic ("thermal phonons") components [5].

Table 1: Width of forbidden band, with direct allowed transition, Urbach's energy and steepness parameter

Temperature	100	150	200	250	300
E_{g_d} eV	2.13	2.11	2.10	2.08	2.06
E_u meV	39.70	44.40	48.00	51.00	55.50
Stepness parameter	0.217	0.291	0.359	0.422	0.465

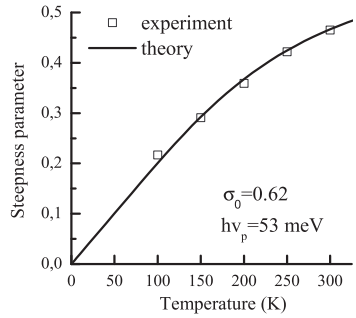

Figure 4: Steepness parameters as function of temperature for p-98 mol% $TlGaSe_2$ – 2 mol% ZnSe; the solid line represents a fitting curve using the equation $\sigma(T) = kT\Delta(\ln\alpha)/\Delta(h\nu)$

The steepness parameter from the experimental data on the slopes of the tails of the absorption edge is shown in Figure 4. In the entire range under study, it is approximated by the expression for the absorption edge which is formed with the participation of electron-phonon interaction [5].

References

[1] Gurbulak B 2005 *Czechoslovak J. Phys.* **55** (1) 93
[2] Myronchuk G, Zamurueva O, Ożga K 2015 *Arch. Metall. Mater.* **60** (2) 1051
[3] Gamal G 1990 *Semicond. Sci. Technol.* **13** (2) 185
[4] Urbach F 1953 *Phys. Rev.* **B 92** (5) 1324
[5] Myronchuk G 2014 *J. Mater. Sci. - Mater. Electron.* **25** (7) 3226

Redistribution of Valence Electrons Due to Changes in Synthesis Conditions and Ion Charge State Influence on Electrochemical Properties of Lithium Power Sources

Ya. V. Zaulychnyy[1], Y. V. Yavorskyi[1], O. I. Dudka[1], I. M. Kozak[1], M. V. Karpets[2]

[1] *Physical Engineering Faculty, National Technical University of Ukraine "Kyiv Polytechnical Institute" Politekhnichna 35, 03056 Kyiv, Ukraine*

[2] *Frantsevich Institute for Problems of Materials Science Krzhyzhanivsky 3, 03680 Kyiv, Ukraine*

The energy conditions and electronic mechanisms of interaction of the surface ions of nanoparticles and surrounding environments were determined as a result of the study of the redistribution of valence electrons in the dispersion process of nanosized materials with different types of the bonding and atomic-crystalline structure.

We show that narrowing the energy distribution of valence electrons in nanosystems is a result of the disappearance of the splitting of energy levels and that changes of their position are a result of relaxation processes at the breaking of atomic bonds.

The migration of electrons from high-energy non-binding states of anions to the energy levels of cations was detected due to the increase in the number of broken ionic-covalent bonds when the sizes of oxide nanoparticles were reduced. This leads to an increase in the surface energy of nanosize oxides and the abilityto interact with other systems.

The influence of shock-vibration treatment of mixtures of nanooxides and pyrogenic synthesis of nanocomposites on their electronic structure is studied. It is shown that when shock-vibration processing amorphous and crystalline nanosize particles interconnect, there is formation in the interface of their $(O-O)p\pi$-bonds, due to the overlap of Op-orbitals and additional splitting of energy levels and filling of the electron binding transitioned from metal [1,2]. Therefore, the increase in the charges of anions leads to increased Coulomb attraction of Li^+ ions to the anions on the surface and structural defects of nanocomposites. This leads to a sharp increase in the charge capacity of the lithium power sources with composite cathodes.

The inability of Li^+ to recombination with Op-bound electrons and recovery of lithium is established. Therefore, lithium oxide film is not formed on the surface of nanoparticles and the level of introduction of lithium in the cathode increases 1.5 times after the 2nd cycle of deintercalation.

It was also shown that an increase in the filling of high-energy non-binding and anti-binding levels by electrons leads to the recovery of lithium due to the recombination of $Li^+ + e^- = Li$.

References

[1] Zaulychnyy Ya V, Ilkiv V Ya, Yavorskyi Y V, Gunko V M, Zarko V I, Karpets M V 2015 *Physics and Chemistry of the Solid State* **16** (2) 425
[2] Yavorskyi Y V, Zaulychnyy Ya V, Ilkiv V Ya, Dudka O I, Chmeruk A P, Zarko V I, Karpets M V 2015 *Physical Surface Engineering* **13** (3) 371

$FeF_3 \cdot 0.33H_2O$ and $FeF_3 \cdot 0.33H_2O/C$ as Cathode Materials for Lithium Power Sources

L. Zbihlei[1], V. Moklyak[2], O. Khemii[1]

[1] *Vasyl Stefanyk Precarpathian National University*
Shevchenko 57, 76025 Ivano-Frankivsk, Ukraine

[2] *G. V. Kurdyumov Institute for Metal Physics, Nat. Acad. of Sci. of Ukraine*
Ac. Vernadsky Av. 36, 03142 Kiev, Ukraine

The lithium-ion battery is the most promising battery candidate among various available storage technologies to store chemical energy and deliver electrical energy with high conversion efficiency without gaseous emission. As the dominant power source for electric vehicles and hybrid electric vehicles, rechargeable lithium batteries need to be further improved to compete with traditional petrol vehicles [1]. Therefore, intensive research efforts on searching for battery cathode materials with higher energy densities spring up. Traditional cathode materials, such as $LiCoO_2$, $LiMn_2O_4$, $LiFePO_4$, etc., have a limited actual specific capacity in the range of 120–160 A·h/kg, which depend on Li^+ intercalation/deintercalation that use only one unit valence change per cation. Recently, transition metal fluorides, such as CoF_2 [2] and FeF_3 [3–6] have been studied as a promising new class of cathode materials, which exhibit large theoretical capacities and high discharge voltages due to their highly ionic metal-ligand bonds and small atomic weight.

Fluoride iron is regarded today as one of the most promising cathode materials for lithium power sources (LPS). The advantages of their use in power sources are: a relatively high open-circuit voltage of ~ 4 V and the specific capacity of ~ 200 A·h/kg. However, these materials are characterized by low conductivity and they are dielectrics with a wide band gap (4.485 eV). This makes it difficult to transport electrons into the flow of electrochemical reactions, and reduces the specific characteristics of the LPS formed on their basis. One solution to this problem is the use of nanostructured iron fluoride forms and their nanocomposites from conductive materials.

The materials were prepared by a simple liquid-phase method. $FeF_3 \cdot 0.33H_2O$ was obtained by heat treatment at 180°C for 4 h in a tube furnace with an argon flow. As a result, according to the XPA and Mössbauer spectroscopy data, we obtained the following monophase materials: HTB-$FeFR_3 \cdot 0.33H_2O$ with a structure of hexagonal tungsten bronze (PDF: 76–1262) with an average size of coherent scattering regions up to 26 nm. The $FeF_3 \cdot 0.33H_2O/C$ nanocomposite was obtained by the ultrasonic dispersion method using acetylene black (AB) (weight ratio of iron fluoride: AB= 80 : 20). The cathodes for the lithium cells were fabricated by mixing the acetylene black and a polyvinylidene fluoride (PVDF) binder with a weight ratio of 75 : 15 : 10 in N-methyl pyrrolidinone, which were then pasted on aluminum foil. The testing cells were assembled with the cathodes thus fabricated, a metallic lithium anode, a film

separator, and 1 M $LiBF_4$ electrolyte. The testing cells were assembled in an argon-filled glove box. All the cells were allowed to age before testing, the specific capacity was based on the weight of the nanocomposite material.

Although the electrochemical reaction mechanism of FeF_3 has been investigated fully, the electrochemical reaction mechanism of $FeF_3 \cdot 0.33H_2O$ and $FeF_3 \cdot 0.33H_2O/C$ still remains unknown. The galvanostatic charge/discharge measurements were carried out in a wide voltage range (0.5–4.5 V) to explore the reaction mechanisms of these iron fluorides and compare their electrochemical properties. $FeF_3 \cdot 0.33H_2O$ and $FeF_3 \cdot 0.33H_2O/C$ as cathodes during the first cycles with the current density of 0.1 C in the voltage of 0.5–4.5 V at room temperature showed a well-defined three-staged discharge with the voltage plateau above 3.0–2.7 and 2.0–1.4 V, followed by a flat voltage discharge at 1.4–0.5 V, demonstrating a three-step electrochemical reaction process. Notably, $FeF_3 \cdot 0.33H_2O$ shows a maximum initial discharge capacity of 603 A·h/kg, and $FeF_3 \cdot 0.33H_2O/C$ shows – 819 A·h/kg, which are probably attributed to a three-step electrochemical reaction including the Li+ insertion and the reversible conversion reaction.

References

[1] Goodenough J B, Kim Y 2009 *Chem. Mat.* **22** (3) 587
[2] Fu Z W et al. 2005 *J. Electrochem. Soc.* **152** (2) E50
[3] Nishijima M et al. 2009 *J. Power Sources* **190** (2) 558
[4] Plitz I et al. 2005 *J. Electrochem. Soc.* **152** (2) A307
[5] Yamakawa N et al. 2009 *J. Am. Chem. Soc.* **131** (30) 10525
[6] Li T et al. 2010 *J. Phys. Chem. C* **114** (7) 3190

INDEX OF AUTHORS